AD-773 597

INVESTIGATION OF ADVANCED STRUCTURAL CONCEPTS FOR FUSELAGE

Robert J. Mayerjak, et al

Kaman Aerospace Corporation

Prepared for:

Army Air Mobility Research and Development Laboratory

October 1973

DISTRIBUTED BY:

NTIS

National Technical Information Service
U. S. DEPARTMENT OF COMMERCE
5285 Port Royal Road, Springfield Va. 22151

DISCLAIMERS

DISPOSITION INSTRUCTIONS

Unclassified

Security Classification

AD773577

DOCUMENT CONTROL DATA - R & D

(Security classification of title, body of abstract and indexing annotation must be entered when the overall report is classified)

1. ORIGINATING ACTIVITY (Corporate author) Kaman Aerospace Corporation Division of Kaman Corporation Bloomfield, Connecticut	2a. REPORT SECURITY CLASSIFICATION Unclassified 2b. GROUP

3. REPORT TITLE

INVESTIGATION OF ADVANCED STRUCTURAL CONCEPTS FOR FUSELAGE

4. DESCRIPTIVE NOTES (Type of report and inclusive dates)

Final Report

5. AUTHOR(S) (First name, middle initial, last name)

Robert J. Mayerjak
William A. Smyth

6. REPORT DATE	7a. TOTAL NO OF PAGES	7b. NO. OF REFS
October 1973	144	12

8a. CONTRACT OR GRANT NO DAAJ02-72-C-0057 b. PROJECT NO Task 1F162208A17001 c.	9a. ORIGINATOR'S REPORT NUMBER(S) USAAMRDL Technical Report 73-72 9b. OTHER REPORT NO(S) (Any other numbers that may be assigned this report) Kaman Aerospace Report R-1164

...UTION STATEMENT

...ed for public release; distribution unlimited.

11. S...	12. SPONSORING MILITARY ACTIVITY Eustis Directorate U. S. Army Air Mobility R&D Laboratory Fort Eustis, Virginia

13. ABSTRACT

Design concepts are presented and evaluated for the application of fiber reinforced composite materials to fuselage structures. The concepts are evaluated on the basis of cost-effectiveness and performance when specifically applied to the aft fuselage of the Army AH-1G helicopter. Comparisons to the existing metal structure show that several of the new concepts provide significant advantages in initial acquisition cost, life-cycle cost, weight, safety, reliability, and maintainability.

157

DD FORM 1 NOV 65 1473 REPLACES DD FORM 1473, 1 JAN 64, WHICH IS OBSOLETE FOR ARMY USE.

Unclassified

Security Classification

12

Unclassified
Security Classification

14 KEY WORDS	LINK A		LINK B		LINK C	
	ROLE	WT	ROLE	WT	ROLE	WT
Design						
Composite materials						
Structures						
Fuselage						
AH-1G						
Helicopter						
Costs						

Unclassified
Security Classification

DEPARTMENT OF THE ARMY
U. S ARMY AIR MOBILITY RESEARCH & DEVELOPMENT LABORATORY
EUSTIS DIRECTORATE
FORT EUSTIS, VIRGINIA 23604

This report was prepared by the Kaman Aerospace Corporation under the terms of Contract DAAJ02-72-C-0057.

The information contained in this report is a result of research conducted to extend the basic understanding of advanced design concepts and composite materials and their application to aircraft fuselage primary structures.

This effort is one of two parallel studies to investigate advanced structural concepts for helicopter fuselages. The associated study program, under the same title, was conducted by The Boeing Company. Vertol Division, under the terms of Contract DAAJ02-72-C-0056.

Numerous design approaches, material selections, and fabrication techniques were investigated for the AH-1G Cobra helicopter tail section. A quantitative method (math model) for ranking the proposed design concepts was developed. Although each individual concept possesses specific areas of advantages and disadvantages, it was determined that a monocoque/sandwich structure was the preferred design concept.

The report has been reviewed by the Eustis Directorate, U.S. Army Air Mobility Research and Development Laboratory and is considered to be technically sound. It is published for the exchange of information and the stimulation of future research.

The technical monitor for this program was Mr. L. Thomas Mazza, Technology Applications Division.

Task 1F162208A17001
Contract DAAJ02-72-C-0057
USAAMRDL Technical Report 73-72
October 1973

INVESTIGATION OF ADVANCED STRUCTURAL CONCEPTS FOR FUSELAGE

Final Report

Kaman Aerospace Report R-1164

By

Robert J. Mayerjak
William A. Smyth

Prepared by

Kaman Aerospace Corporation
Bloomfield, Connecticut

for

EUSTIS DIRECTORATE
U.S. ARMY AIR MOBILITY RESERACH AND DEVELOPMENT LABORATORY
FORT EUSTIS, VIRGINIA

Approved for public release; distribution unlimited.

ii

SUMMARY

The objective of this program is to prepare and evaluate several design concepts for the application of fiber-reinforced composite materials to fuselage structures. The concepts are evaluated on the basis of cost effectiveness and performance when specifically applied to the aft fuselage of the Army AH-1G helicopter.

It is concluded from these studies that when compared to the existing metal structure, the preferred new concepts provide life-cycle cost savings, weight savings, increased safety, reliability, and maintainability.

The preferred concepts are identified herein as boom-fin concept 3, elevator concept 4, and cover concept 3.

FOREWORD

This design study of advanced concepts for fuselage structures was performed under Contract DAAJ02-72-C-0057, Task 1F162208A17001 from the Eustis Directorate, U. S. Army Air Mobility Research and Development Laboratory, Fort Eustis, Virginia, and was under the general technical cognizance of Mr. Thomas Mazza of the Technology Applications Division.

The authors acknowledge important contributions made to this program by Messrs. Herbert Guay, Dr. John Hsu, Durwood Lathrop, Andrew Mank, Harold Showalter, Peter Sevenoff, Frank Starses, and William Whiteside, all of the Kaman Aerospace staff.

Preceding page blank

TABLE OF CONTENTS

Preceding page blank

Page

LIST OF ILLUSTRATIONS

LIST OF TABLES

LIST OF SYMBOLS

Symbols are listed in four categories. The categories are presented in the order of their appearance in the text.

MATERIAL SYMBOLS

E	E Glass
D	E. I. DuPont PRD-49
G	graphile
PVC	polyvinyl chloride
R300	rigid, closed-cell, expanded PVC foam at 3 lb/cu ft
R400	rigid, closed-cell, expanded PVC foam at 4 lb/cu ft (R300 and R400 are B. F. Goodrich designations)
S	S Glass
T	thickness, in.
U	uniaxial
120	woven fabric, 120 style
181	woven fabric, 181 style
913	woven fabric, 913 style (913 is a Ferro Corporation designation for a zero twist fabric of a twill weave with 53.7% of the fibers in the warp direction)

LAMINATE CODE SYMBOLS

In this report, a laminate code is used to describe a specific laminate uniquely. The code is very similar to that described in Reference 1 for description of orientation. Herein, the code is extended to the description of material, style, angle, and thickness. The elements of the code used in this report are listed below.

A	Each lamina is denoted by a symbol, A, B, C, etc., denoting its material, style, angle, or thickness.
A/B	Individual adjacent laminae are separated by a slash, if their materials, styles, angles, or thicknesses are different.

(A/B) The laminae are listed in sequence from one laminate face to the other, with parentheses indicating the beginning and end of the code.

(A_N) Adjacent laminae of the same material, style, angle, or thickness are denoted by a numerical subscript.

$(A/B)_S$ A subscript S indicates a symmetric laminate. Only one-half of the laminate is shown.

STRUCTURAL ANALYSIS SYMBOLS

11,22,12 The properties of the individual lamina are described with reference to a local orthogonal axis system identified by the numbers 1 and 2. In general, the 1-axis is chosen colinear with the reinforcement. The subscript 11 denotes a property along the 1-axis. The subscript 22 denotes a property along the 2-axis. The subscript 12 denotes a property (such as shear or Poisson's ratio) along both the 1 and 2 axes.

xx, yy, xy The properties of the total laminate are described with reference to a local orthogonal axis system identified by the letters x and y. These axes lie in the plane of the laminate. In general, the x-axis is chosen to be nearly parallel to the central axis of the structure. The use of the subscripts is similar to that described for 11, 22, 12.

X,Y,Z The stiffnesses of the total cross-section and the loads upon a cross-section are described with reference to a local orthogonal axis system identified by the letters X, Y, and Z. In general, the local X axis lies along the axis of the structure, be it boom or fin. The local Y lies perpendicular to the midplane of the aircraft and is positive to the left. When used alone, X, Y, and Z denote coordinate positions. When used in a subscript, X, Y, or Z denotes a quantity along or about the axis.

AST area of stringer, in.^{2}

c compression, used in superscripts

E modulus of elasticity, ksi

F allowable limit stress, ksi

f stress, ksi

G	shear modulus, ksi
I	bending stiffness/basic E, $in.^4$
J	torsional stiffness/basic G, $in.^4$
N	allowable limit load intensity, kips/in.
n	load intensity, kips/in.
s	shear, used in superscripts
T	thickness, in.
t	tension, used in superscripts
TF	factor used to calculate contribution of cover in bending analyses
μ	principal Poisson's ratio, strain along 2-axis/strain along 1-axis for load applied along 1-axis

<u>COST MODEL SYMBOLS</u>

C_A	attrition costs per aircraft life cycle
C_{AS}	cost of air shipping tail section from CONUS
C_C	cost of shipping container
C_{ER}	cost of special ground support equipment required
C_O	acquisition cost for one tail section
C_{LC}	total tail section costs per aircraft life cycle
C_M	average cost of material per repair
C_{MD}	depot level labor rate
C_{MH}	organizational/intermediate-level labor rate
C_{MS}	shipping cost of material per repair as a fraction of material cost
C_{PS}	shipping preparation cost
C_{RD}	depot-level repair costs
C_{RO}	organizational/intermediate-level repair costs
C_S	initial spares cost per aircraft life cycle

C_{SC}	container surface shipping cost
C_{SD}	depot-level scrap costs
C_{SO}	organizational/intermediate-level scrap costs
C_{SS}	tail section surface shipping cost to CONUS
C_{TM}	total operating costs per aircraft life cycle
C_{TO}	total initial costs per aircraft life cycle
C_W	cost adjustment for weight
D_{RD}	average material and equipment costs per tail section repaired at depot level
D_W	dollar value per pound of structural weight
K_{RD}	fraction of damaged sections repaired at depot level
K_{RI}	fraction of damaged sections repaired at intermediate level
K_{RO}	fraction of damaged sections repaired at organizational level
K_{SD}	fraction of damaged sections scrapped at depot level
K_{SO}	fraction of damaged sections scrapped at organizational/intermediate level
K_{TS}	total fraction of damaged sections scrapped
L	aircraft life cycle, flight hours
M_1	MMH to inspect and determine damage
M_2	same as M_1
M_3	MMH to inspect and determine damage, remove and replace tail section, requisition and obtain replacement
M_4	MMH to receive and inspect at depot
M_5	MMH at depot level to receive, inspect, and dispose of scrap
MMH	maintenance man-hours

MTBD	tail section mean time between damage, hr
N_A	number of tail sections lost to attrition per life cycle
N_D	number of damaged tail sections per aircraft life cycle
T_{RO}	mean field repair time, including time to remove and replace 1.3% of damaged tail sections
W_S	weight of existing tail section minus weight of new concept
Y	aircraft life cycle, yr

INTRODUCTION

Aluminum sheet is today the bargain among aircraft materials. It costs roughly 50 cents per pound. However, a conventional aft fuselage made from this aluminum sheet costs about $35 per pound, even for good designs in quantity production. The material is inexpensive, but its fabrication and assembly are dear. The reason lies in the concept itself, namely, the hand assembly of many individual pieces using fasteners. The concept also contributes to future maintenance costs because of fatigue cracking at or near thousands of fasteners.

Fibrous composite materials offer an opportunity to escape these costs and in addition to get, pound-for-pound, a safer, more reliable structure. The opportunity will be wasted, however, if old concepts are retained. To take full advantage of the opportunity for low life-cycle cost, and the designer must use new design concepts that:

1. Reduce the number of parts
2. Eliminate production operations
3. Simplify assembly
4. Improve field maintainability

These precepts were applied to develop new design concepts for the aft fuselage of the AH-1G helicopter. The aft fuselage assembly is considered herein to consist of three components: the boom-fin, the elevators, and the covers over the drive shaft. Each of these components has a distinctly different function and presents a different problem for design. In this report, four new concepts are presented for each of the three components for a total of 12 new design concepts.* The presentation includes estimates for production costs and weight for each new concept. Production costs and weight are also shown for four aft fuselage assemblies. Each assembly consists of a boom-fin concept combined with the lowest cost elevators and lowest cost drive shaft covers if required.**

In addition, the total life-cycle costs are presented for each of the four new concepts for aft fuselage assemblies and also for the existing metal aft fuselage. The life-cycle costs for the existing fuselage provide the baseline for comparisons of the new concepts to conventional construction. The life-cycle cost model includes all the significant costs incurred in the support of a fleet of 1000 helicopters over a 10-year life cycle. The principal categories of cost in the model are initial cost, operational cost, and attritional cost.***

* Tables I, II, and III summarize the basic characteristics.
** Table XX summarizes production costs and weights.
*** Tables XXI and XXIII summarize life-cycle costs.

The concepts were developed within the following design constraints:

1. Low life-cycle cost shall be a principal objective. This objective guarantees that consideration is given to low initial cost, high reliability, and good repairability.

2. The new concepts shall provide improved safety. This requires high tolerance to ballistics damage in addition to adequate strength for design loads.

3. The weight of new concepts for the aft fuselage assembly shall not exceed that of the existing structure. In this program, the emphasis is upon life-cycle cost rather than weight reduction per se. The dollar value of weight reduction is accounted for as one of many elements in a comprehensive model for life-cycle cost.

4. The new concepts shall be dynamically compatible with the aircraft. Adequate stiffness must be provided to keep the natural frequencies well positioned in relationship to the principal exciting forces at main rotor harmonics.

5. The structure shall be constructed principally from composite materials.

6. The new concepts shall be interchangeable with the existing aft fuselage.

7. The existing tail rotor, gearboxes, and drive shafts shall be used.

DESCRIPTION

EXISTING STRUCTURE

Figure 1, from Reference 2, shows the structural skeletons for the existing boom-fin and the elevator. In Reference 3, the manufacturer provides the following structural descriptions:

> "The tail boom is of semimonocoque construction, composed of 75ST6 aluminum skins, longerons and stringers. The primary bending structure consists of four longerons, one located in each of the four corners, and several stringers spaced between longerons. Each longeron is a built-up section consisting of one or more hats bonded and riveted together to form one part. A standard "J" section is used for the stringers on the sides and bottom of the boom. Two 90° angles, equally spaced from the vertical center line act as stringers on the upper skin surface. These angles also support the tail rotor drive shaft cover, which is a nonstructural fairing extending the length of the boom.
>
> The longerons and stringers are supported by frames spaced at approximately 21.0 inches. Five of these bulkhead frames are considered basic structure as they either re-distribute or introduce load. These bulkheads are located at boom stations* 41.32, 59.50, 143.28, 206.0, 227.0.
>
> The vertical fin is a sandwich construction cambered airfoil having an aluminum core and 7075-T6 aluminum skins. The internal structure consists of a front spar, rear spar, trailing edge and several intermediate ribs. These components are made of 7075-T6 and 2024-T4 aluminum alloys. The leading edge of the vertical fin is a honeycomb fiberglas door which hinges off of the front spar to allow access to the tail rotor drive shaft. It extends from the top of the boom to the 90° gear box.
>
> The elevator is a swept airfoil of semimonocoque construction made of 2024-T3 aluminum. The elevator is actuated and supported by a 2024-T3 aluminum alloy spar. The leading edge is made from .050 2024-T4 aluminum in order to resist the impact of the shell casings and/or ammunition clips ejected from the GAU-2B/A Minigun and the XM-129 40 mm grenade launcher."

---

* Abbreviated B.S. throughout this report

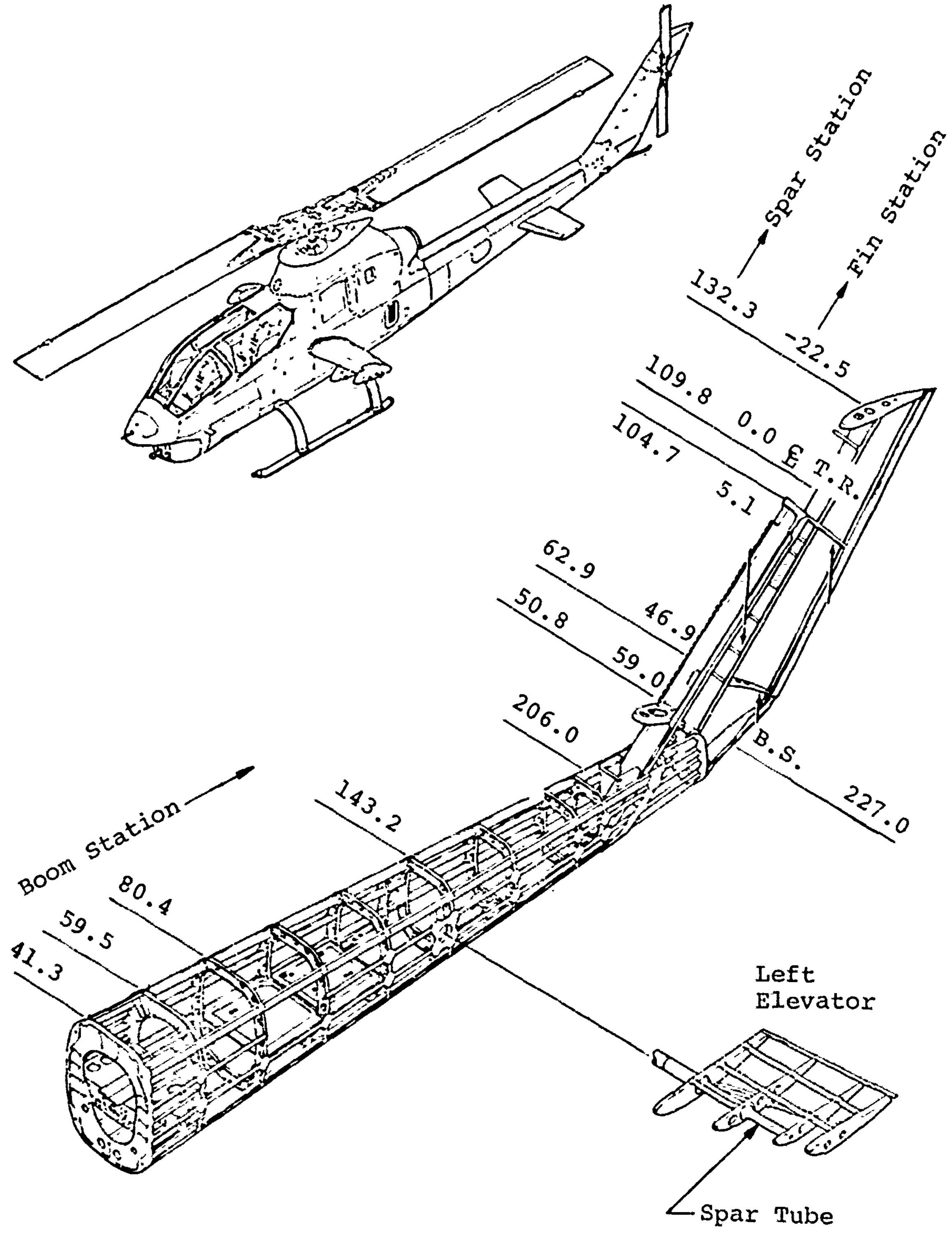

Figure 1. Structural Skeleton of Existing Aft Fuselage.

The manufacturer also provides the following assembly descriptions:

> "The vertical fin is assembled (permanently) to the tail boom between B.S. 206 and B.S. 227. Support for the vertical fin is provided by the bulkheads at Boom stations 206 and 227. At B.S. 206 the forward spar of the vertical fin assembles to the canted bulkhead. At B.S. 227 the aft spar and trailing edge are assembled to the bulkhead through fittings. Additional continuity is provided by shear attachments between the fin panels and boom structure.
>
> The horizontal stabilizer is part of the cyclic control system. As part of this system it helps to maintain the proper helicopter attitude. To install the stabilizer the left and right hand spars are inserted into the 209-001-908 Horn Assembly at Boom Sta. 140.35. This ties the elevator into the cyclic control system. The installation is supported by brackets and fittings extending between the B.S. 143.28 bulkhead and a partial frame at B.S. 137.42.
>
> The tail boom, vertical fin and horizontal stabilizer (elevator) together form one installation which is readily assembled to the forward fuselage at F.S. 299.57 by four bolts. These bolts are installed from the forward fuselage into barrel nut fittings located at the end of each longeron. Fuselage sta. 299.57 corresponds to boom sta. 41.32."

The drive train for the tail rotor is mounted on top of the boom and in front of the forward spar of the fin. It includes two intermediate supports at B.S. 80 and B.S. 143, a 42° gearbox at the junction of the boom and the fin, and a 90° gearbox at F.S. 0.

The forward end of the boom contains shelves of sandwich construction for the support of electronic equipment. The electronic equipment can be reached from the forward fuselage and through an access panel on the left side at B.S. 90. Two other large access panels are located on the bottom of the fuselage at B.S. 133 and B.S. 174.

A landing skid is located at the aft end of the boom. It is attached to the bulkheads at B.S. 206 and B.S. 227. A pair of small access panels is provided for the installation of the skid.

BOOM-FIN CONCEPTS

General

In this report, a design concept is defined as a single combination of:

1. structural configuration
2. fabrication process

The boom-fin concepts presented herein differ in structural configuration rather than in fabrication process. The configurations for the boom include four external contours and two internal arrangements. Each variation seeks to achieve greater structural efficiency through improved geometrical effectiveness. For all contours, a side silhouette view of the boom-fin would be unchanged. A plan view, however, would show less taper in the boom for contours 2, 3, and 4. The greatest difference would be seen at B.S. 194. Aft of this station all contours fair in gradually to produce a conventional, streamlined boat tail. Figure 2 shows cross sections at B.S. 194 for each contour.

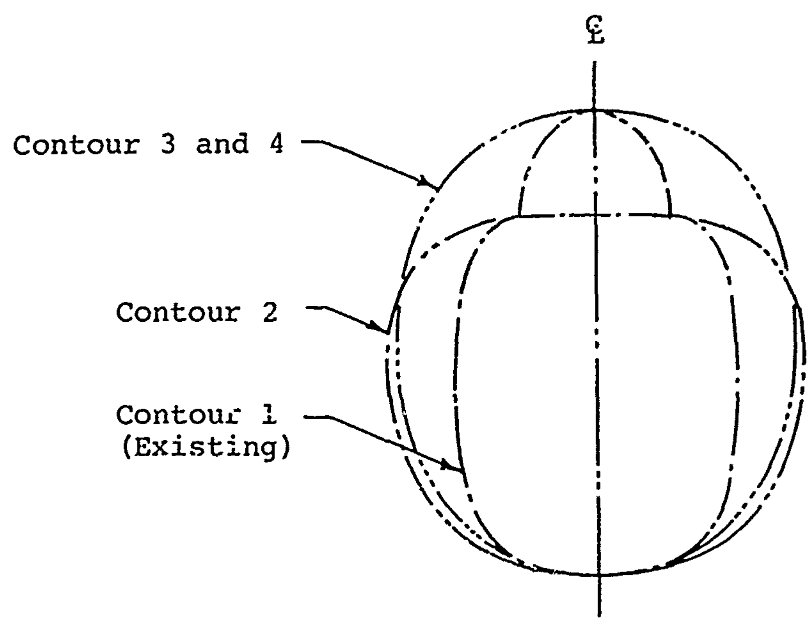

Figure 2. Contours at B.S. 194.

Only one fabrication process is used for all boom-fin concepts because no other process was found to compete with it on a cost-plus-quality basis. Essentially, it is a method for a large single-phase bondment. Details of the fabrication plan are described in the discussions for boom-fin concept 1.

It is noted that the definition of a design concept excludes the materials of construction. Thus, it would be possible to consider a single design concept executed in several alternative materials and to make comparative cost evaluations. The scope of this study, however, did not permit such evaluations to be made. Instead, only one combination of materials is shown for each concept. These combinations do provide the required strength and stiffness characteristics. In general, the prime material candidate for all concepts is glass-filament reinforced epoxy. Glass deserves first consideration because of its low cost, high strength, ease of fabrication, and ease of lightning protection. However, graphite and PRD-49 are used for boom-fin concept 1 to achieve the required stiffness and low weight using the existing contour. Details of the type and placement of materials are presented in the discussion which follows for each concept.

Table I summarizes the basic characteristics of the four new concepts and the existing structure which is numbered 0.

TABLE 1. BOOM-FIN CONCEPTS, BASIC CHARACTERISTICS

No.	Position of Drive Shaft	Contour	Type	Principal Material
0	External	Existing	Stiffened Sheet	Aluminum
1	External	Existing	Sandwich	PRD-49, Graphite
2	External	New No. 2	Sandwich	S Glass
3	Internal	New No. 3	Sandwich	S Glass
4	Internal	New No. 4*	Corrugated	S Glass

*The outer envelope of the corrugations is coincident with Contour 3.

Boom-Fin 1

Figure 3 shows the structural configuration for boom-fin concepts 1 and 2. The principal element is a thin sandwich shell that forms the boom and gradually changes shape to become the fin. Several internal frames, bulkheads, and a rib distribute concentrated loads to the shell and also contribute to its stability. When completed by the attachment of the fin

spars and the support panel for the 42° gearbox, the shell itself becomes a single cell tube that supports all moments, shears, and torques without the aid of stringers or longerons. The tail rotor drive shaft and gearboxes, not shown in Figure 3, are located on top of the shell and are enclosed by covers shown in phantom in Figure 3.

An important feature of the concept is its fabrication using a method developed prior to the present study by Mr. Frank Clark at Kaman Aerospace. The method produces with only one cure cycle a finished high-quality shell at low cost using low-cost tooling. Raw materials are placed in a female mold; a finished product emerges. The finished shell is a sandwich with filament reinforcement and a foam core of PVC. The use of a heat-formable foam is a source of large savings of cost. The core can be purchased in flat sheets and then preformed to any shape after preheating it to 220° F for 10 minutes. The core also accommodates itself to steps in the thickness of facings by yielding at the cure temperature. Upon cooling, the mechanical strength of the core returns. Through such procedures, the expensive steps of carving of cores and pre-curing of facings can be eliminated.

Tooling appropriate for the AH-1G boom-fin is shown in Figure 4. The following bond sequence can be used:

1. Preform foam core segments.
2. Position preimpregnated composites for the outer face into the left-hand and right-hand female molds.
3. Position inserts such as attachment angles and local facing reinforcements.
4. Position the four fittings at B.S. 41.3.
5. Position the PVC core and local core reinforcements.
6. Position preimpregnated composites for the inner face into the left-hand and right-hand female molds.
7. Position attachment angles for frames.
8. Place inner mandrel into right-hand mold.
9. Rotate right-hand mold and inner mandrel to place them into left-hand mold.
10. Position splices and splice inserts.

A

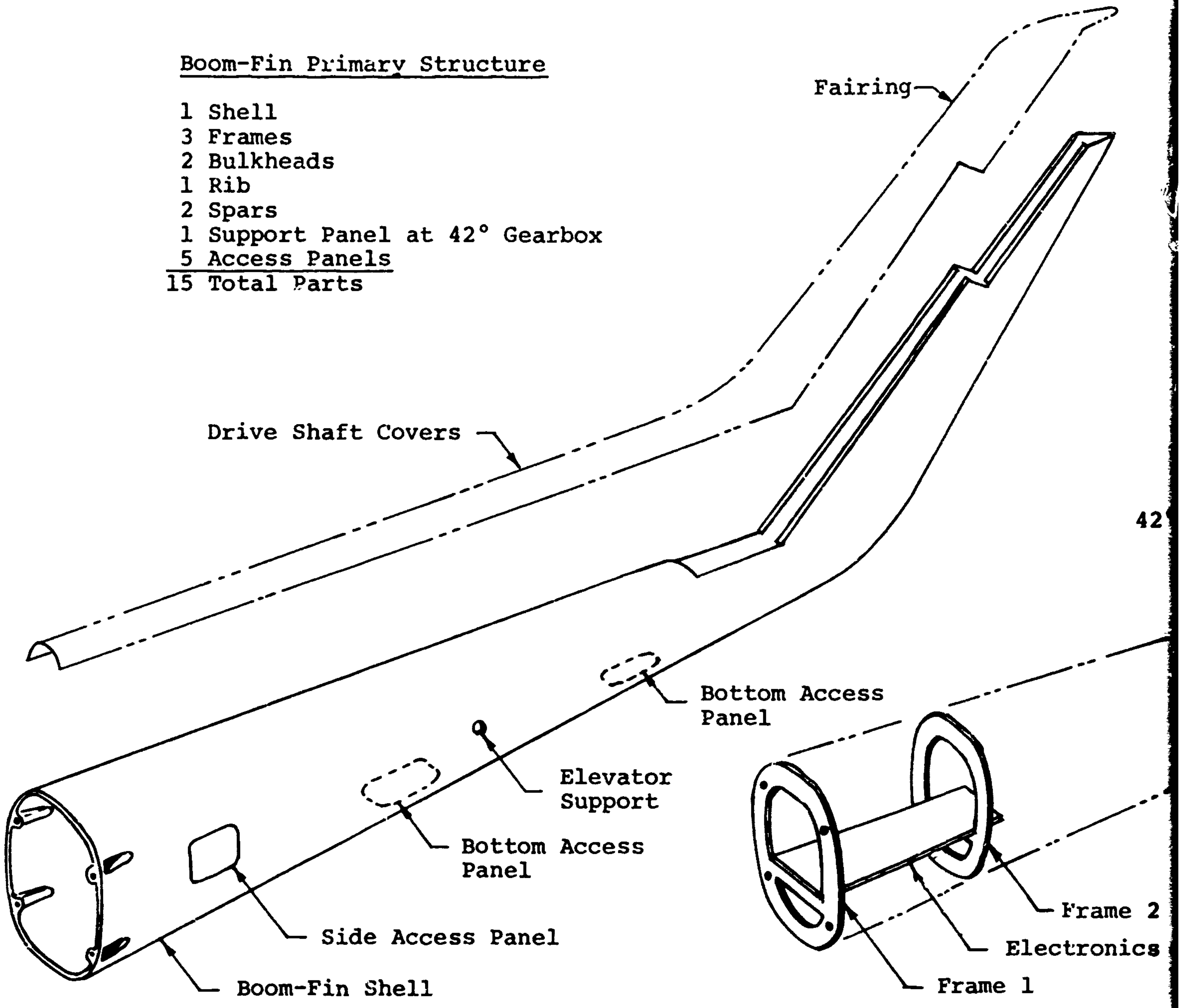

Figure 3. Structural Configurations for Boom-Fin Concepts 1 and 2.

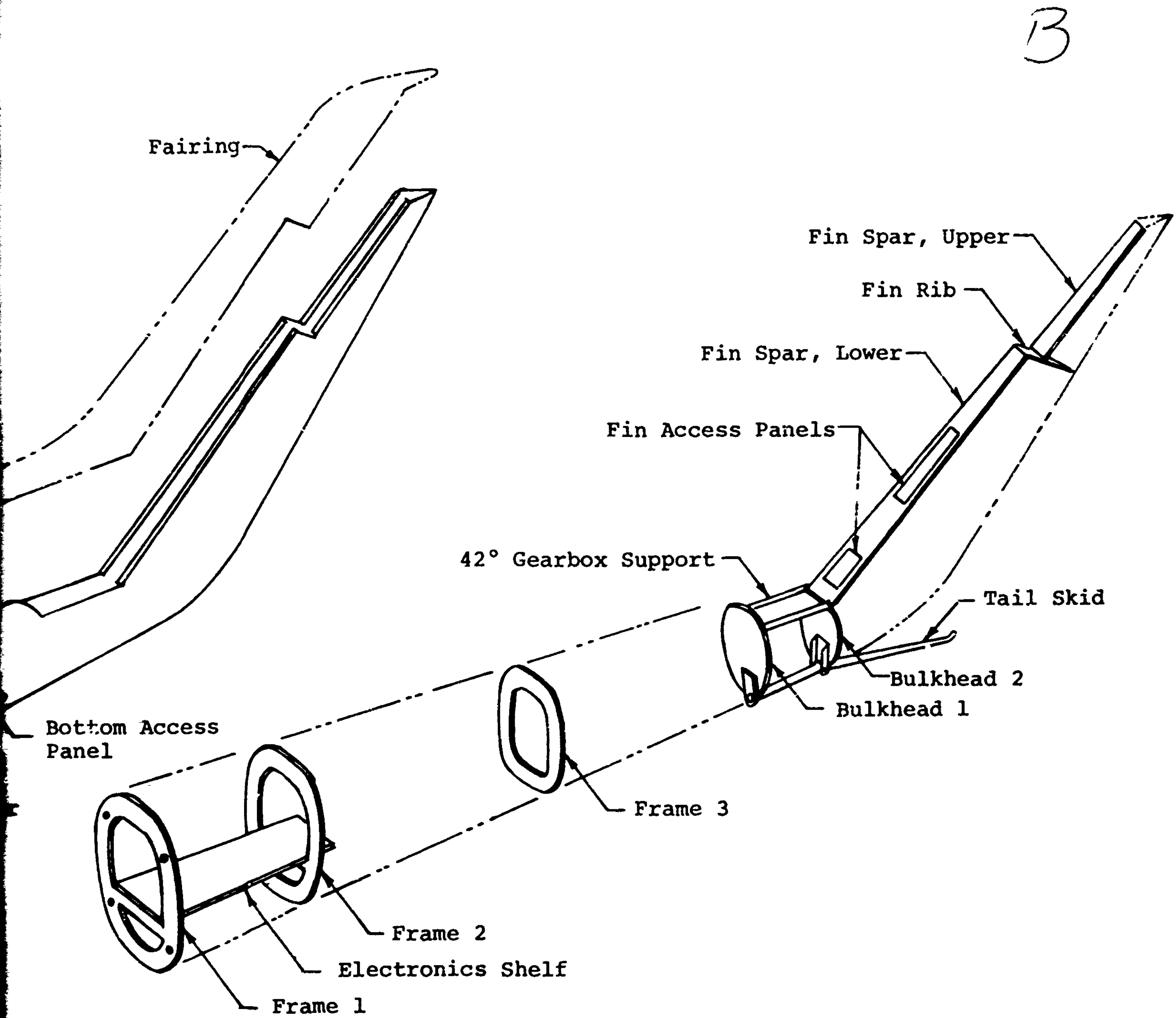

B
Fairing
Fin Spar, Upper
Fin Rib
Fin Spar, Lower
Fin Access Panels
42° Gearbox Support
Tail Skid
Bulkhead 2
Bulkhead 1
Bottom Access Panel
Frame 3
Frame 2
Electronics Shelf
Frame 1

for

A

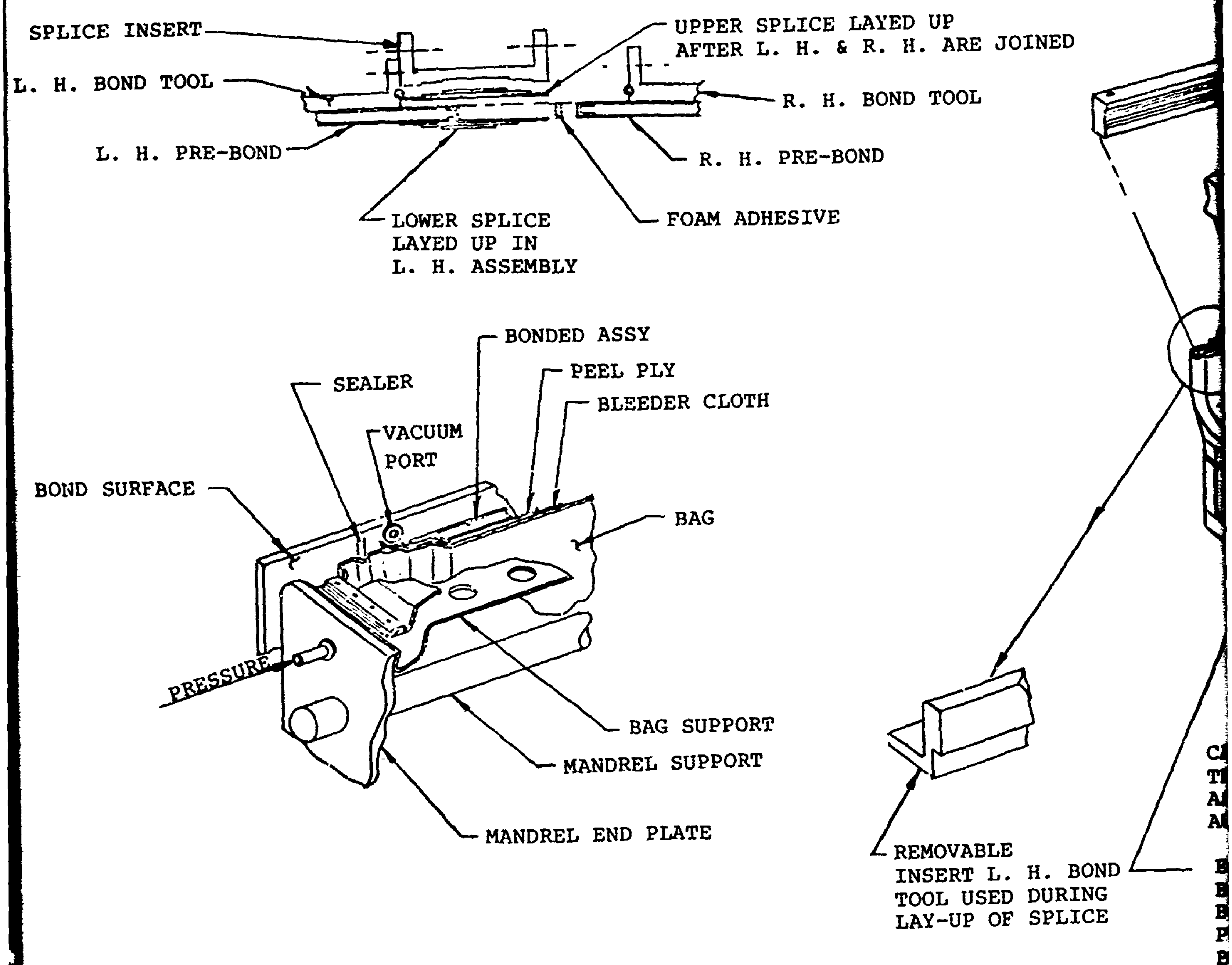

Figure 4. Bond Tooling for Boom-Fin.

Preceding page blank

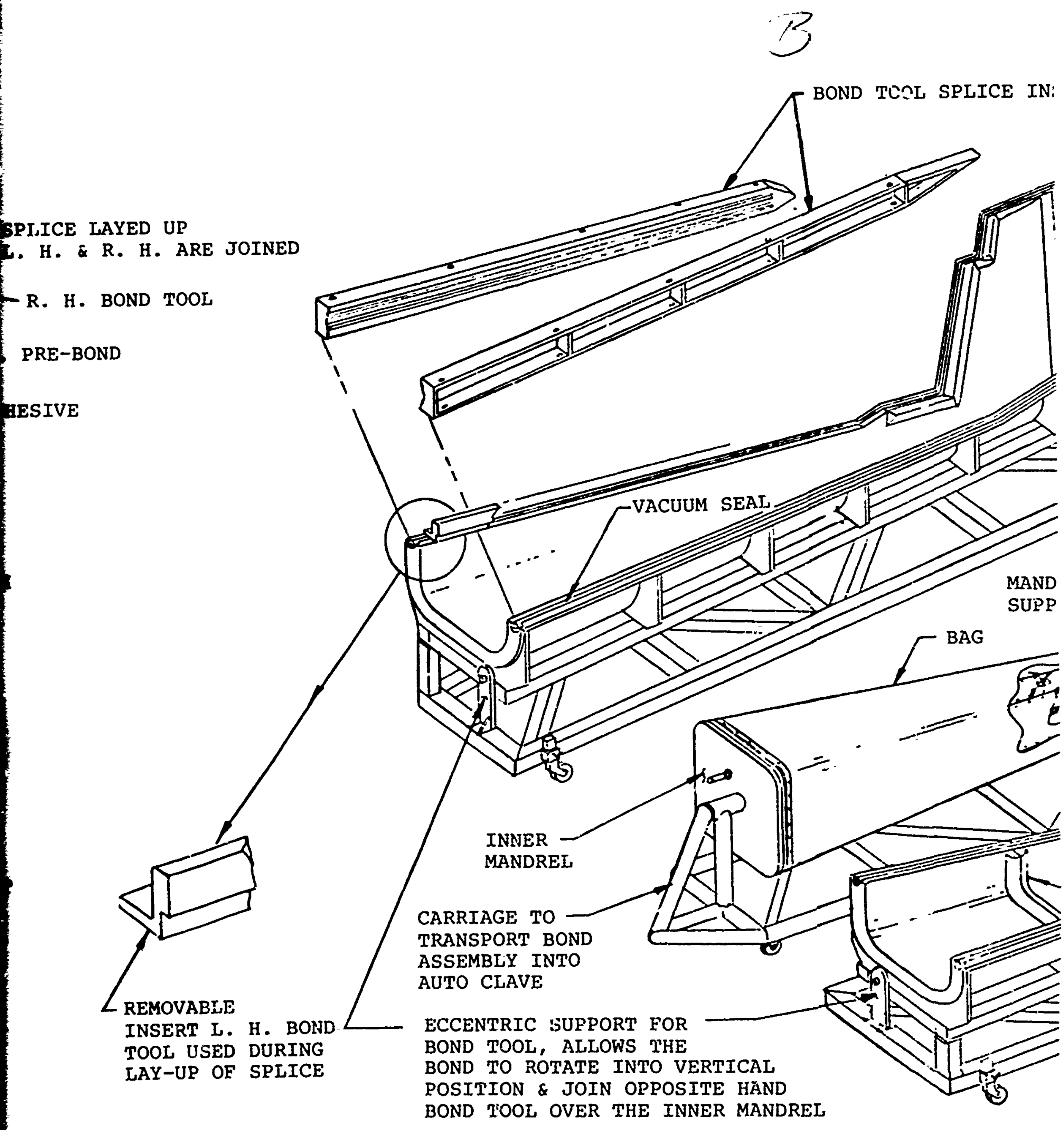

B
BOND TOOL SPLICE IN:
SPLICE LAYED UP
L. H. & R. H. ARE JOINED
R. H. BOND TOOL
PRE-BOND
HESIVE
VACUUM SEAL
MAND
SUPP
BAG
INNER
MANDREL
CARRIAGE TO
TRANSPORT BOND
ASSEMBLY INTO
AUTO CLAVE
REMOVABLE
INSERT L. H. BOND
TOOL USED DURING
LAY-UP OF SPLICE
ECCENTRIC SUPPORT FOR
BOND TOOL, ALLOWS THE
BOND TO ROTATE INTO VERTICAL
POSITION & JOIN OPPOSITE HAND
BOND TOOL OVER THE INNER MANDREL

C

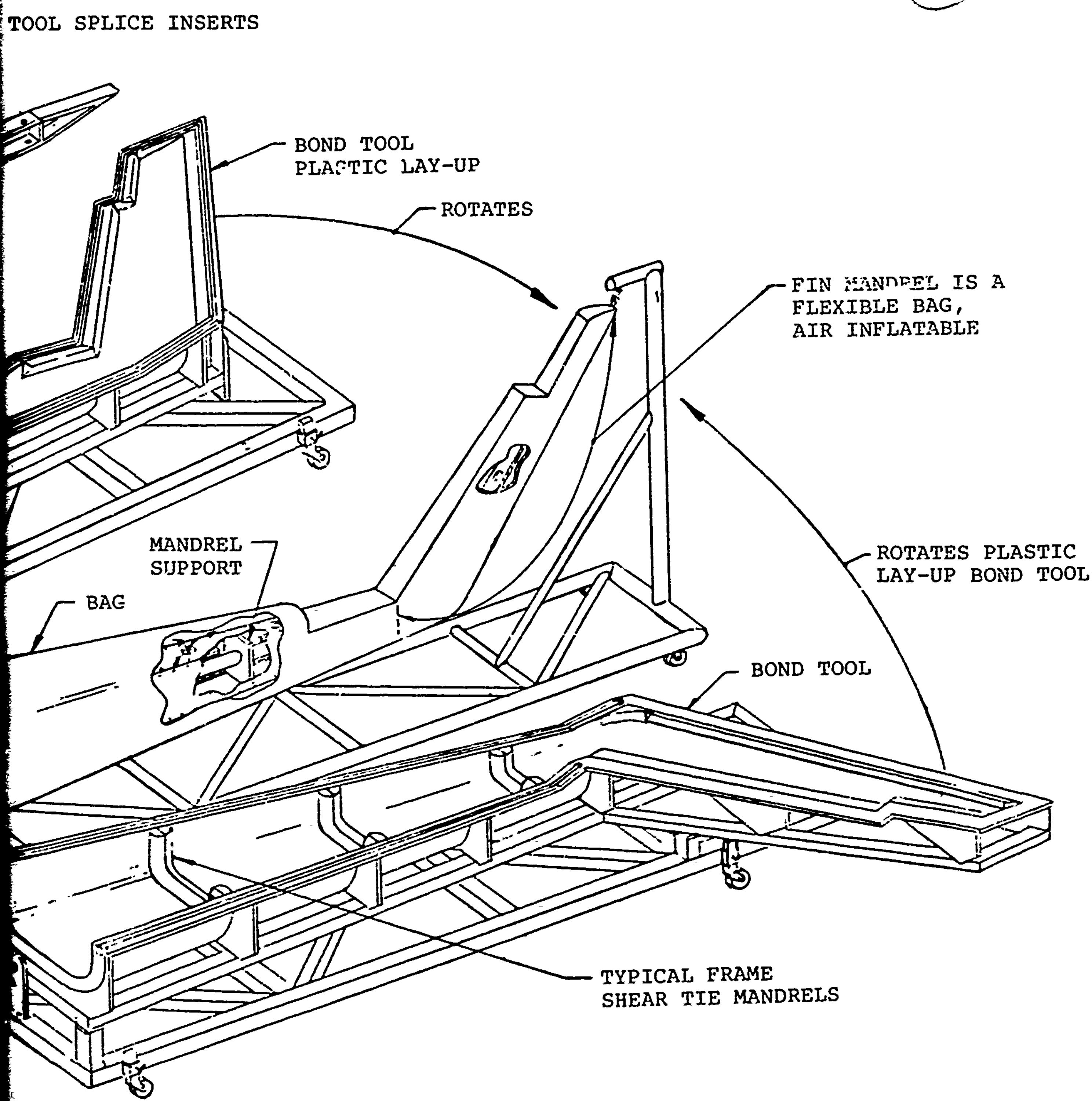
TOOL SPLICE INSERTS
BOND TOOL
PLASTIC LAY-UP
ROTATES
FIN MANDREL IS A
FLEXIBLE BAG,
AIR INFLATABLE
MANDREL
SUPPORT
BAG
ROTATES PLASTIC
LAY-UP BOND TOOL
BOND TOOL
TYPICAL FRAME
SHEAR TIE MANDRELS

11. Seal and pressure test.

12. Cure in autoclave.

Figure 5 shows a cross section through the boom and indicates construction typical throughout the length of the boom. Each face of the sandwich is a balanced laminate. The inner and outer surfaces of each face are woven plies of PRD-49 style cloth oriented at 45° to the boom axis. Between the plies of PRD-49, uniaxial graphite is located at 0° to the axis of the boom. Typically, the core is PVC R-400 rigid foam .25 inch thick.

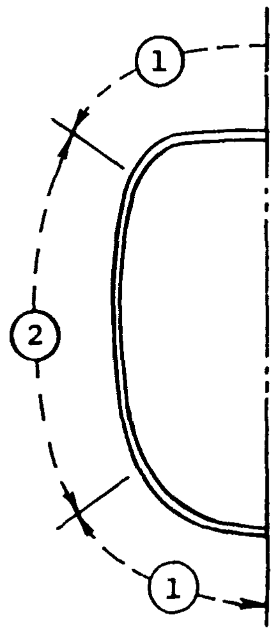

Symbols are defined on page xiv. Orientation is in degrees from boom axis.

Face	Region	Material	Style	Angle (deg)	T	Σ T
Outer	1	D/G/D	181/U/181	45/0/45	.011/.0065/.011	.0285
	2	D/G/D	181/U/181	45/0/45	.011/.0130/.011	.0350
Inner	1	D/G/D	181/U/181	45/0/45	.011/.0065/.011	.0285
	2	D/G/D	181/U/181	45/0/45	.011/.0130/.011	.0350

Figure 5. Materials for Boom in Boom-Fin Concept 1.

Preceding page blank

Such construction provides a structure with the following characteristics:

1. High survivability. The structure is highly redundant because its primary load paths are distributed nearly uniformly around its perimeter. A single bullet cannot cause disproportionate damage by striking a concentrated longeron. Typical damage from a ballistic strike will be quite local. Figure 6 shows a test panel that received a broadside hit from a .30-06 rifle bullet at approximately 20 feet. The bullet was tumbled by six .25-inch plywood baffles. The test specimen is a flat sandwich with two-ply, E glass style 181 facings on a PVC R-400 rigid foam core .25 inch thick.

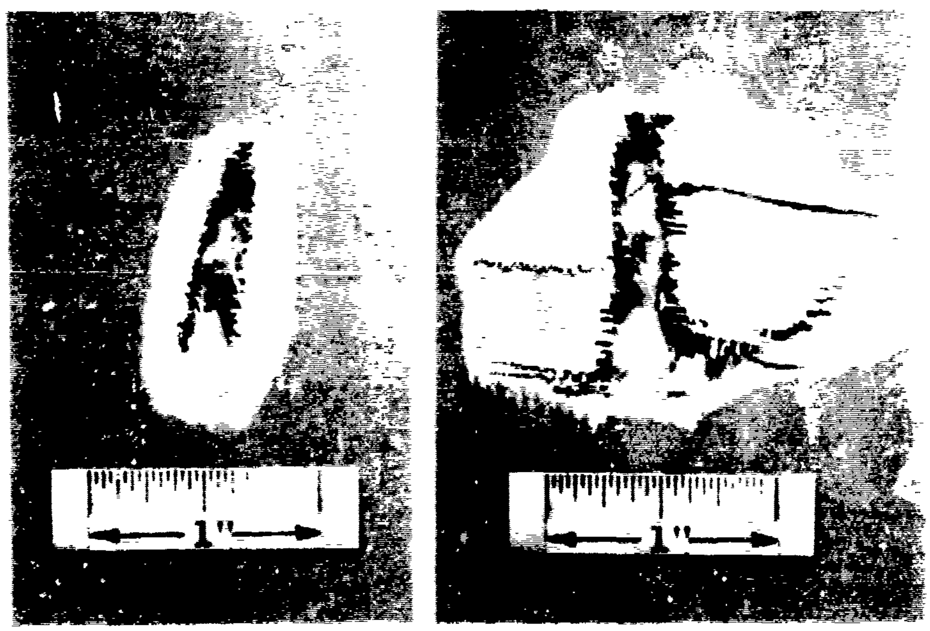

Entrance Exit

Figure 6. Typical Damage From a Tumbled .30-06 Rifle Bullet.

2. Good repairability. Again as a consequence of the nearly uniform distribution of load paths, the load intensity per running inch of perimeter is very low. For example, at limit load, at the most critical location, the highest direct load, n_x, in each face is less than 600 pounds per inch. Repair in such a low stress field is easily accomplished by simple lap joints.

3. Good low-velocity impact resistance. The poor low-velocity impact toughness of graphite is overcome by the extensive mix with PRD-49, which has very good impact properties. The faces are by volume more than two-thirds PRD-49.

4. Low weight. Stiffness requirements are a very significant factor in the design of the boom. The use of graphite provides the required stiffness with low weight.

The attachment of the boom to the forward fuselage is a critical area for strength, alignment, and maintainability. This attachment is accomplished with four aluminum fittings that are bonded into the shell and actually become a portion of the shell that is partially wrapped around the line of action of the bolt. Figure 7 shows an isolated view of a typical fitting. Figure 8 shows the final relationships between the boom, fitting, and frame at B.S. 41.3. Forged aluminum fittings are used to provide adequate strength. The fittings are subject to multiaxial stresses and require the interlaminate shear capabilities of a metal for efficient design. Precise alignment and mating to the forward fuselage is assured by final machining and drilling of the contact faces after final cure and assembly of the interior structure. Good maintainability is assured by the fact that the bolt nuts are directly accessible and visible from the exterior of the boom.

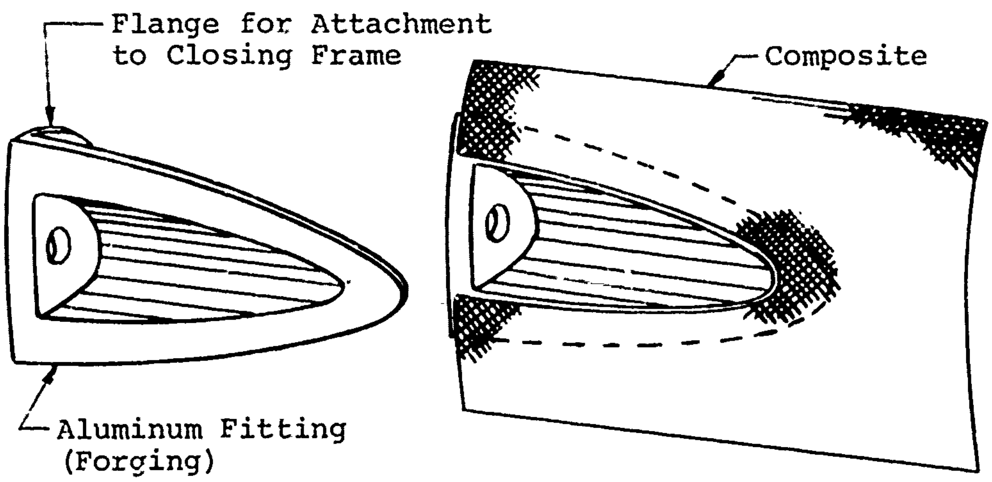

Figure 7. Fitting at B.S. 41.30.

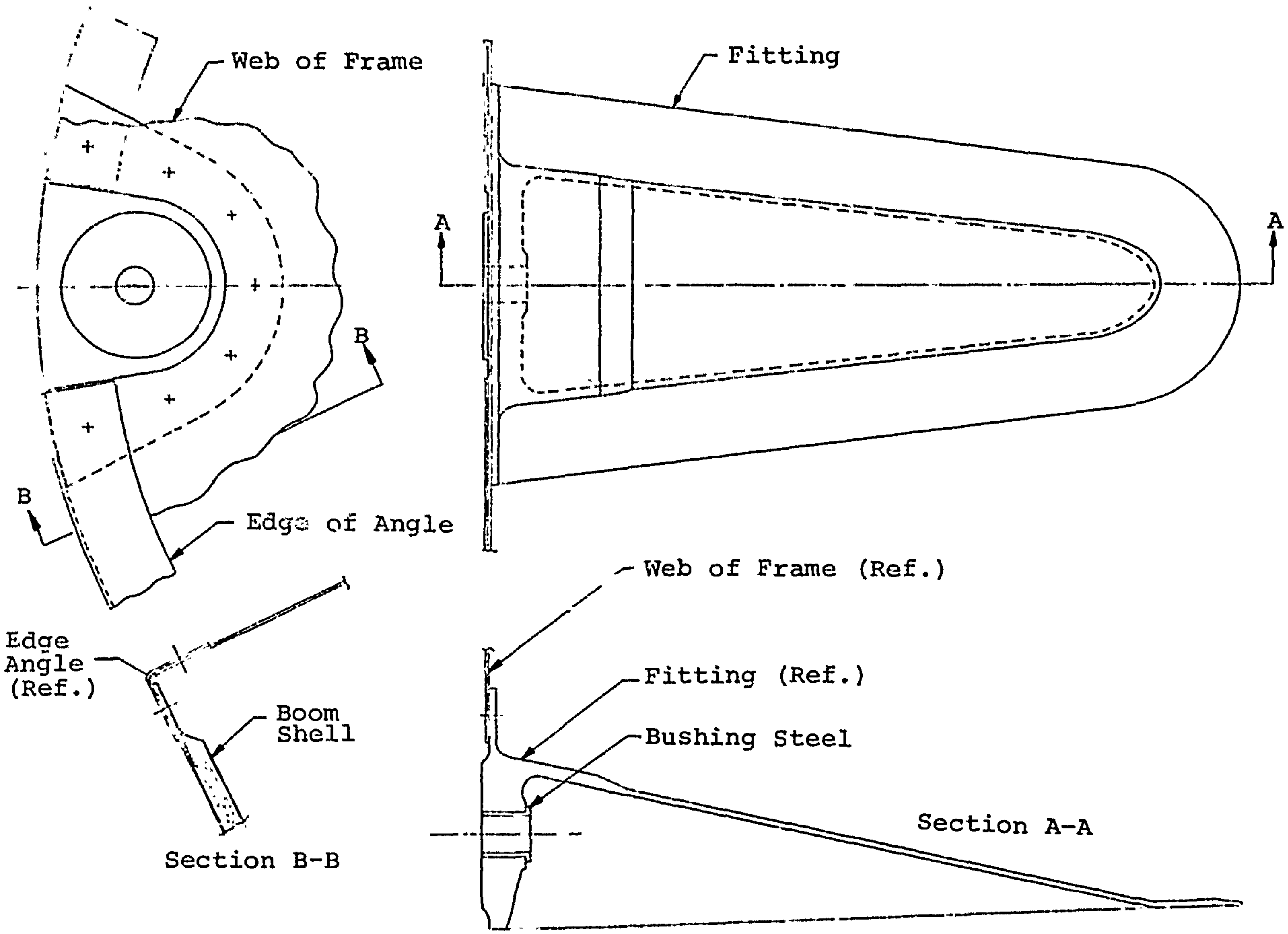

Figure 8. Assembly at B.S. 41.30.

The fitting concept shown in Figure 7 provides several advantages. These include:

1. The elimination of mechanical fasteners. The aluminum fitting is bonded to the composite material to make a preassembly for insertion into the female mold for the boom fin.

2. The opportunity to use higher pressure for the bond between the fitting and the composite.

3. The opportunity to inspect critically the fitting assembly before its use in the boom-fin bondment.

4. The opportunity to retain bolt preload with a high degree of reliability. Bolt loosening is unlikely because little wear is possible in the stackup of clamped parts due to broad areas of contact and because a conventional nut with a large nylon self-locking ring is specified for one-time usage.

5. The opportunity for easy in ection in the field. A torque stripe painted be en the nut and the fitting allows easy detection of rotation of the nut and possible loosening of the connection.

6. Low weight, low cost, and simplicity.

Figure 8 also shows the attachment of the frame at B.S. 41.30. The frame is riveted directly to the flange on the fitting and indirectly to the shell through four angles. The use of mechanical fasteners in this area is very desirable because they are highly loaded and a high-quality secondary bond would be difficult to achieve. The frame also serves as a terminal board for electrical connectors and a support for the forward end of the electronics shelf. The electronics shelf itself is a simple sandwich supported by and attached to the frames by only four bolts. The shelf is restrained in the fore-and-aft direction by two angle struts that connect it to the shell at B.S. 41.3.

Figure 9 shows a cross section through the fin and details for the attachment of the front cover, the spar and access panels. When the front cover is opened, the drive shaft and the control cables are exposed. Two large, removable panels in the spar provide access to the interior of the fin. These panels facilitate repair of extensive ballistics damage to the fin and also permit periodic inspections of the interior facings. Figure 10 indicates the materials of construction for the fin.

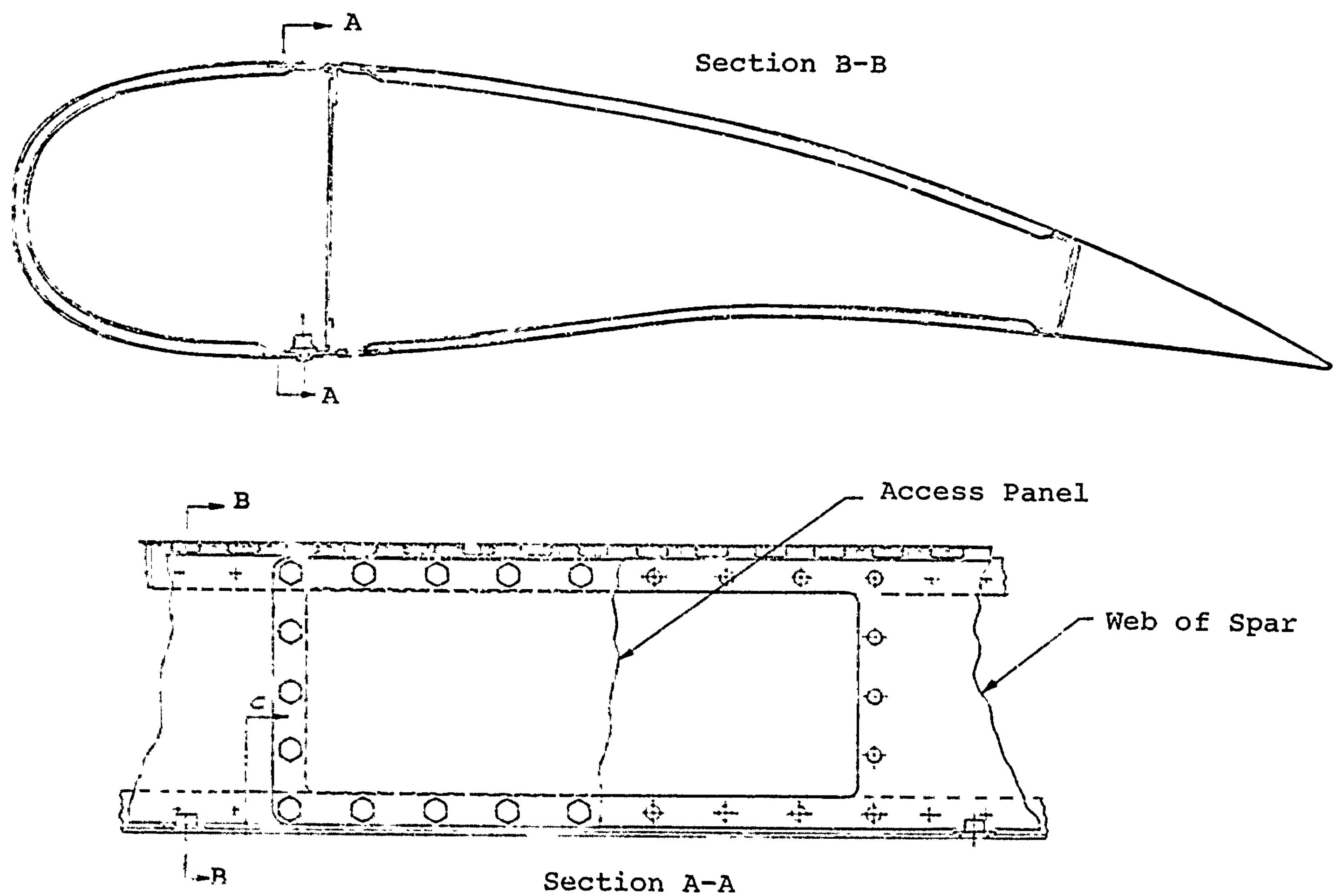

Figure 9. Fin Sections.

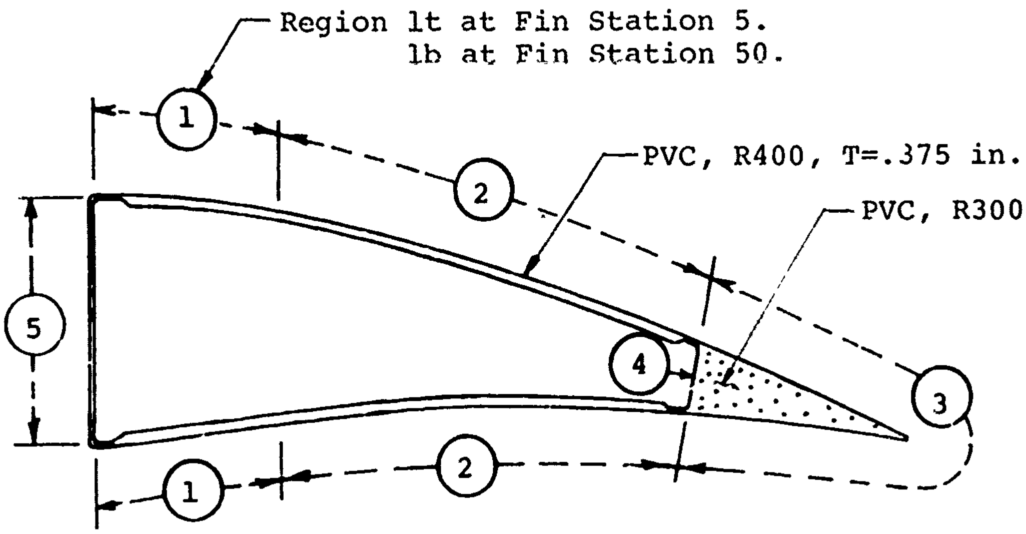

Symbols are defined on page xiv.
Orientation is in degrees from boom axis.

Face	Region	Material	Style	Angle (deg)	T	ΣT
Outer	1t	$(D/D)_S$	$(181/181)_S$	$(0/45)_S$	$(.011/.011)_S$	.044
	1b	$(D/D/G)_S$	$(181/181/U)_S$	$(0/45/0)_S$	$(.011/.011/.026)_S$	.096
	2	D/D	181/181	0/45	.011/.011	.022
	3	E/E	181/181	0/45	.009/.009	.018
	4	$(E/E)_S$	$(181/181)_S$	$(0/45)_S$	$(.009/.009)_S$	.036
	5	Aluminum			.050	.050
Inner	1t	$(D/D)_S$	$(181/181)_S$	$(0/45)_S$	$(.011/.011)_S$	.044
	1b	$(D/D/G)_S$	$(181/181/U)_S$	$(0/45/0)_S$	$(.011/.011/.013)_S$	.070
	2	D/D	181/181	0/45	.011/.011	.022

Figure 10. Materials for Fin in Boom-Fin Concept 1.

Boom-Fin 2

Boom-Fin 2 differs from boom-fin 1 only in contour and materials. The new contour has already been described and shown in Figure 2. It is considerably more efficient. For example, at B.S. 194, an equal weight of material uniformly distributed on contour 2 produces a 38% increase in torsional stiffness and a 76% increase in lateral bending stiffness over that for contour 1. The improvement is less at all other stations, and zero at B.S. 41.30 where the contours 1 and 2 are identical. The stability is also improved by the increased curvature of the shell. The improved efficiency of contour 2 permits an all-glass boom-fin having the stiffness of existing metal structure with less weight. Figure 11 shows the construction that is typical throughout the length of the boom. Figure 12 shows the materials for the fin.

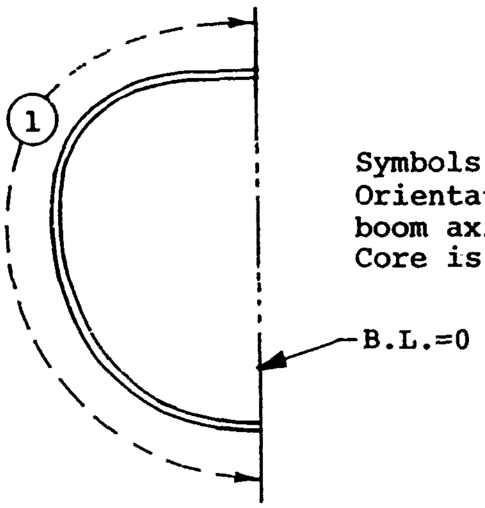

Symbols are defined on page xiv.
Orientation is in degrees from boom axis
Core is PVC R400, T=.25 inch.

Face	Region	Material	Style	Angle (deg)	T	ΣT
Outer	1	S/S/S	913/U/913	45/0/45	.010/.030/.010	.050
Inner	1	S/S/S	913/U/913	45/0/45	.010/.010/.010	.030

Figure 11. Materials for Boom in Boom-Fin Concept 2.

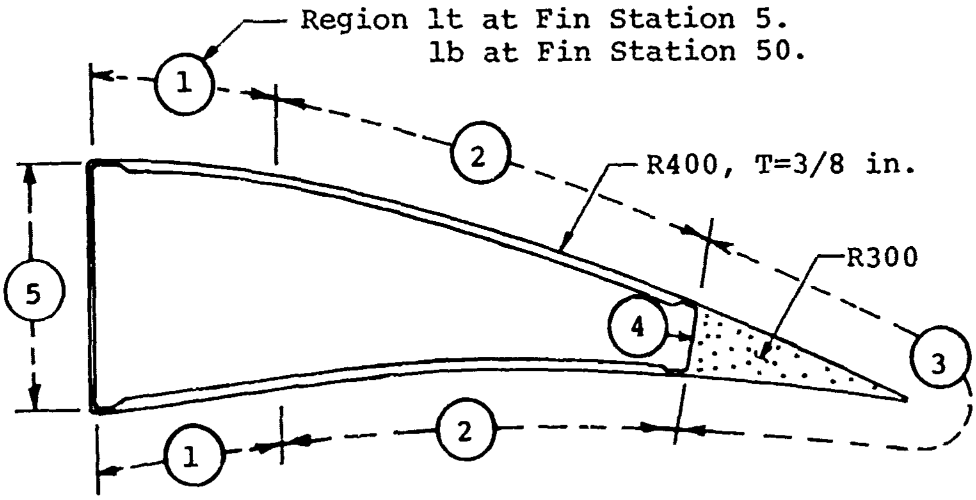

Symbols are defined on page xiv.
Orientation is in degrees from boom axis

Face	Region	Material	Style	Angle (deg)	T	ΣT
Outer	1t	$(S/S)_S$	$(913/913)_S$	$(0/45)_S$	$(.010/.010)_S$	.040
	1b	$(S/S/S)_S$	$(913/913/U)_S$	$(0/45/0)_S$	$(.010/.010/.040)_S$	.120
	2	S/S	913/913	0/45	.010/.010	.020
	3	E/E	181/181	0/45	.009/.009	.018
	4	$(E/E)_S$	$(181/181)_S$	$(0/45)_S$	$(.009/.009)_S$	.036
	5	Aluminum				
Inner	1t	$(S/S)_S$	$(913/913)_S$	$(0/45)_S$	$(.010/.010)_S$	.040
	1b	$(S/S/S)_S$	$(913/913/U)_S$	$(0/45/0)_S$	$(.010/.010/.020)_S$	.080
	2	S/S	913/913	0/45	.010/.010	.020

Figure 12. Materials for Fin in Boom-Fin Concepts 2, 3 and 4.

Boom-Fin 3

Figure 13 shows the structural configuration for boom-fin concepts 3 and 4. In these concepts, the fin is identical to that for concept 2. The boom, however, is changed appreciably. The boom is fabricated as an open shell with a 12-inch-wide gap at its top, running along its entire length. This gap is closed by a system of removable structural panels. The drive shaft is located within the contour of the boom. The bearings for the drive shaft are supported directly by the two intermediate frames. Hinged doors are provided at these locations for access to the drive shaft bearings and couplings for daily inspections. The control system can also be inspected through these doors. Figure 14 shows additional details for the covers.

Favorable characteristics of concept 3 include:

1. Low weight. Concept 3 uses the entire available envelope with corresponding increase in structural efficiency. At B.S. 194, an equal weight of material, uniformly distributed on contour 3, increases torsional, vertical, and lateral stiffnesses by 68%, 50%, and 71%, respectively,over that for contour 1.

2. Excellent access to the interior of the boom.

3. Elimination of secondary covers for drive shaft.

4. Elimination of two bottom access panels.

The principal disadvantage is the requirement for removal of structural panels to replace drive train components. Figure 15 shows typical construction throughout the length of the boom.

Boom-Fin 4

Boom-Fin 4 has the same structural layout as boom-fin 3. However, it uses single-walled construction over major portions of the boom. Stability is provided by longitudinal corrugations without the use of stringers or longerons. The corrugations are tapered both in depth and in width over the length of the boom. At the forward end, B.S. 41.30, the convolutions provide a natural transition to the attachment fittings. Sandwich construction is used at selected locations, such as the top covers, the edge of the opening for the covers, the areas around the side access panel, and the areas around the attachment of the elevators. Figure 16 shows construction at a typical section through the boom. The fin is identical to that described for boom-fin 2.

A

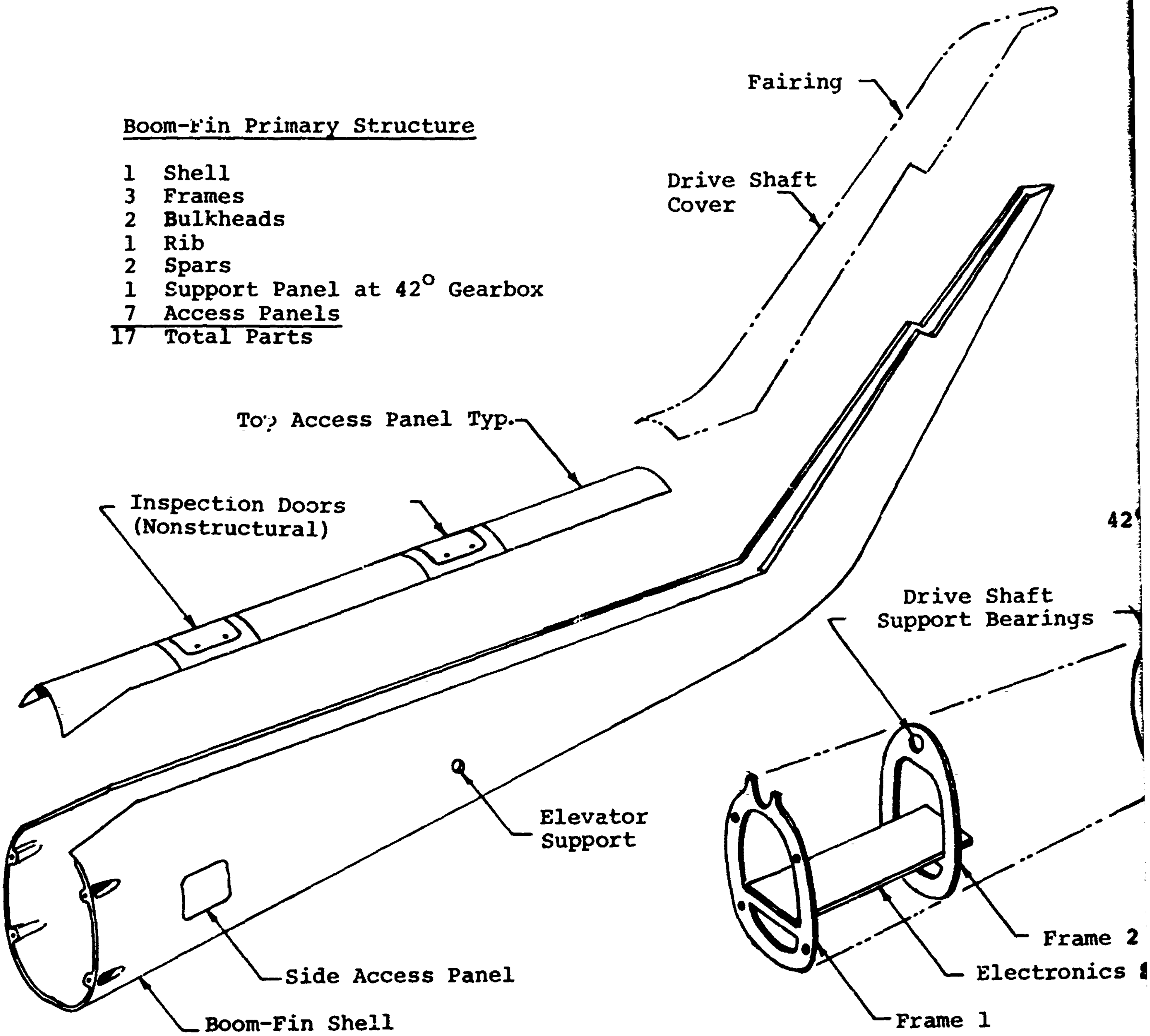

Figure 13. Structural Configurations for Boom-Fin Concepts 3 and 4.

B

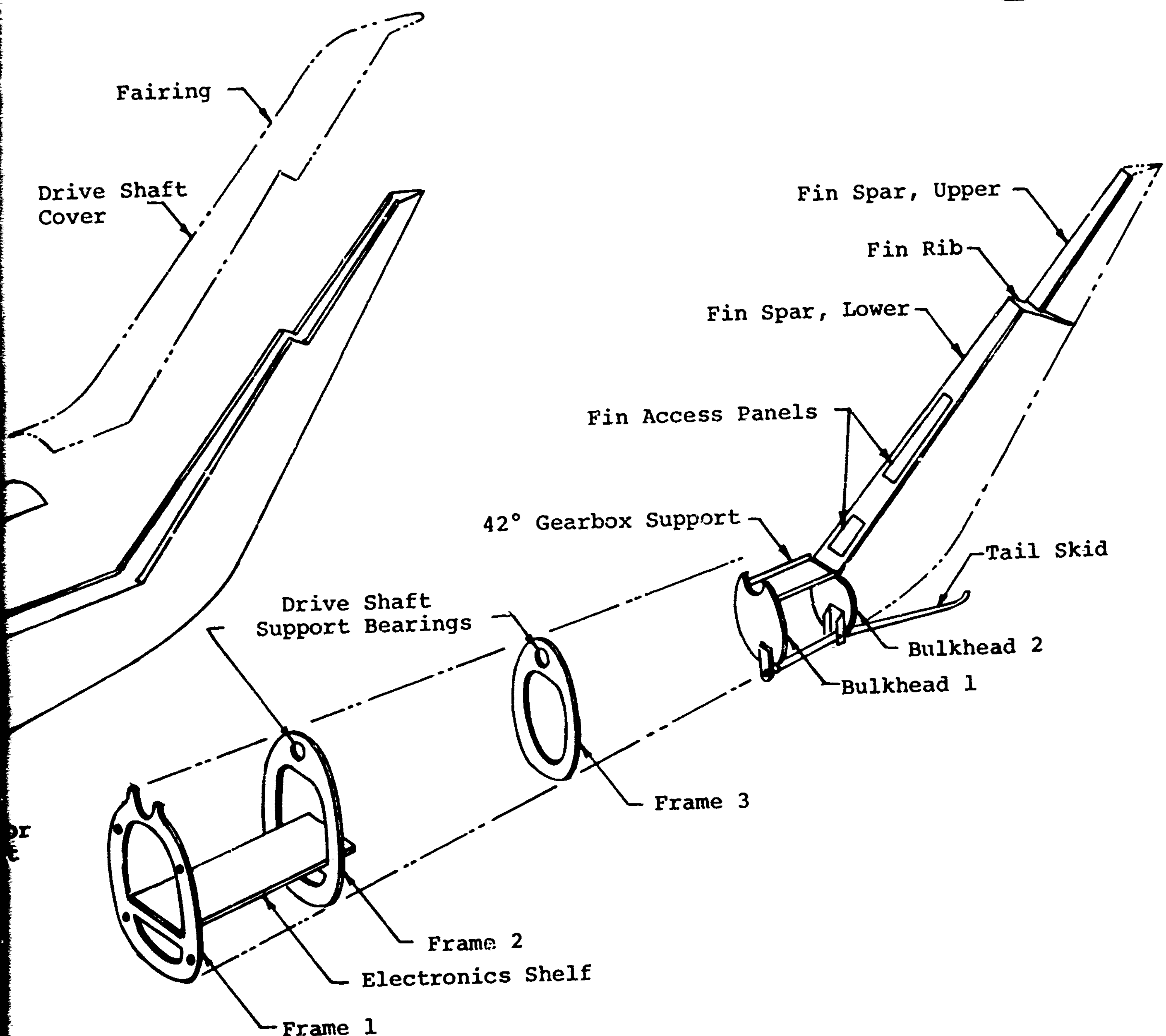
Fairing
Drive Shaft Cover
Fin Spar, Upper
Fin Rib
Fin Spar, Lower
Fin Access Panels
42° Gearbox Support
Tail Skid
Drive Shaft Support Bearings
Bulkhead 2
Bulkhead 1
Frame 3
Frame 2
Electronics Shelf
Frame 1

or
t

s for
4.

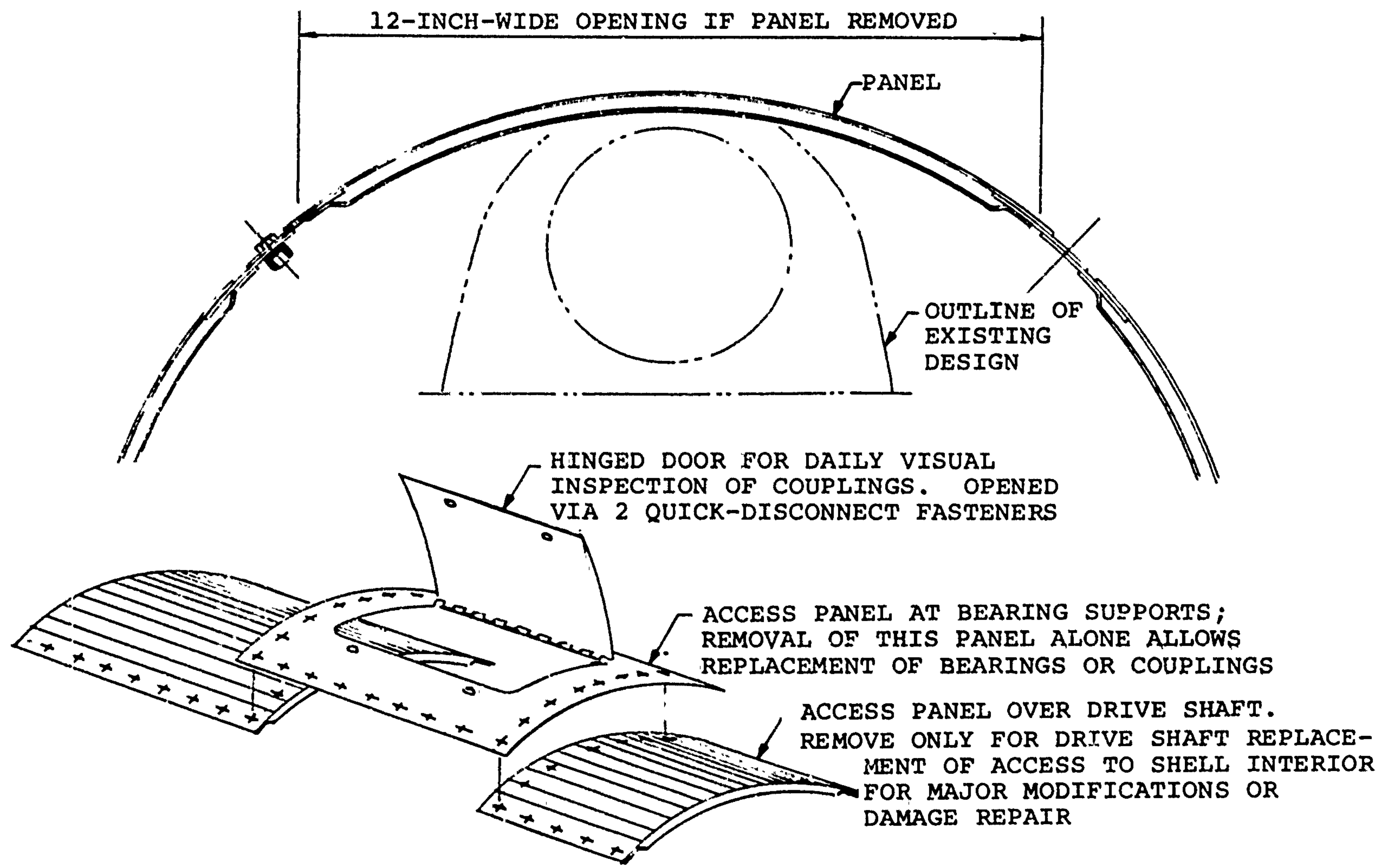

Figure 14. Access Panels for Boom-Fin Concepts 3 and 4.

Preceding page blank

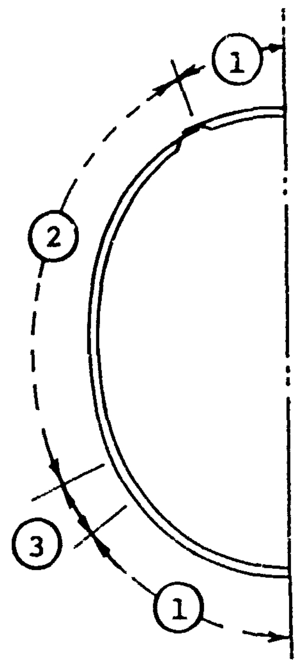

Symbols are defined on page xiv
Orientation is in degrees from boom axis.
Core is PVC R400, T=.25 inch.

Face	Region	Material	Style	Angle (deg)	T	ΣT
Outer	1	E/S/S	120/U/913	45/0/45	.004/.010/.010	.024
	2	E/S/S	120/U/913	45/0/45	.004/.030/.010	.044
	3	E/S/S	120/U/913	45/0/45	.004/.020/.010	.034
Inner	1	E/S/E	120/U/120	45/0/45	.004/.010/.004	.018
	2	E/S/E	120/U/120	45/0/45	.004/.030/.004	.038
	3	E/S/E	120/U/120	45/0/45	.004/.020/.004	.028

Figure 15. Materials for Boom in Boom-Fin Concept 3.

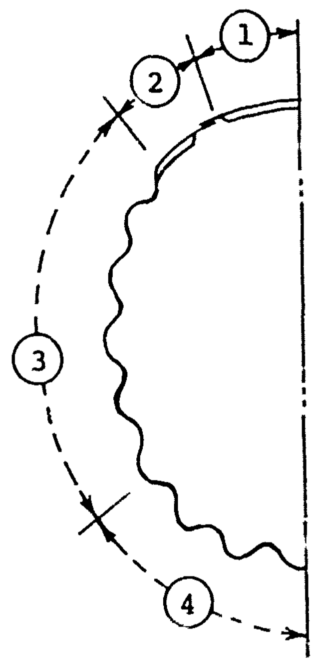

Symbols are defined on page xiv.
Orientation is in degrees from boom axis.
Core is PVC R400, T =.25 inch.

Face	Region	Material	Style	Angle (deg)	T	ΣT
Outer	1	E/S/S	120/U/913	45/0/45	.004/.010/.010	.024
	2	S/S/S	913/U/913	45/0/45	.010/.040/.010	.060
	3	S/S/S	913/U/913	45/0/45	.010/.050/.010	.070
	4	$(S/S/S)_S$	$(913/913/U)_S$	$(45/0/0)_S$	$(.010/.010/.005)_S$	.050
Inner	1	E/S/E	120/U/120	45/0/45	.004/.010/.004	.018
	2	S/S/S	913/U/913	45/0/45	.010/.010/.010	.030

Figure 16. Materials for Boom in Boom-Fin Concept 4.

ELEVATOR CONCEPTS

General

The four elevator concepts presented herein differ both in structural configuration and fabrication process. The sequential numbering of the concepts is also the historical order of their development, and it will be found that each concept evolves from its predecessor. The last is the simplest, and cost analysis also shows it to be clearly the best. Table II summarizes the characteristics of each concept.

TABLE II. ELEVATOR CONCEPTS, BASIC CHARACTERISTICS

No.	Bending Element	Facing Type	Principal Materials	
			Spar	Facings
0	Internal tubular spar	Stiffened sheet	Aluminum	Aluminum
1	Internal tubular spar	Shell & sandwich	Aluminum	E-Glass
2	Internal tubular spar	Shell & sandwich	Aluminum	E-Glass
3	External faces	Shell & sandwich	E-Glass	E-Glass
4	External faces	Sandwich	E-Glass	E-Glass

Elevator 1

Concept 1, shown in Figure 17, contains an aluminum tubular spar and attachment fittings similar to those in the existing structure. This spar tube is the main structural element that supports the bending moments and transfers them by socket action to a cross tube located in the boom. Two aluminum ribs, bonded to the tube, support the outer envelope, which consists of a leading-edge "C" and a trailing-edge arrow, both made from glass fabric. The leading edge is a symmetric laminate with a total thickness of six plies. The trailing-edge arrow is a sandwich with two-ply facings over a core of PVC R-300 rigid foam. The extreme trailing edge of the arrow also contains an aluminum strip 2 in. x .032 in. to provide resistance to handling impacts.

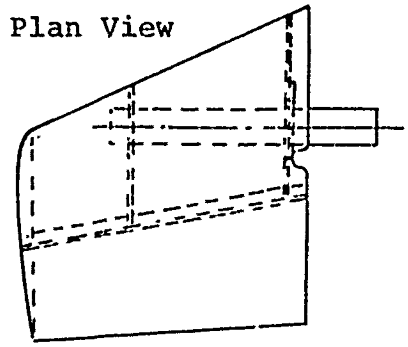

<u>Elevator Primary Structure</u>

1 Spar Tube
1 Attachment Fitting, Bonded to Tube
2 Ribs
1 Leading-Edge "C"
1 Trailing-Edge Arrow
1 Tip Cap
2 Clip Angles
9 Total Parts

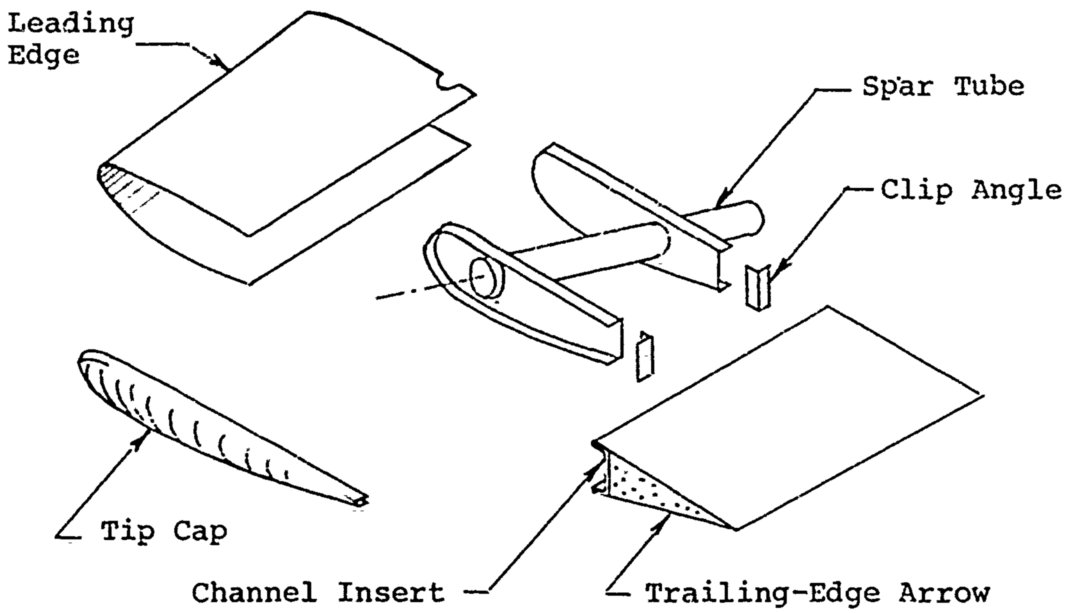

Figure 17. Structural Configuration for Elevator Concept 1.

The following lay-ups are used:

Item	Material	Style	Angle (deg)	ΣT
L. E. "C"	$(S/E/E)_S$	$(913/181/181)_S$	$(0/0/45)_S$	.06
T. E. Arrow	E/E	181/181	0/45	.02

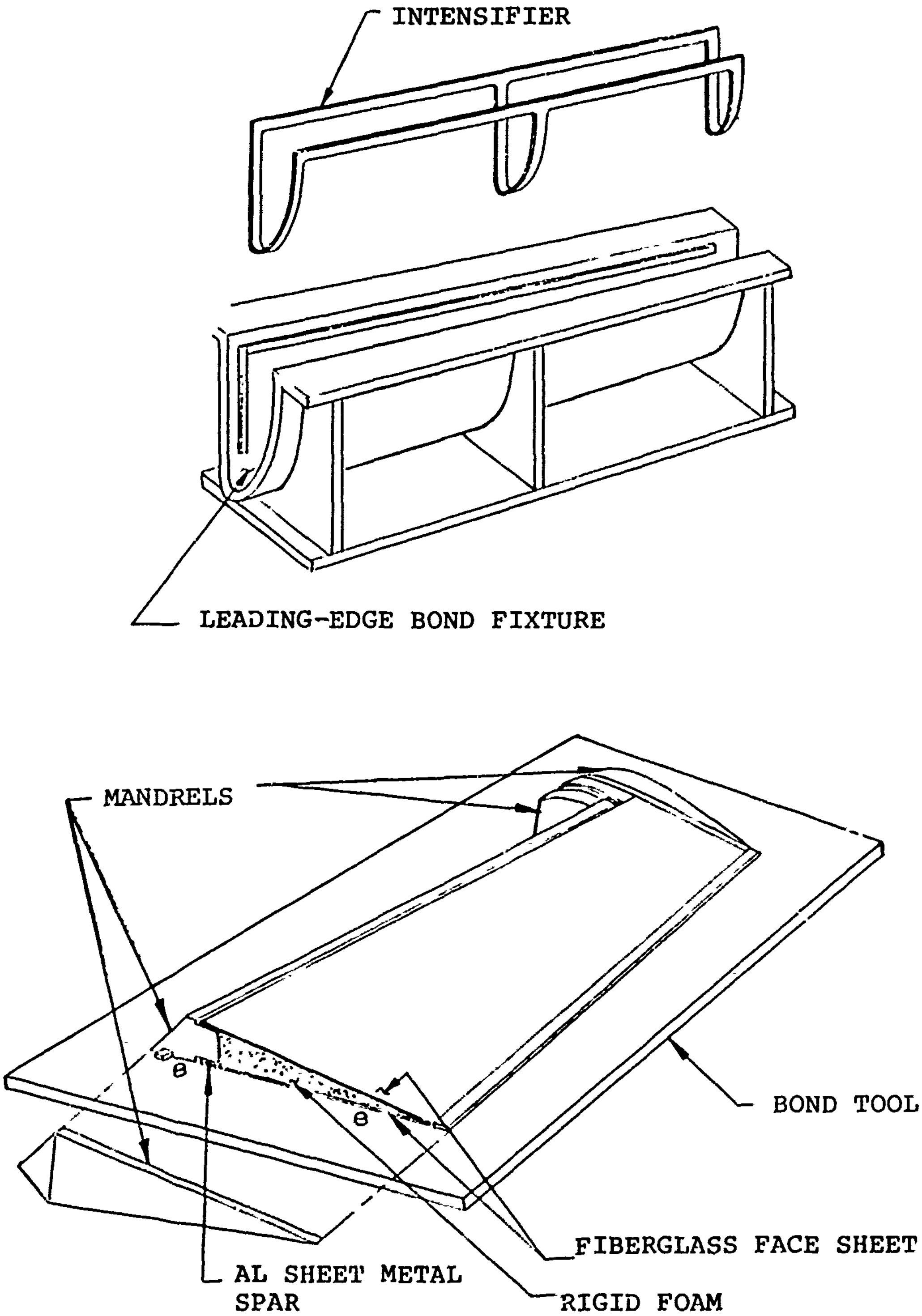

Figure 18. Bond Fixtures for Elevator Concept 1.

Elevator 2

Concept 2 is similar to concept 1 in layout and materials. It differs principally in that the outer envelope is made in a one-phase bondment as shown in Figures 19 and 20. This method produces a D-shaped leading edge of all-fiberglass construction.

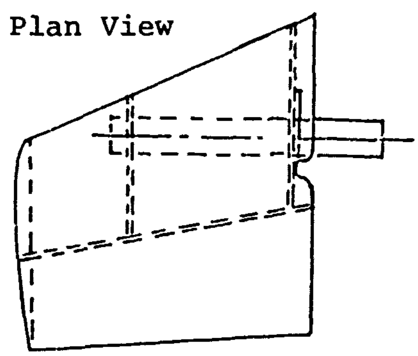

Elevator Primary Structure

1 Spar Tube
1 Attachment Fitting, Bonded to Tube
2 Ribs
1 Envelope
1 Tip Cap
2 Clip Angles
8 Total Parts

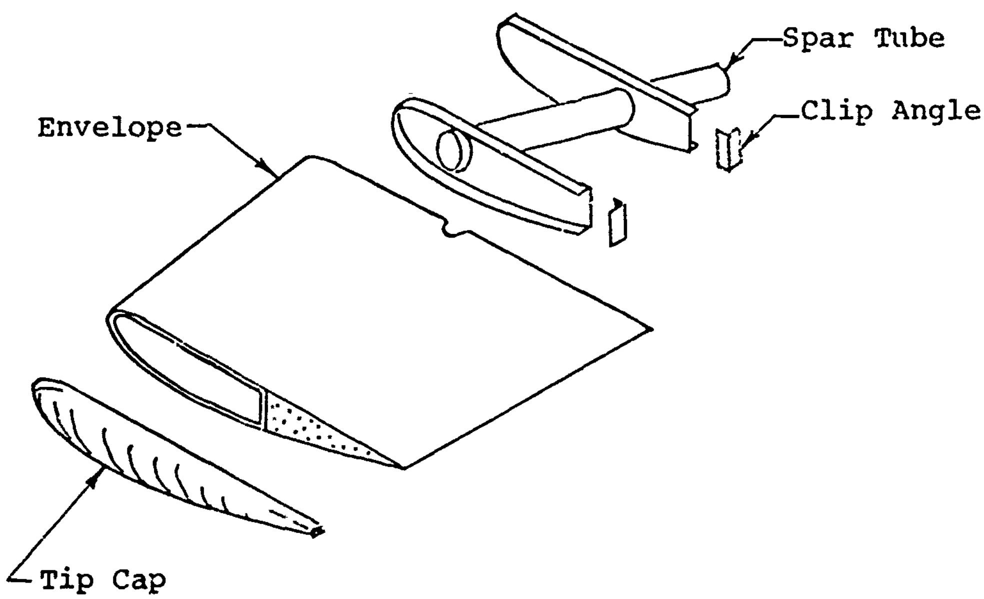

Figure 19. Structural Configuration for Elevator Concept 2.

Elevator 3

In concept 3, the aluminum tubular spar is eliminated. In its place a fiberglass spar is used. For most of its length, the spar has a channel shape. At its root end, however, it changes to become circular. A hard-coated, thin-walled, .06-inch aluminum tube is bonded over the spar to provide wear-resistant bearing surfaces for socket action with the cross-tube within the boom.

The outer envelope itself is the load path for bending moments. Figure 21 shows that the outer envelope and the tip cap are made as a single unit. The outer envelope is both bonded and riveted to the spar. The outer envelope can be divided into three general regions: the leading edge forward of the spar, the middle region aft of the spar, and a trailing-edge arrow. Lay-ups for these regions are listed below.

Region	Material	Style	Angle (deg)	ΣT
Fwd. of Spar	$(E_4)_S$	$(181_4)_S$	$(0/0/45/45)_S$	.08
Aft of Spar	$(E_4)_S$	$(181_2)_S$	$(0/45)_S$	.04
T. E. Arrow	E/E	181/181	0/45	.02

The envelope also contains plies of uniaxial E-Glass oriented sparwise at the location of the spar. On the average the uniaxial cap is .04" x 4.0". The trailing edge is a sandwich similar to that used in concepts 1 and 2, including the aluminum strip for handling impacts.

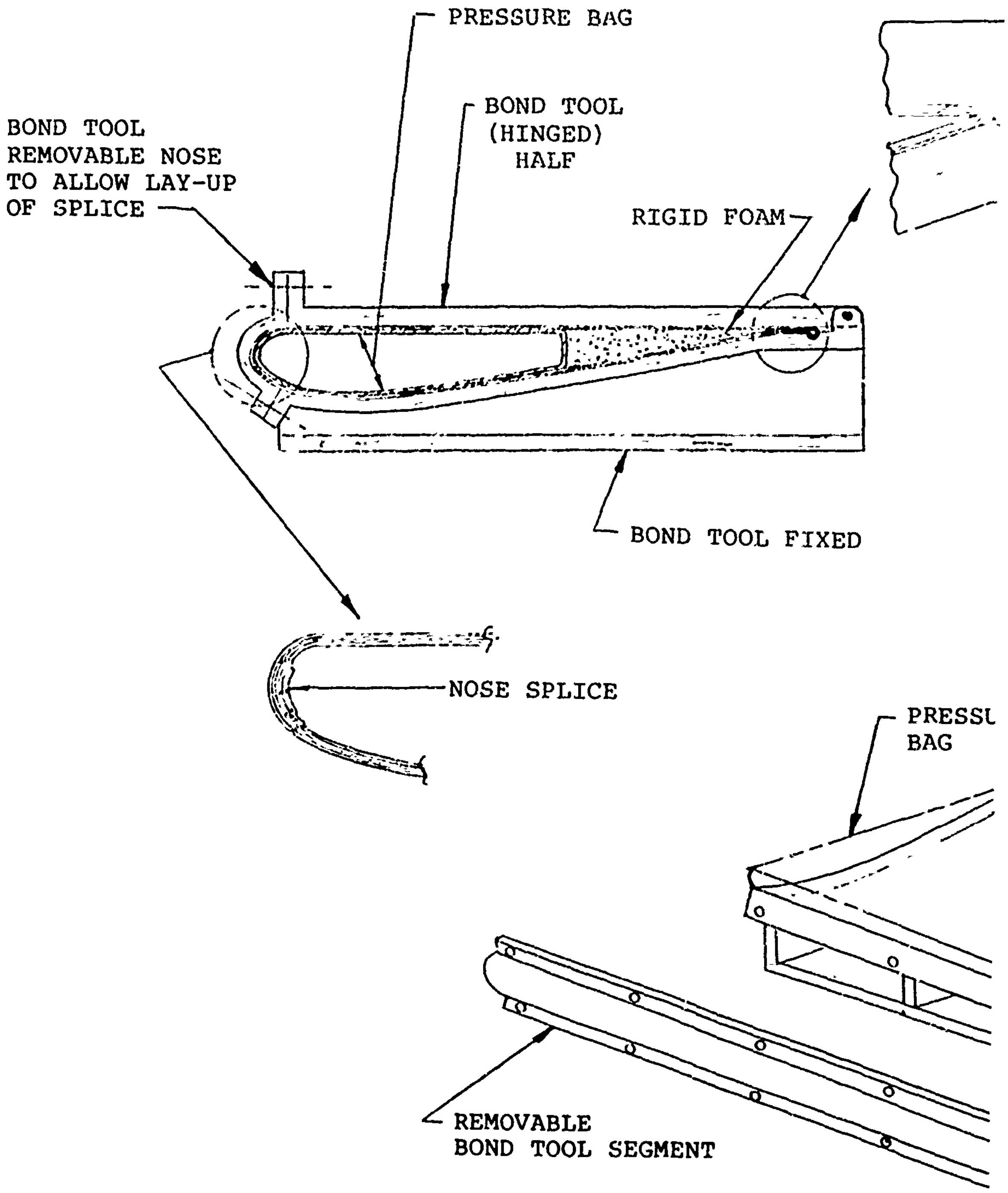

Figure 20. Bond Fixtures for Elevator Concept 2.

A

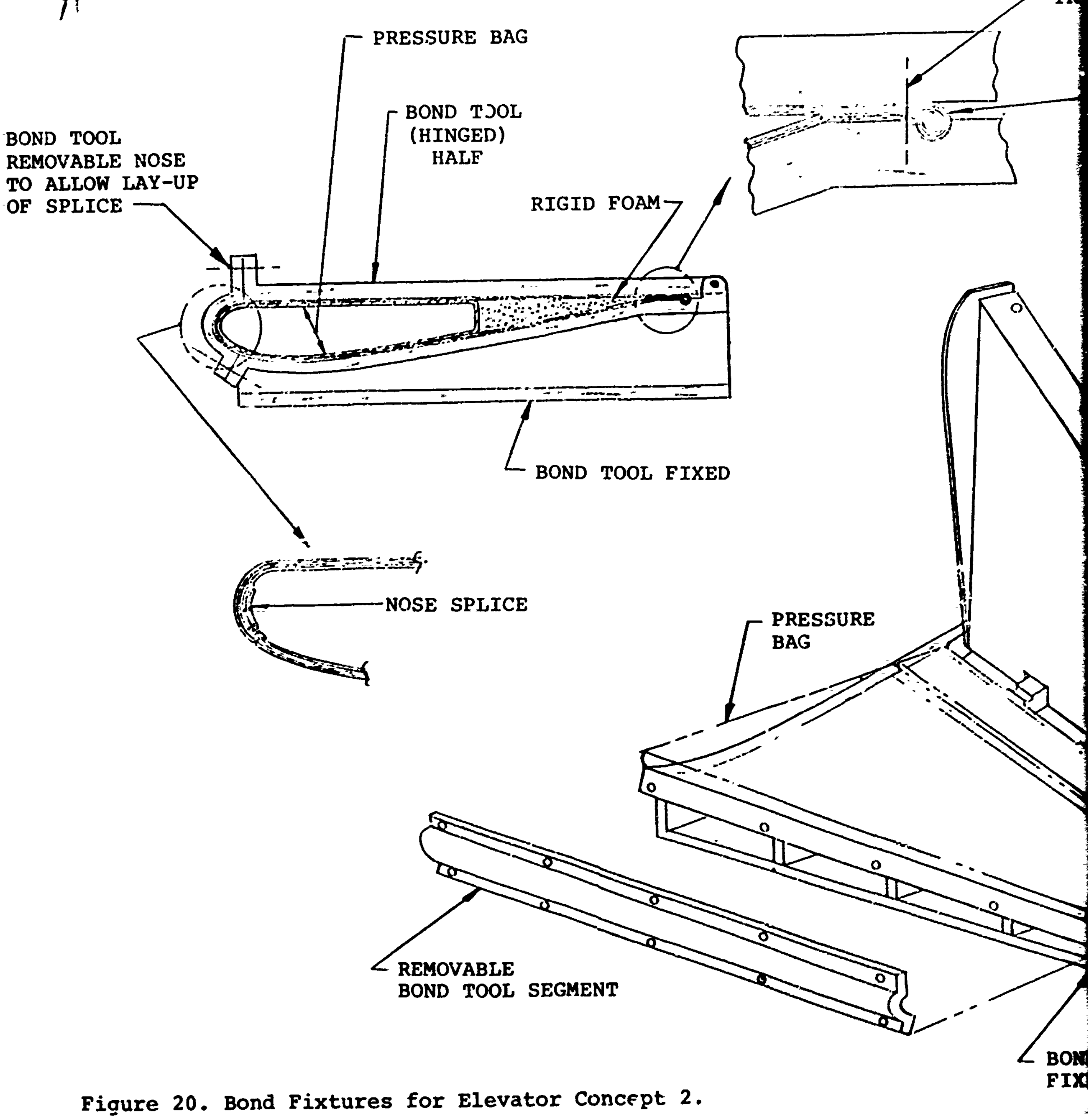

Figure 20. Bond Fixtures for Elevator Concept 2.

B

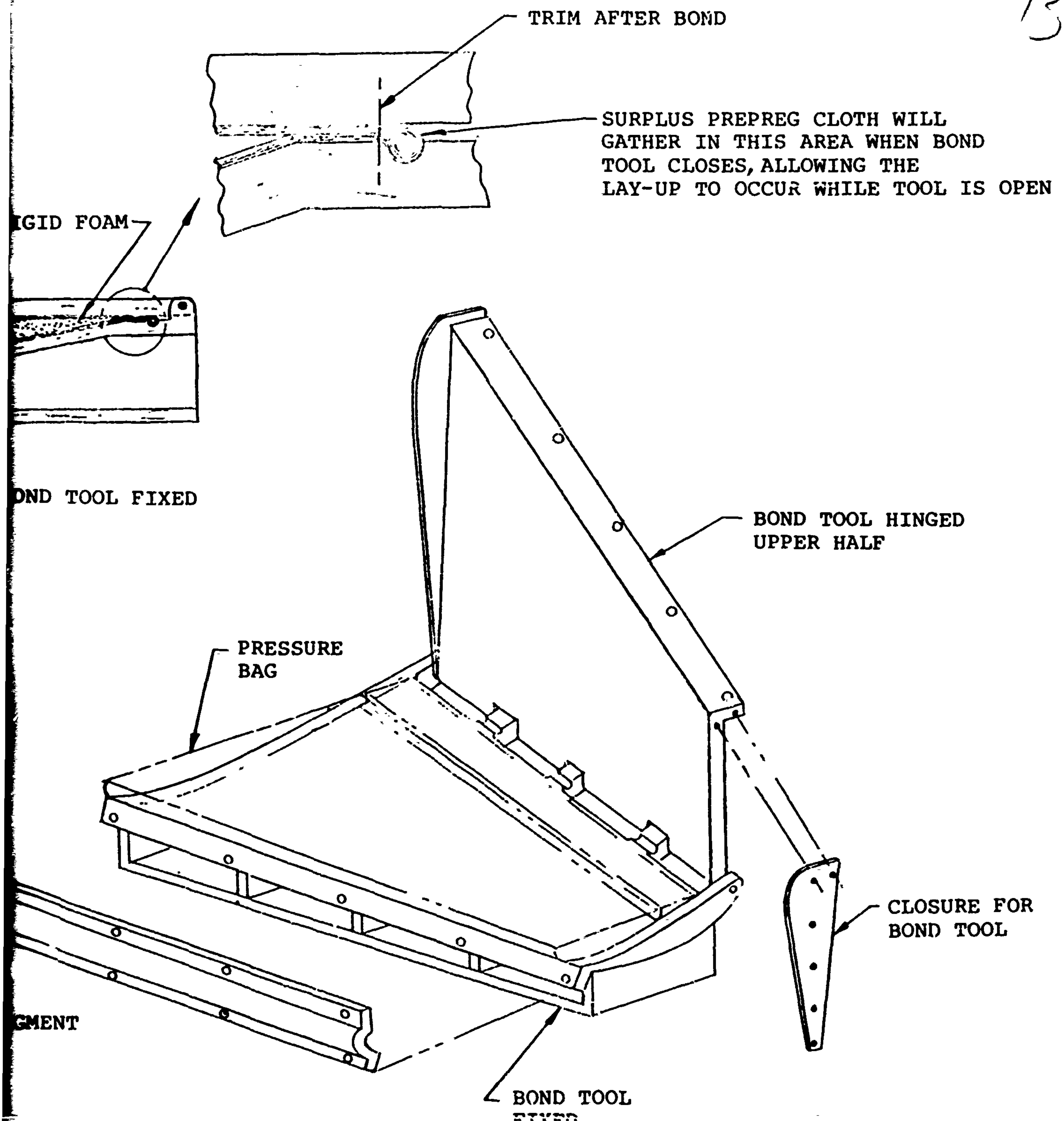

TRIM AFTER BOND
SURPLUS PREPREG CLOTH WILL GATHER IN THIS AREA WHEN BOND TOOL CLOSES, ALLOWING THE LAY-UP TO OCCUR WHILE TOOL IS OPEN
IGID FOAM
OND TOOL FIXED
BOND TOOL HINGED UPPER HALF
PRESSURE BAG
CLOSURE FOR BOND TOOL
GMENT
BOND TOOL FIXED

Concept 2.

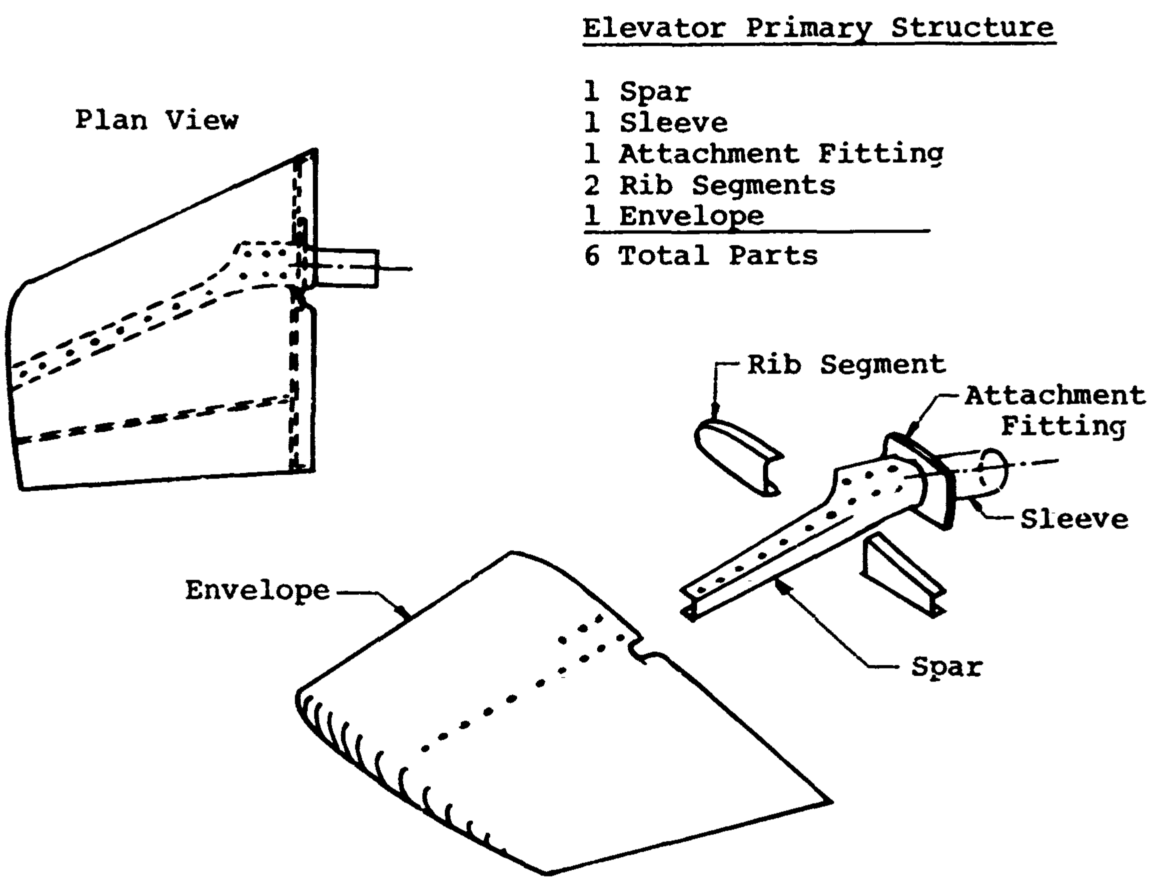

Figure 21. Structural Configuration for Elevator Concept 3.

Elevator 4

Figures 22 and 23 show the structural configuration and the bond fixture for concept 4. In this concept the entire outer surface, tip cap, end rib, interior spars and interior rigid foam are laid up and cured in one step. A single-piece aluminum forging is then fastened to the elevator to complete the assembly. This concept has several advantages, which include: low cost, low weight, extremely low parts count, and excellent strength, reliability, aerodynamics, salvageability and repairability.

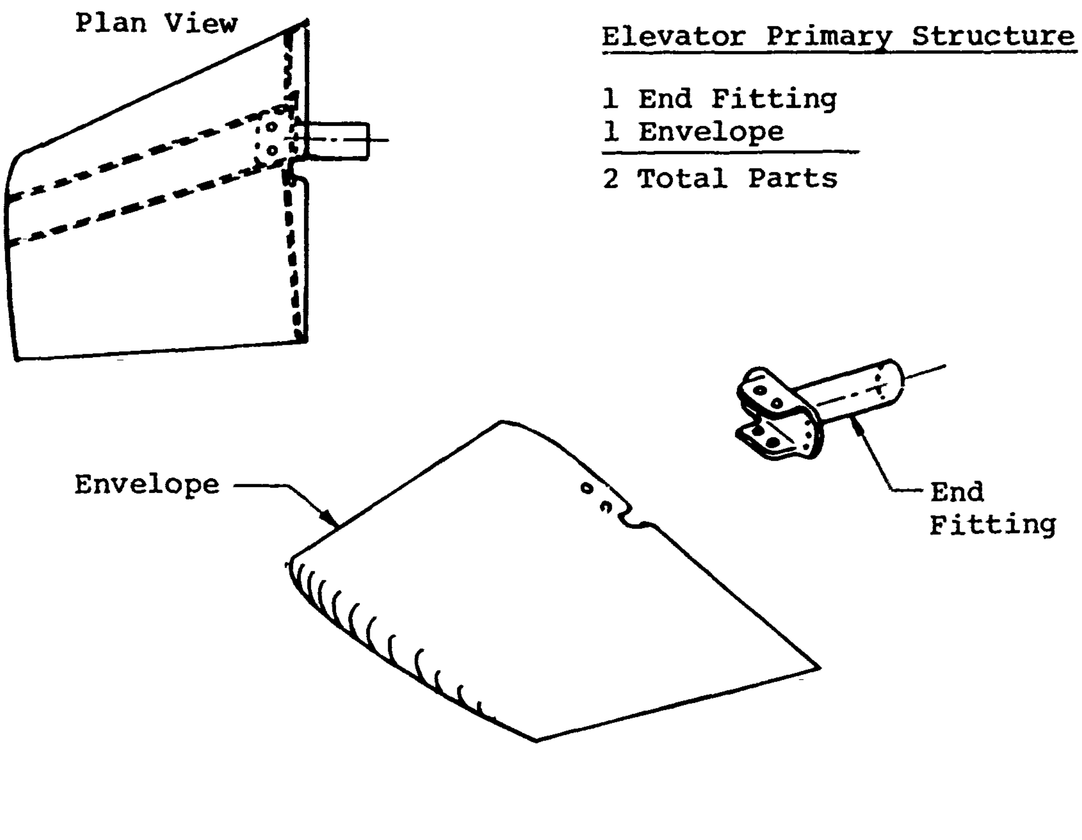

Figure 22. Structural Configuration for Elevator Concept 4.

A

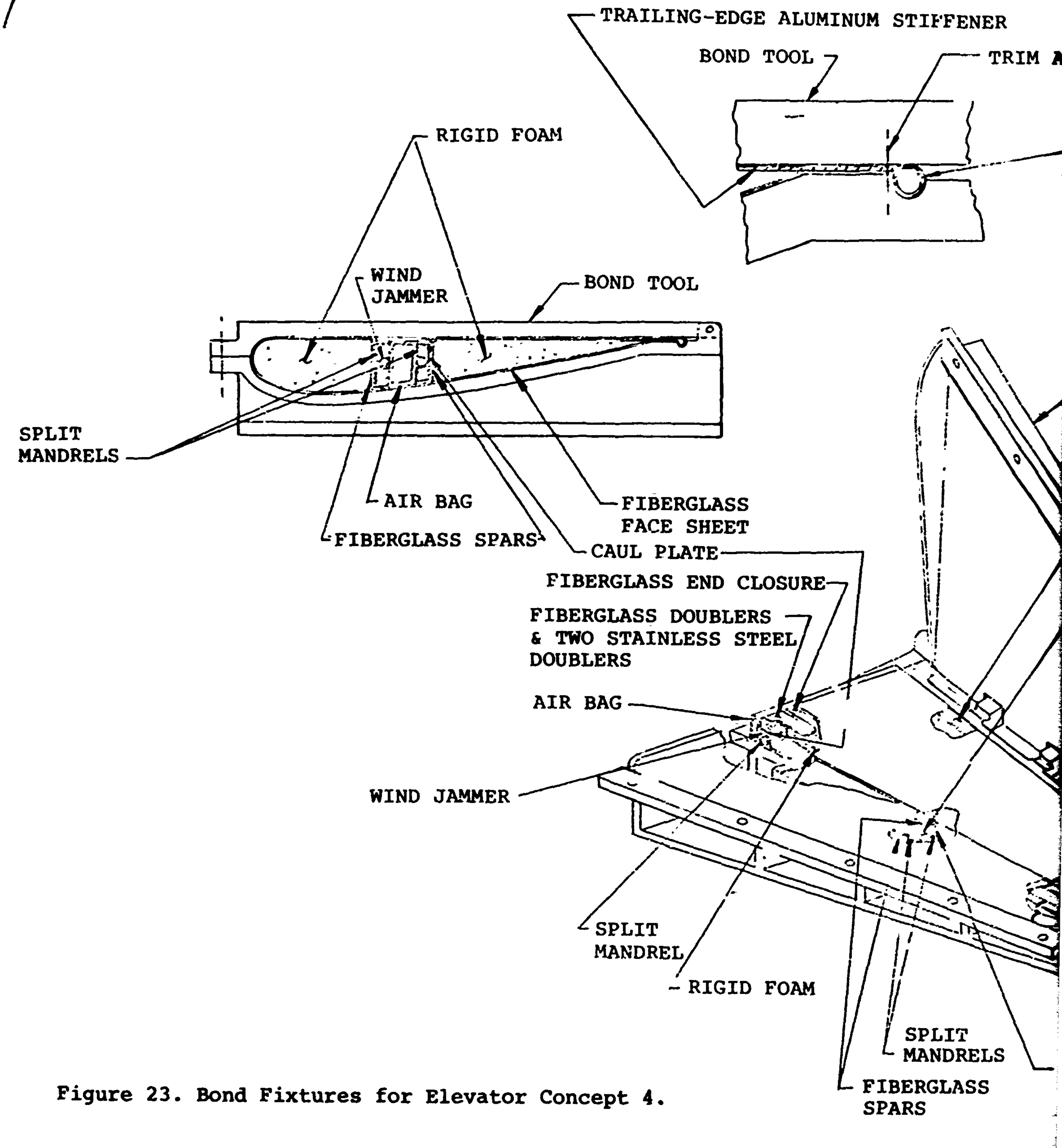

Figure 23. Bond Fixtures for Elevator Concept 4.

B

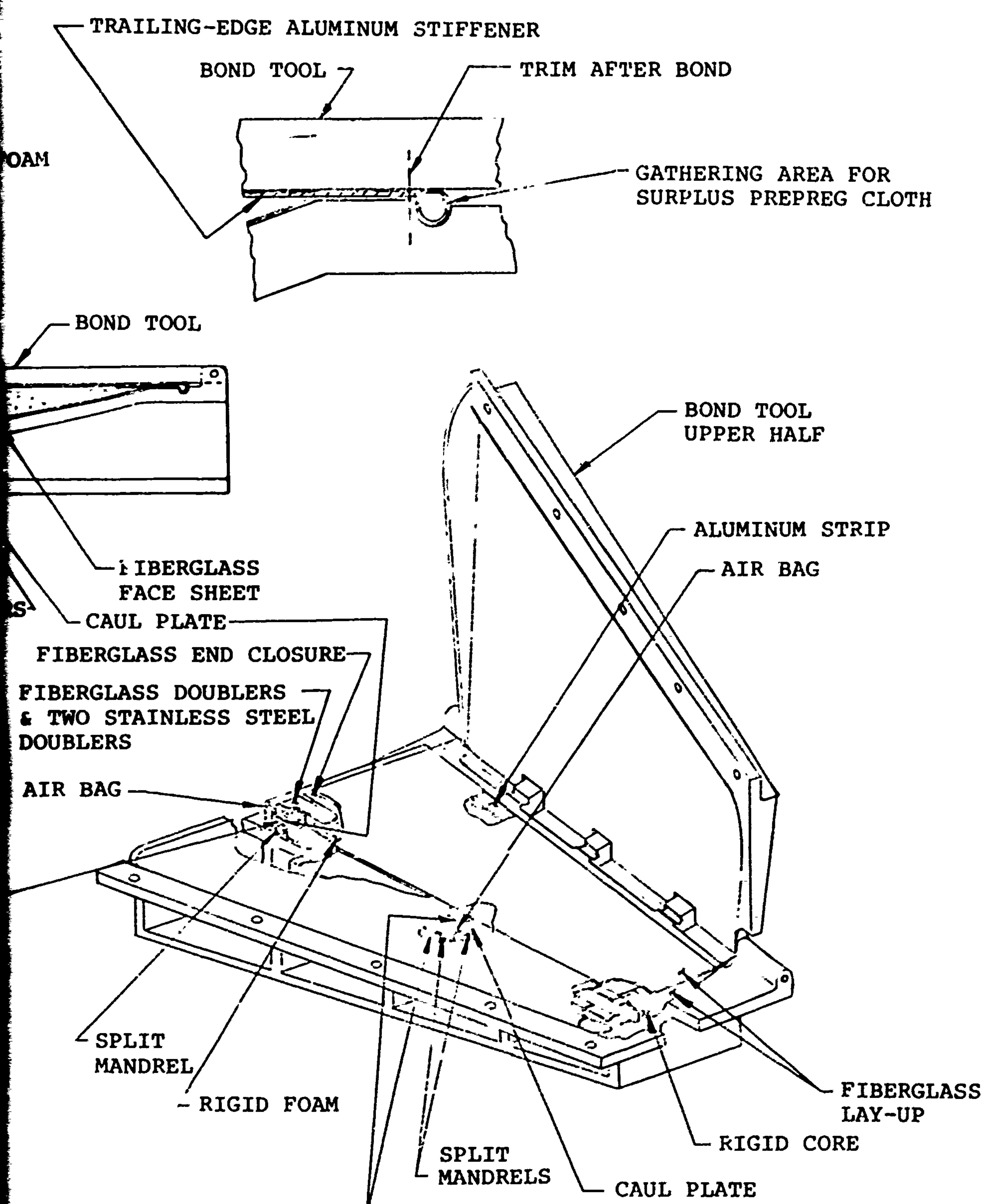

TRAILING-EDGE ALUMINUM STIFFENER
BOND TOOL
TRIM AFTER BOND
OAM
GATHERING AREA FOR SURPLUS PREPREG CLOTH
BOND TOOL
BOND TOOL UPPER HALF
ALUMINUM STRIP
AIR BAG
IBERGLASS FACE SHEET
CAUL PLATE
FIBERGLASS END CLOSURE
FIBERGLASS DOUBLERS & TWO STAINLESS STEEL DOUBLERS
AIR BAG
SPLIT MANDREL
RIGID FOAM
SPLIT MANDRELS
FIBERGLASS SPARS
CAUL PLATE
RIGID CORE
FIBERGLASS LAY-UP

Concept 4.

Structurally, the principal element is a box beam formed by the two channel-shaped spars and the outer envelope. Stainless steel doubler plates are interleaved into the lay-up to assist in the transfer of the loads at the attachment to the end fitting. The end fitting itself is a single-piece aluminum forging that interfaces properly with the existing cross tube in the boom.

Typical lay-ups for the envelope are shown below:

Region	Material	Style	Angle (deg)	ΣT
Fwd. of Box	E_4	181_4	$(0/45)_S$	.04
Over Box *	E_8	$(181_2/U_2)_S$	$(0/45/0/0)_S$	.08
Aft. of Box	E/E	181/181	0/45	.02

* Average values, more uniaxial at root, less at tip

COVER CONCEPTS

Table III summarizes the principal characteristics of four concepts presented for covers to enclose the drive shaft over the boom. Concept 3 is the best of the group, with an outstandingly low life-cycle cost and good durability.

TABLE III. COVER CONCEPTS, BASIC CHARACTERISTICS

No.	Hinge	Cover Type	Principal Materials	
			Hinge	Cover
0	1 Side, Continuous	Chem-Milled Sheet	Aluminum	Aluminum
1	1 Side, Discrete	Sandwich	Aluminum	E-Glass
2	1 Side, Continuous	Reinforced Sheet	Polyalomer*	"
3	1 Side, Continuous	Formed Sheet	"	Polyalomer*
4	2 Sides, Continuous	Formed Sheet	"	"

* Propylene-ethylene type crystalline copolymer

Preceding page blank

Cover 1

Figure 24 shows cover concept 1. Like the boom, it is a sandwich shell made in a single-phase bondment. Typical lay-ups are:

Item	Material	Style	Angle (deg)	ΣT
Outer face	E/E	181/120	0/45	.014
Inner face	E	181	0	.010

The core is R400 with a thickness of .25 inch. The core extends over the central regions. At the ends, single-wall construction is used to simplify the mechanical attachment of the hinges and the quarter turn fasteners. The lower longitudinal edges are also single wall to facilitate fabrication and trimming. The perimeter is locally reinforced with additional plies of cloth and a small aluminum sheet at the fastener holes.

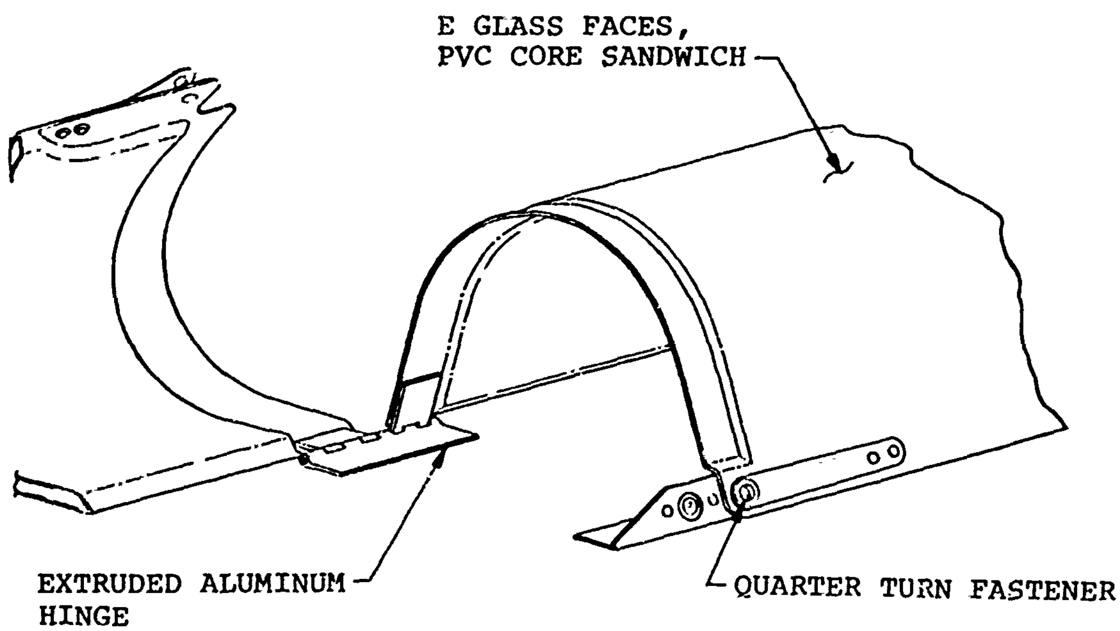

Figure 24. Cover Concept 1.

One feature of this design is the attachment of each cover to the hinge by only two fasteners per cover. This provides economy in assembly and replacement, and also allows convienent removal of the cover for obstruction-free maintenance of the drive train. Another feature is the short length of the hinges. Each hinge is attached with only two fasteners to the

shell of the boom. The hinges can also be very durable with permanently entrapped hinge pins.

Cover 2

Concept 2, shown in Figure 25, is conventional. It is very similar in concept to the existing metal cover. However, it should be superior to the existing cover because of better impact resistance. Its only new feature is the use of a plastic hinge; polypropylene and polyalomer are leading candidates for the hinge.

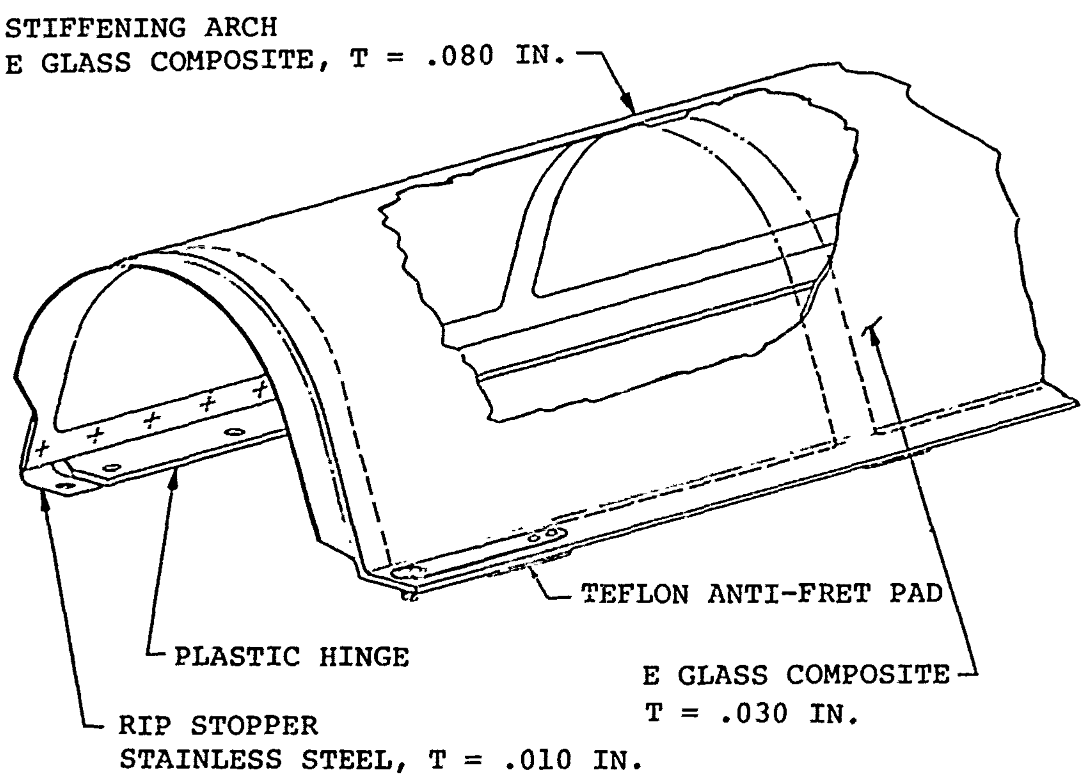

Figure 25. Cover Concept 2.

Cover 3

Figure 26 shows cover concept 3. This cover is vacuum molded in one piece from a .10-inch-thick sheet of polyalomer or polypropylene. It features extremely low cost and excellent tolerance to impact and mishandling. One concern is failure of the hinge, loss of the cover, and damage to the tail rotor. Such behavior is precluded by the presence of a small steel strap, called a rip stopper. It is a standby load path that comes into play only if the hinge begins to fail. The rip

stopper restrains the cover and prevents the progressive failure of the hinge.

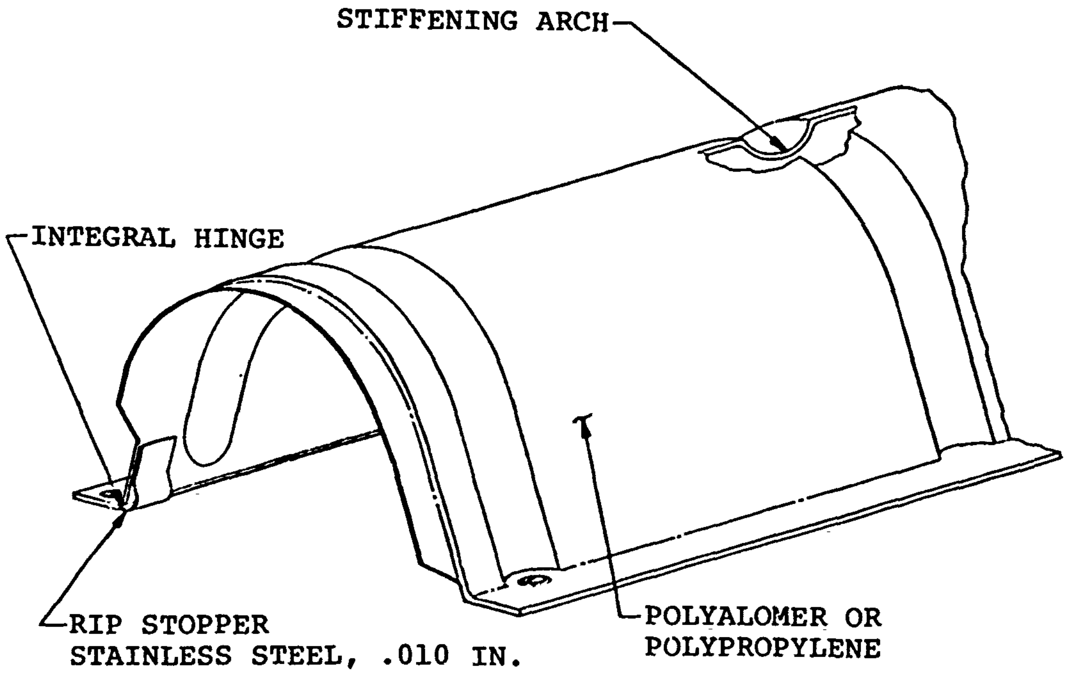

Figure 26. Cover Concept 3.

Cover 4

Concept 4, shown in Figure 27, uses the same fabrication process as concept 3. It differs only in configuration. Hinges are provided on both sides, permitting service from either side of the aircraft. This is a mixed blessing, however. It increases serviceability, but it also increases the likelihood of forgetting to secure both sides of the cover. In addition, the presence of the hinge precludes carrying the stiffening arch to the base, and thus concept 4 has less lateral resistance than concept 3. On the whole, concept 3 is the better design.

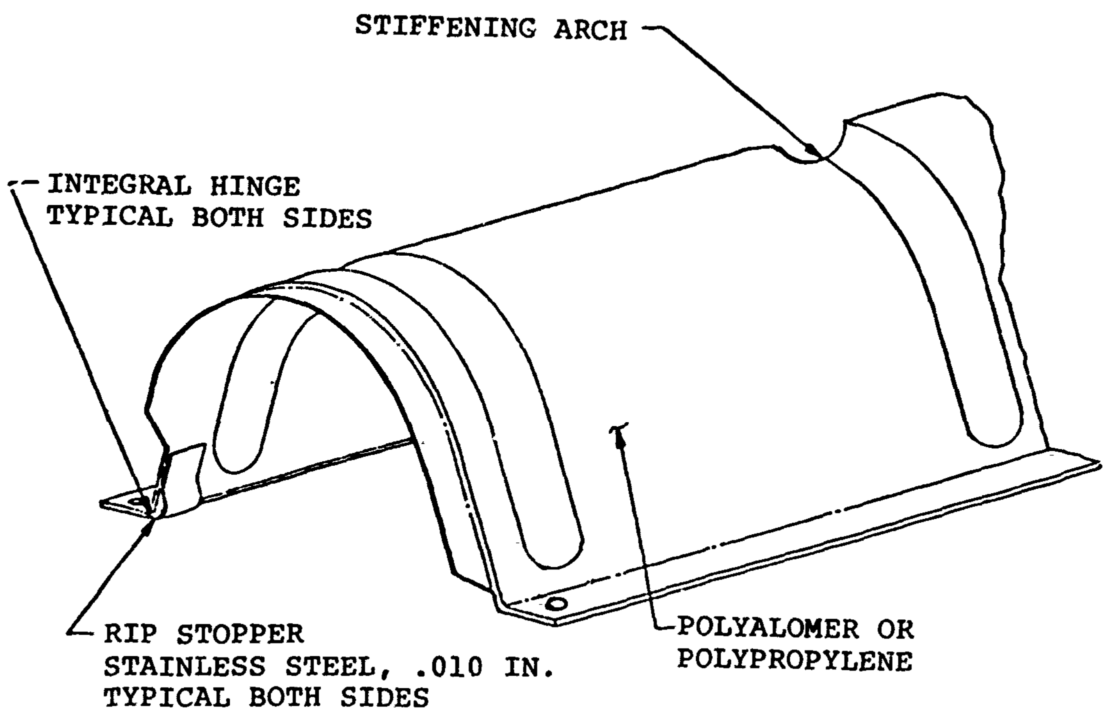

Figure 27. Cover Concept 4.

DESIGN CRITERIA

SIGN CONVENTIONS

In this report, two local coordinate systems, shown in Figure 28, are used to define the loadings on the boom-fin. In each system, a consistent left-hand sign convention is used for coordinates, forces, and moments. The local X-directions lie in the midplane of the aircraft and along the axis of the boom and along the forward spar of the fin. The positive sense for the X-directions has an aft component. The Y-direction lies perpendicular to the midplane of the aircraft and is positive to the left; the Z-direction is orthogonal to X and Y with left-hand sense. Forces and moments are positive when their vectors lie in the direction of the positive sense of the coordinate axes. In all tables of internal loads, the stated loads are those acting upon the forward segment, as shown in Figure 28.

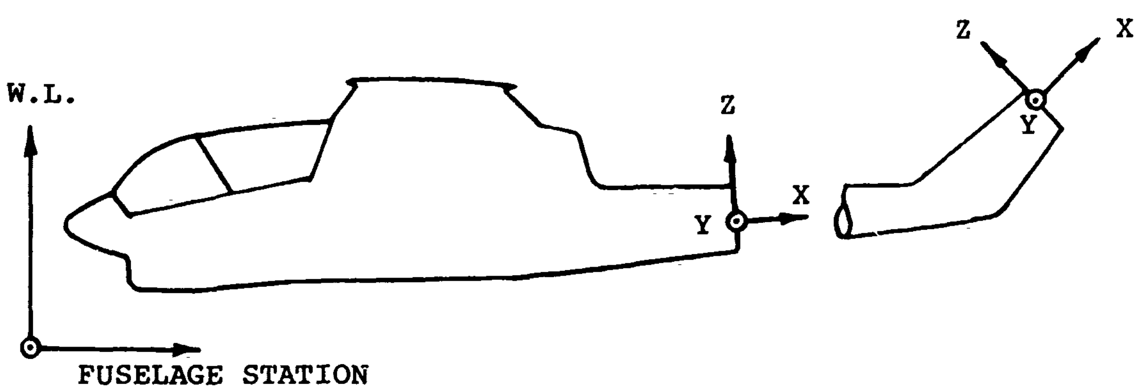

Figure 28. Coordinates for Boom and Fin Loads.

LIMIT LOADS

According to Reference 3, the critical design conditions for the boom are: condition Vb, yaw + 15^{o} recover; condition Vb, yaw - 15^{o} recover; and condition XIV, tail-down landing. In the present study, these conditions are identified as cases .12, .13, and .15, respectively. The critical design conditions for the fin are cases .12 and .13 only. Tables IV and V summarize the limit loads for the boom and fin.

TABLE IV. LIMIT LOADS FOR BOOM							
Case	BOOM Sta.	F_x (kips)	F_y (kips)	F_z (kips)	M_x (in.-kips)	M_y (in.-kips)	M_z (in.-kips)
.12	41.32	-0.09	-2.66	-1.45	75.91	-166.46	-597.78
	59.50	-0.08	-2.73	-1.35	80.12	-140.15	-549.73
	80.44	-0.08	-2.73	-1.35	83.64	-11.89	-492.86
	101.38	-0.07	-2.96	-1.13	85.12	-83.62	-435.86
	122.33	-0.07	-2.96	-1.13	81.60	-61.52	-492.73
	143.28	-0.03	-3.03	-0.47	92.16	-37.80	-312.78
	164.23	-0.03	-3.03	-0.47	96.07	-27.82	-249.59
	185.18	-0.02	-2.92	-0.28	102.15	-17.95	-186.54
	194.30	-0.02	-2.92	-0.28	103.84	-15.28	-159.19
.13	41.32	-0.09	1.67	-1.43	-57.98	-165.30	406.26
	59.50	-0.08	1.74	-1.33	-61.10	-189.32	376.14
	80.44	-0.08	1.74	-1.33	-63.35	-111.47	339.75
	101.38	-0.07	2.00	-1.11	-63.99	-83.61	293.24
	122.33	-0.07	2.00	-1.11	-65.98	-60.11	261.11
	143.28	-0.03	2.09	-0.49	-67.81	-38.63	220.05
	164.23	-0.03	2.09	-0.49	-70.52	-28.44	176.39
	185.18	-0.02	2.00	-0.29	-75.51	-18.25	132.82
	194.30	-0.02	2.00	-0.29	-76.67	-15.52	114.01
.15	41.32	0.11	0.0	1.85	0.0	367.04	0.0
	59.50	0.11	0.0	1.85	0.0	333.39	0.0
	80.44	0.11	0.0	1.85	0.0	294.63	0.0
	101.38	0.11	0.0	1.85	0.0	255.87	0.0
	122.33	0.11	0.0	1.85	0.0	217.09	0.0
	143.28	0.11	0.0	1.85	0.0	178.31	0.0
	164.23	0.11	0.0	1.85	0.0	139.53	0.0
	185.18	0.11	0.0	1.85	0.0	100.75	0.0
	194.30	0.11	0.0	1.85	0.0	83.87	0.0

Notes:

1. For cases .12 and .13, the points of application of the loads lie at aircraft B.L. = 0 and W.L. = 63.09.
2. For case .15, the points of application of the loads lie at aircraft B.L. = 0 and W.L. = 76.81.
3. The above loads were calculated from load data presented in Reference 3, pg. 4.003 by applying a rotation of -3.55° about the Y-axis and appropriate sign changes to transform the loads into the local (true) axes for the boom.

TABLE V. LIMIT LOADS FOR FIN							
Case	SPAR Sta.	FIN Sta.	SPAN Sta.	F_y (kips)	M_x (in.-kips)	M_y (in.-kips)	M_z (in.-kips)
.12	39.55	70.25	0	-3.21	12.26	-18.95	-164.2
	60.00	49.80	14.22	-2.69	11.65	-18.95	-105.9
	80.00	29.80	28.13	-2.18	10.91	-18.95	- 57.03
	100.00	9.80	42.03	-1.69	10.42	-18.95	- 18.40
	112.61	3.00	50.80	- .27	2.40	0	.18
.13	39.55	70.25	0	2.36	3.51	-18.95	129.[illegible]
	60.00	49.80	14.22	2.06	2.96	-18.95	86.[illegible]
	80.00	29.80	28.13	1.75	3.39	-18.95	47.37
	100.00	9.80	42.03	1.43	3.93	-18.95	14.85
	112.61	3.00	50.80	.16	-.02	0	.02

Notes:

1. Spar stations have the same sense as the local X direction.
2. Fin stations run down the spar. Their origin is at the location of the tail rotor; see Figure 1. Fin station = 109.8 - spar station.
3. Span stations are used in Reference 2. They are related to aircraft waterline positions as follows: Span station = W.L. - 67.5.
4. F_x and F_z are zero.
5. Points of application of load lie along the center line of the forward spar.
6. The above loads were calculated from load data presented in Reference 3, pages 5.01 and 5.02 by applying a rotation of -44.05° about the Y-axis and appropriate sign changes to transform the loads into the local (true) axes for the fin.

STIFFNESS

Stiffness criteria are required to achieve two objectives:

1. To avoid resonances with main rotor harmonics, particularly 1/rev and 2/rev.

2. To assure that changes in the angle of attack of the fin as a result of lateral loads are similar to those that occur in the existing structure.

The first objective avoids excessive vibration levels. The second objective avoids changes in the lateral control of the aircraft. Such control changes may not be harmful, perhaps even desirable, but their investigation would be beyond the scope of this study and thus, to be safe, are avoided.

One approach to defining stiffness criteria would be to require that the bending and torsional stiffness match the corresponding unbuckled stiffnesses* of the existing structure at each station along the boom and fin. This approach will lead to satisfactory new designs if the total mass and its distribution are similar to those of the existing structure. Such is the general case because approximately one half of the total mass of the assembly is composed of nonstructural items common to all designs. The match-stiffness-everywhere approach is undesirable as a rigid requirement, however, because it restricts design freedom unnecessarily and, in some concepts, requires that the structure be heavier and more costly than necessary.

An alternative, less restrictive, and still valid, approach can achieve the stated objectives. The stiffness criteria can be defined by deflection requirements. Consider the aft fuselage to be cantilevered in normal position from a rigid wall. Then the following three deflections must be satisfied:

1. The vertical deflection from a vertical load of 1 kip applied at the tail rotor 90° gearbox shall be between 100% and 120% of the corresponding deflection for the existing aft fuselage, calculated to be 1.136 inches.

---

*Unbuckled stiffnesses for the existing structure were calculated. They are presented and compared to stiffness of the new concepts. See page 68 and Figures 35 and 39.

2. The lateral deflection from a lateral load of 1 kip applied at the tail rotor 90° gearbox shall be between 90% and 100% of the corresponding deflection for the existing aft fuselage, calculated to be 2.81 inches.

3. The change in angle of attack of the fin at the location of the tail rotor 90° gearbox from a 1-kip load applied laterally at the 90° gearbox shall be between 80% and 120% of the corresponding change in angle of attack for the existing aft fuselage, calculated to be 1.062 degrees.

The above deflection requirements are based upon the observation that the tail rotor, the 90° gearbox, and the fin together constitute 28% of the total mass of the aft fuselage. This mass dominates the behavior because it is in the antinodal position for the first two natural modes of vibration in both the lateral and vertical directions. Thus, when the stiffness for this important mass is maintained similar to that of the existing structure, the frequencies cannot deviate significantly.

Figures 29 and 30, from Reference 4, show the positions of the natural frequencies of the existing aircraft in relationship to the main rotor harmonics. From Figure 29, it is seen that the first vertical mode lies between 1/rev and 2/rev, being much closer to 2/rev, and that the second mode lies between 2/rev and 4/rev, being closer to 4/rev. Thus, it is apparent that some reduction of stiffness in the vertical direction is desirable and should be allowed. Accordingly the criteria state that the allowable vertical deflections are 100% to 120% of those in the existing structure. Figure 30 shows that the first lateral mode lies almost midway between 1/rev and 2/rev. The second mode lies, unfortunately, in resonance with 4/rev. It is believed that the good position of the first mode should not be disturbed, even if it allows the second mode to be in resonance. Accordingly, the criteria state that the allowable lateral deflections are 90% to 110% of those in the existing structure.

WEIGHT

It is required that the new concepts weigh no more than the existing aft fuselage. Figures 31 and 32 provide concise summaries of the weight and balance of the existing aft fuselage. Table VI further identifies the items of weight in the existing structure. These figures and tables were prepared from data presented in Reference 5.

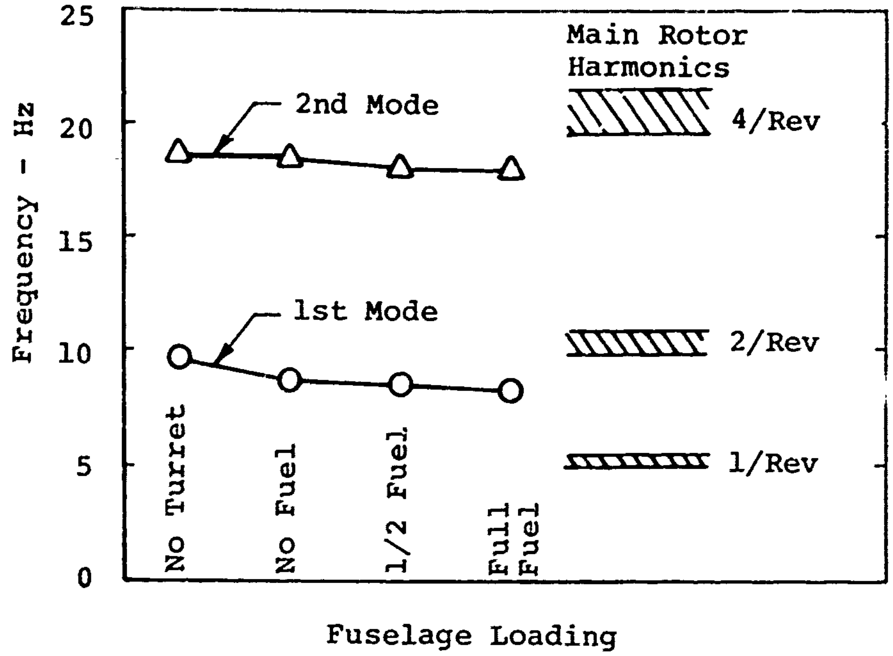

Figure 29. Peak Turret Response Frequencies Versus Fuselage Loading for Vertical Excitations.

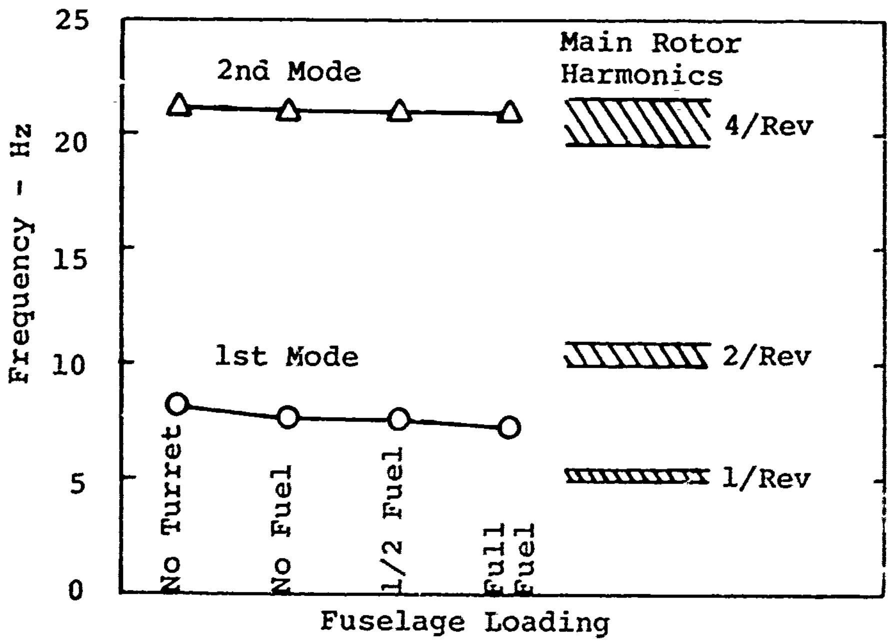

Figure 30. Peak Turret Response Frequencies Versus Fuselage Loading for Lateral Excitations.

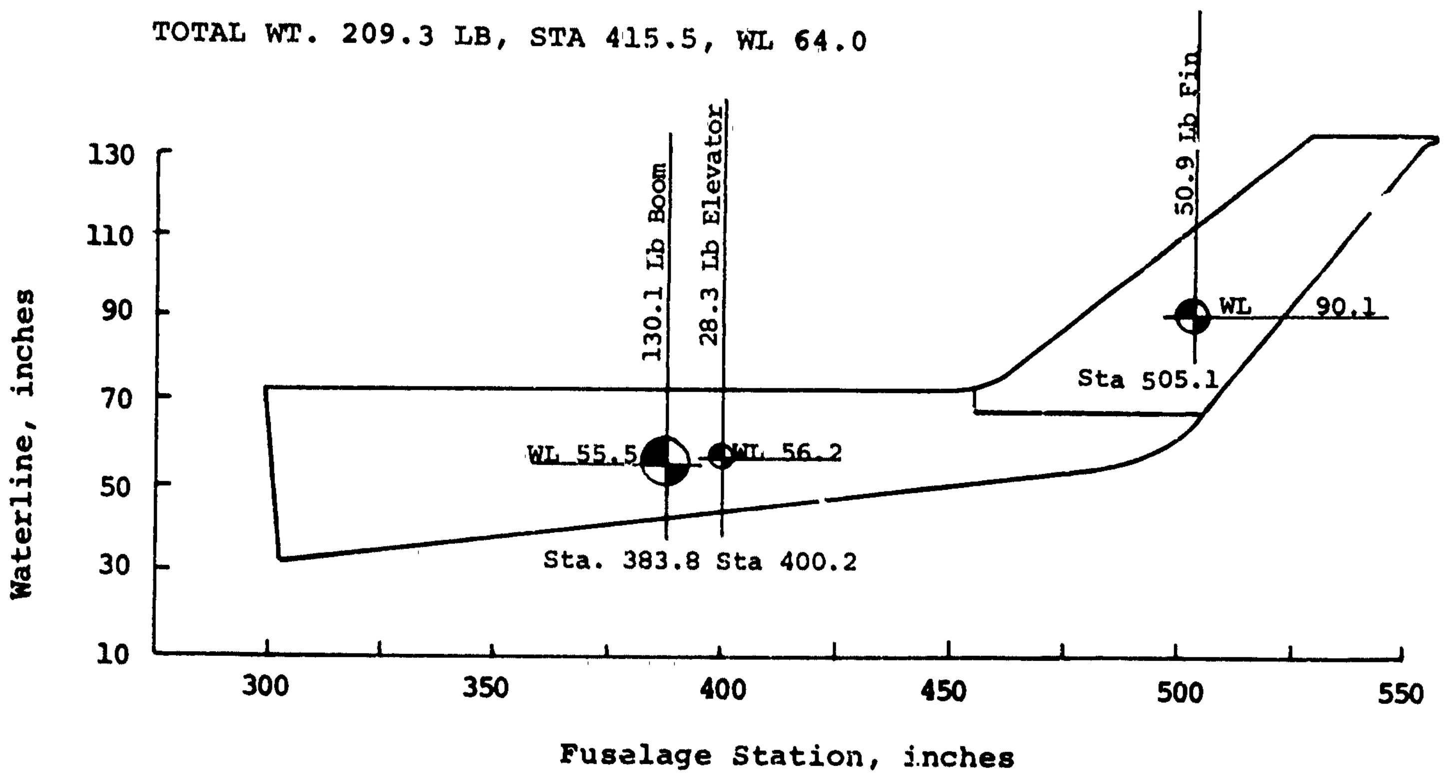

Figure 31. Structural Mass Items for Existing Aft Fuselage.

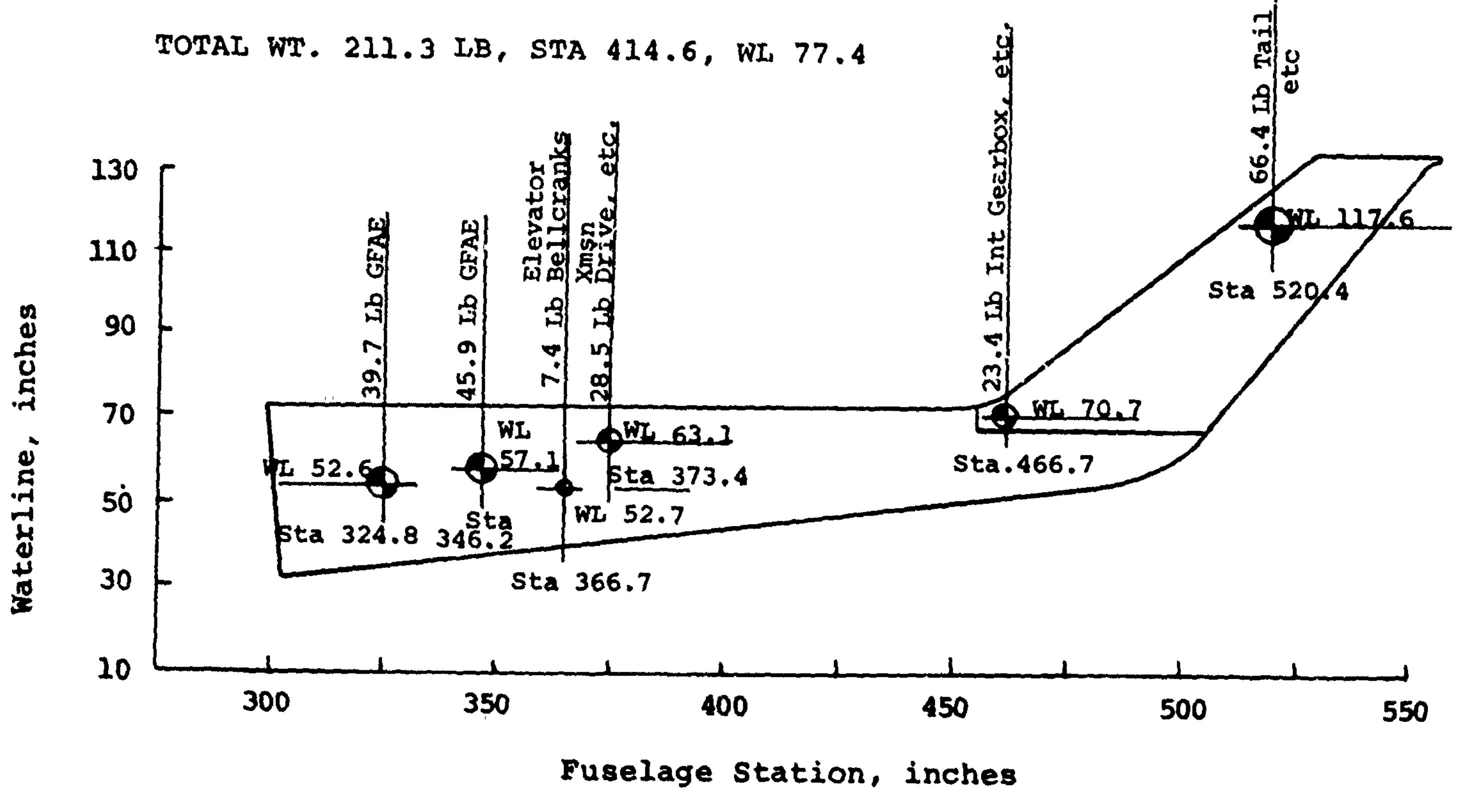

Figure 32. Total Equipment and Hardware for Existing Aft Fuselage.

TABLE VI. STRUCTURAL MASS ITEMS FOR EXISTING AFT FUSELAGE

Item	Boom	Fin	Elevators
Bulkheads, frames, ribs	13.7	2.0	2.2
Cover	56.8	19.9	10.4
Fittings	2.6	1.0	0.8
Formers, stiffeners, angles	2.6	2.8	-
Longerons	22.7	-	-
Stringers	13.3	-	-
Spars	-	15.4	10.2
Doors and frames, access	6.0	4.0	-
Fairings and fillets	2.3	3.9	0.4
Exterior finish	2.5	0.7	-
Hardware, miscellaneous	3.1	1.2	1.0
Bumper, aux. tail gear	4.5	-	-
Trailing-edge strips	-	-	0.4
Supports	-	-	2.9
TOTAL WEIGHT, POUNDS =	130.1	50.9	28.3

STRUCTURAL ANALYSIS

MATERIAL

Material analyses were made to determine elastic constants and limit strengths for the specific laminates used in the design concepts. Limit loads and limit strengths are used throughout this report.

Composite theory as described in Reference 6 was used to calculate the laminate properties from the properties of the individual lamina. Table VII presents the input properties for the individual lamina and the sources for the data. Table VIII presents the calculated properties for the laminates.

It is believed that tests would show that the calculated strengths are underestimated because the following conservative assumptions are made in the failure theory.

1. Limit strength for each lamina is taken as .5x strength. In effect, this provides an extra 33% margin in ultimate strength over that normally required by aircraft specifications.

2. Failure of the total laminate is assumed when any individual lamina reaches its limiting strain. The limiting strains can be found from the data in Table VII by dividing the allowable limit stresses by the corresponding elastic constant.

In general, no weight penalty is incurred by the use of these conservative strengths because stiffness requirements, rather than strength, control the selection of thicknesses.

Figure 33 shows a typical envelope of allowable stresses. For the laminates used in this study, the allowable design space is typically a rectangle or a near rectangle.

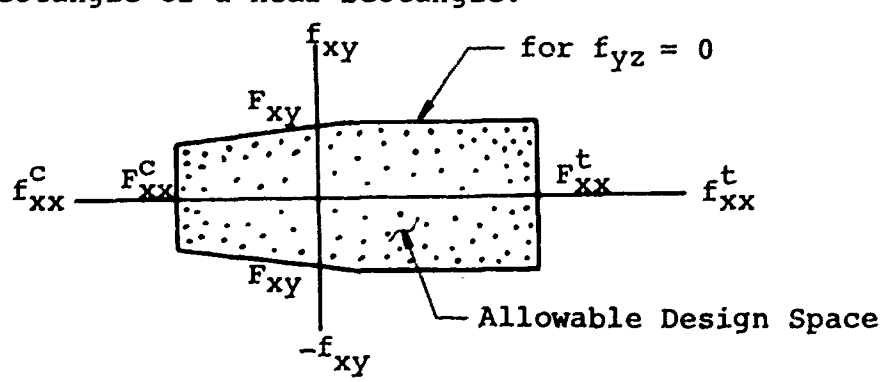

Figure 33. Typical Envelope of Allowable Stresses.

TABLE VII. LAMINA PROPERTIES									
Material, Style	Allowable Limit Stresses (ksi)					Elastic Constants (ksi)			
	F^c_{11}	F^t_{11}	F^c_{22}	F^t_{22}	F_{12}	E_{11}	E_{22}	G	$\mu 12$
E,120	-28.3	29.1	-24.9	28.90	±6.95	3410.	3210.	570.	.078
D,181	-16.0	35.0	-14.0	34.80	±4.50	4700.	4200.	550.	.10*
G, U	-70.0	92.5	-15.0*	3.50	±5.00*	21000.	1200	700.*	.30*
S, U	-63.0	109.5	-12.5	2.38	±4.53	7100.	1740.	516.	.25
S,913	-39.6	56.8	-39.6	56.80	±7.00*	4420.	4420.	700.*	.10*

Notes

1. Allowable limit stress = .5 x ultimate strength.

2. Properties for E-glass style 120 are based upon those in Reference 7 for style 7781 at 260°F cure. E_{11} and E_{22} are the average of the initial values for tension and compression. G is the secant modulus to .25 x ultimate strength.

3. For PRD-49 style 181, see Reference 8.

4. For Graphite uniaxial style, see Reference 9, SP-286 T2.

5. For S-Glass uniaxial style, see Reference 10, 1002S.

6. For S-Glass 913 style, see Reference 11.

*Data reported in the literature is often incomplete. In such cases, estimates have been made for the missing properties. These estimates are identified by an asterisk.

TABLE VIII. LAMINATE PROPERTIES										
Location		Allowable Limit Loads (kips/in.)			Allowable Limit Stresses (ksi)			Elastic Constants (Curvature=0) (ksi)		
Concept	Region	N_{xx}^c	N_{xx}^t	N_{xy}	F_{xx}^c	F_{xx}^t	F_{xy}	E_x	E_y	G
Boom 1	1	-1.178	1.558	.630	-20.67	27.33	11.05	6204.	2254.	1725.
	2	-2.092	2.766	.692	-29.89	39.51	9.89	8970.	2152.	1535.
Boom 2	1	-1.152	2.596	.888	-14.40	32.45	11.10	4693.	2228.	1263.
Boom 3	1	-.592	1.303	.429	-14.10	31.02	10.21	4438.	2071.	1164.
	2	-1.824	-3.484	.610	-22.24	42.49	9.84	5753.	1938	848.
	3	-1.179	2.382	.520	-19.02	38.42	8.38	5310.	1991.	955.
Boom 4	1	-.592	1.303	.429	-14.10	31.02	10.21	4438.	2971.	1164.
	2	-1.421	3.126	.932	-15.79	34.73	10.36	4967.	2190.	1180.
	3	-1.456	2.918	.579	-20.80	41.69	8.27	5743.	2053.	943.
	4	-1.012	1.640	.520	-20.24	32.80	10.40	4214.	3192.	1187.
Fin 1	1t	-1.048	1.908	.736	-11.91	21.68	8.36	3498.	3270.	1290.
	1b	-6.488	8.572	1.104	-39.08	51.64	6.65	11722.	2434.	1013.
	2	-.524	.954	.368	-11.91	21.68	8.36	3498.	3270.	1290.
	3	-.403	.415	.231	-22.39	23.06	12.83	2701.	2607.	1054.
	4	-.806	.830	.462	-22.39	23.06	12.83	2701.	2607.	1054.
Fin 2	1t	-2.168	2.168	1.084	-27.10	27.10	13.55	3492.	2392.	1355.
	1b	-5.668	8.880	1.496	-28.34	44.40	7.48	5658.	2499.	851.
	2	-1.084	1.084	.542	-27.10	27.10	13.55	3492.	3492.	1355.
	3	-.403	.415	.231	-22.39	23.06	12.83	2701.	2607.	1054.
	4	-.806	.830	.462	-22.39	23.06	12.83	2701.	2607.	1054.

Notes:

1. See Figures 5, 10, 11, 12, 15, and 16 for further descriptions.
2. The properties for each region include both faces.
3. For boom concept 4, the properties shown above correspond to the descriptions in Figure 16. For the stress and stiffness analysis, the thicknesses shown in Figure 16 for regions 3 and 4 are multiplied by 1.228 to account for the developed length of the corrugations.

Table IX presents allowable limit strengths and stiffnesses for core materials. The values shown are derived from the average test values in the following manner:

1. The allowable limit strength = 4/9 x the average ultimate strength at 70°F. The factor 4/9 is the product of a 2/3 x 2/3. The first 2/3 accounts for a 1.5 factor between limit and ultimate load; the second 2/3 accounts for a reduction in properties for use at 160°F.
2. The elastic constant = 2/3 x the average elastic constant at 70°F. The factor 2/3 again accounts for a reduction in properties for use at 160°F.

It is believed that the average values are attainable in the applications described herein because the modest thicknesses involved permit inspection and subsequent rejection or repair of any area with a significant flaw.

TABLE IX. CORE PROPERTIES

	Density	Allowable Limit Stress (ksi)		Elastic Constants (ksi)	
Material	(lb/cu ft)	F^c	F^s	E^c	G
R200	2.3	.020	.018	1.0	1.0
R300	3.0	.035	.031	1.7	1.7
R400	4.0	.062	.049	3.0	2.3
R500	5.0	.093	.062	4.0	3.0
R600	5.7	.110	.075	4.7	3.7

Notes:

1. Allowable limit stress = 4/9 x average ultimate strength at 70°F.

2. Elastic Constants = 2/3 x average elastic constants at 70°F.

3. Average data obtained by B. F. Goodrich Tests, Reference 12.

STRESS

The boom-fin is a slender beam-like structure suited to conventional analysis over most of its length. Elementary beam and torsion theories are used to determine section properties and stresses.

Table X provides a concise summary of a preliminary study of the load intensities and stresses for each contour. The data in Table X correspond to a shell of uniform thickness and moduli subjected to the limit loading conditions. The following conclusions are apparent:

1. Case .12, yaw +15° recover, produces the highest stresses.

2. The highest stresses occur in the vicinity of B.S. 122.

3. Even the highest stresses are relatively low.

4. On an equal area basis, stresses for contours 2 and 3 are approximately 15% lower than those for the existing contour at B.S. 194.3.

More detailed stress analyses were also performed using the appropriate material properties for the three loading conditions at several stations on the boom and the fin for each design concept. In general, it was found that the materials described for each concept are quite adequate. Tables XI through XIV present typical results from such analyses for the limit loads from Case .12 at B.S. 122.33 for each design concept. The following notes pertain to Tables XI through XIV:

1. The idealized structure for these analyses is shown in Figure 34.

2. The element line refers to either a bending element or a shear element.

3. Tension areas are used for the bending elements. Each bending area is the sum of the transformed areas of the concentrated stringer, AST, and TF x the areas of the shear elements adjacent to the bending element.

4. The margins of safety, M. S., apply only to the bending element. M. S. = F/f - 1.0.

TABLE X. LOAD INTENSITIES AND STRESSES FOR UNIFORM SHELLS

Boom Sta.	Contour	Perimeter (in.)	Limit Load Intensities (kips/in.) Case .12 n_{xx}	Case .12 n_{xy}	Case .13 n_{xx}	Case .13 n_{xy}	Case .15 n_{xx}	Case .15 n_{xy}	Relative Stress for Equal Areas n_{xx}	Relative Stress for Equal Areas n_{xy}
80.4	1	95.3	.686	.115	.521	.096	.376	.060	1.00	1.00
	2	96.8	.662	.119	.492	.096	.371	.058	.98	1.03
	3	102.3	.626	.107	.467	.085	.345	.050	.98	.97
122.4	1	79.5	1.007	.149	.553	.126	.400	.068	1.00	1.00
	2	82.8	.914	.147	.497	.120	.385	.006	.95	1.03
	3	885.	.835	.128	.454	.106	.340	.056	.92	.96
164.2	1	63.6	7.94	.243	.567	.176	.402	.079	1.00	1.00
	2	69.4	.648	.214	.463	.154	.371	.077	.89	.96
	3	74.9	.581	.185	.412	.134	.306	.062	.86	.90
194.3	1	52.2	.749	.356	.541	.257	.361	.089	1.00	1.00
	2	60.2	.537	.278	.389	.201	.314	.085	.83	.90
	3	65.3	.478	.236	.344	.170	.245	.067	.80	.83

Notes:

1. n_{xx} is the maximum direct stress per inch of perimeter. It is a close approximation to consider that both a positive and a negative n_{xx} occur. In reality, the positive and negative values are slightly different because a small axial load exists along the boom. The axial load is a component from the resolution of the vertical shear into the boom axes which are inclined -3.55° to the vertical.

2. n_{xy} is the shear flow.

View Looking Forward

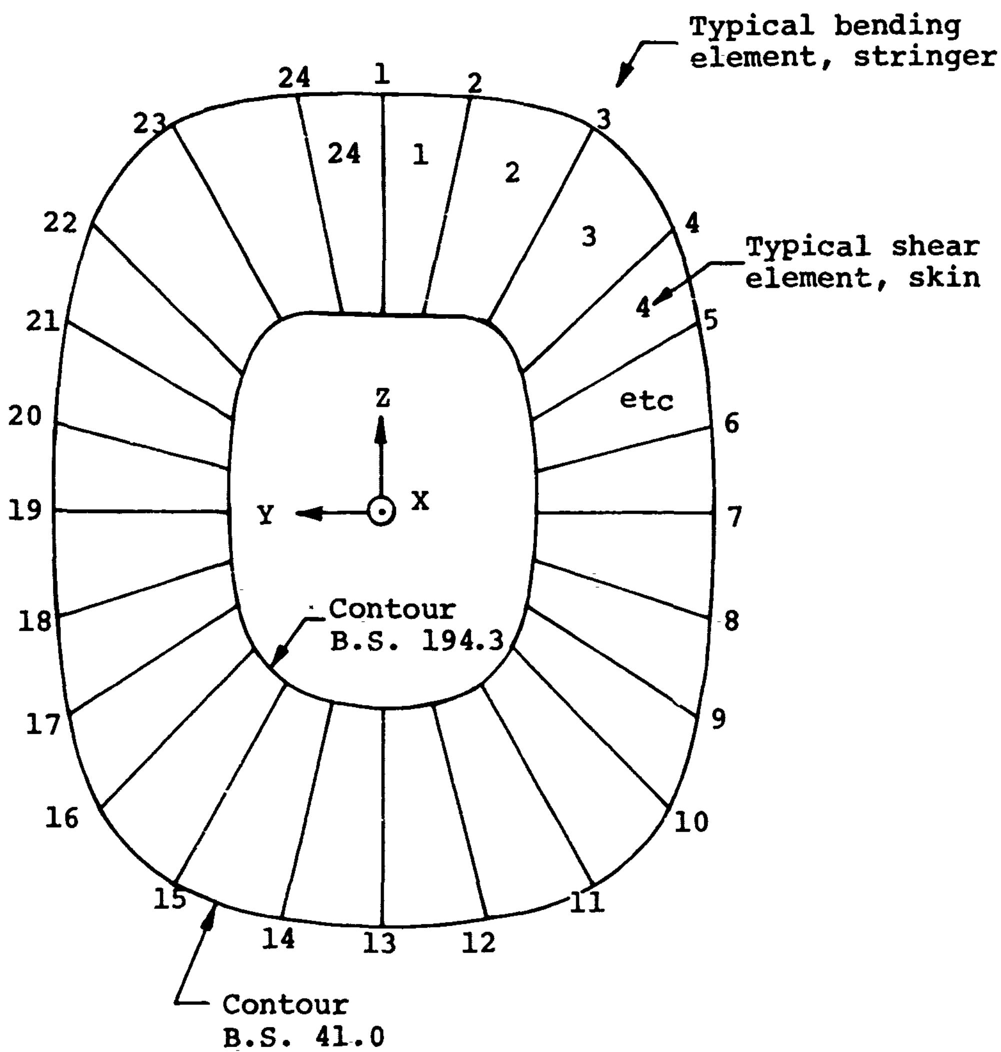

Figure 34. Typical Geometry for Boom Analyses.

TABLE XI. TYPICAL STRESSES FOR BOOM CONCEPT 1

AH-1G BOOM SHELL, CONTOUR 1 B   1-20-73   SHELL-D USES
COND VH-1, YAW +15, LIMIT   INCH-KIP SYSTEM

CASE 5.12
INPUT DATA

BASIC MODULI
STRINGER E = 1000.
SKIN G = 1000.

ELEM.	STATION 122.33 COORDINATES Y	STATION 122.33 COORDINATES Z	STATION 41.00 COORDINATES Y	STATION 41.00 COORDINATES Z	COMP. AREA	TENS. AREA	CRITICAL STRESS COMP.	CRITICAL STRESS TENS.	REL. MOD.	SKIN THICK.	SKIN MOD.	AST	CF	TF
1	0.0	12.938	0.0	17.950	0.0975	0.1570	-20.67	27.33	6.20	0.0570	1725.	0.0000	15.0	0.500
2	-2.75	12.938	-3.82	17.950	0.0975	0.1933	-20.67	27.33	6.20	0.0570	1725.	0.0000	15.0	0.500
3	-6.69	12.073	-9.28	16.750	0.0975	0.2302	-20.67	27.33	6.20	0.0570	1725.	0.0000	15.0	0.500
4	-9.32	8.996	-12.93	12.480	0.1222	0.2214	-20.67	27.33	7.59	0.0700	1535.	0.0000	15.0	0.500
5	-10.10	6.069	-14.01	8.420	0.1470	0.2139	-29.89	39.51	8.97	0.0700	1535.	0.0000	15.0	0.500
6	-10.49	3.013	-14.56	4.180	0.1470	0.2133	-29.89	39.51	8.97	0.0700	1535.	0.0000	15.0	0.500
7	-10.52	0.0	-14.60	0.0	0.1470	0.2173	-29.89	39.51	8.97	0.0700	1535.	0.0000	15.0	0.500
8	-10.44	-3.193	-14.49	-4.430	0.1470	0.2213	-29.89	39.51	8.97	0.0700	1535.	0.0000	15.0	0.500
9	-10.08	-6.300	-13.99	-8.740	0.1222	0.1958	-20.67	27.33	7.59	0.0570	1535.	0.0000	15.0	0.500
10	-9.20	-9.197	-12.76	-12.760	0.0975	0.1862	-20.67	27.33	6.20	0.0570	1725.	0.0000	15.0	0.500
11	-6.75	-11.706	-9.37	-16.240	0.0975	0.1994	-20.67	27.33	6.20	0.0570	1725.	0.0000	15.0	0.500
12	-3.42	-12.744	-4.74	-17.680	0.0975	0.1971	-20.67	27.33	6.20	0.0570	1725.	0.0000	15.0	0.500
13	0.0	-12.938	0.0	-17.950	0.0975	0.1951	-20.67	27.33	6.20	0.0570	1725.	0.0000	15.0	0.500
14	3.42	-12.744	4.74	-17.680	0.0975	0.1971	-20.67	27.33	6.20	0.0570	1725.	0.0000	15.0	0.500
15	6.75	-11.706	9.37	-16.240	0.0975	0.1994	-20.67	27.33	6.20	0.0570	1725.	0.0000	15.0	0.500
16	9.20	-9.197	12.76	-12.760	0.0975	0.1862	-20.67	27.33	6.20	0.0570	1725.	0.0000	15.0	0.500
17	10.08	-6.300	13.99	-8.740	0.1222	0.1958	-20.67	27.33	7.59	0.0700	1535.	0.0000	15.0	0.500
18	10.44	-3.193	14.49	-4.430	0.1470	0.2213	-29.89	39.51	8.97	0.0700	1535.	0.0000	15.0	0.500
19	10.52	0.0	14.60	0.0	0.1470	0.2173	-29.89	39.51	8.97	0.0700	1535.	0.0000	15.0	0.500
20	10.49	3.013	14.56	4.180	0.1470	0.2133	-29.89	39.51	8.97	0.0700	1535.	0.0000	15.0	0.500
21	10.10	6.069	14.01	8.420	0.1470	0.2139	-29.89	39.51	8.97	0.0700	1535.	0.0000	15.0	0.500
22	9.32	8.995	12.93	12.480	0.1222	0.2214	-20.67	27.33	7.59	0.0570	1725.	0.0000	15.0	0.500
23	6.69	12.073	9.28	16.750	0.0975	0.2302	-20.67	27.33	6.20	0.0570	1725.	0.0000	15.0	0.500
24	2.75	12.938	3.82	17.950	0.0975	0.1933	-20.67	27.33	6.20	0.0570	1725.	0.0000	15.0	0.500

TABLE XI - Continued

AM-1G BOOM SHELL, CONTOUR 1 B   1-20-73   SHELL-C USES INCH-KIP SYSTEM
COND VB-1, YAW +15, LIMIT
CASE 5.12   LOAD Y = 0.0   MXX = 81.596   FXX = -0.070
STA. 122.33   POINT Z = 8.48   MYY = -61.516   FXY = -2.957
MXZ = -492.730   FXZ = -1.134

NO.	AXIAL STRESS	M.S.	COMPONENTS OF FORCE X	Y	Z	SHEAR FLOW	SHEAR STRESS	SKIN FORCE COMP. Y	Z
1	-1.79	10.53	-0.281	0.0	0.017	0.131	2.30	-0.353	0.0
2	-4.85	3.26	-0.936	-0.012	0.058	0.138	2.43	-0.453	-0.060
3	-9.11	1.27	-2.092	-0.067	0.120	0.145	2.55	-0.463	-0.283
4	-14.19	0.46	-3.135	-0.139	0.134	0.149	2.13	-0.249	-0.442
5	-17.41	0.72	-3.718	-0.179	0.107	0.151	2.15	-0.088	-0.449
6	-17.42	0.72	-3.711	-0.185	0.053	0.149	2.13	-0.032	-0.455
7	-16.84	0.77	-3.655	-0.183	0.0	0.144	2.06	0.004	-0.454
8	-16.06	0.86	-3.549	-0.177	-0.054	0.136	1.94	0.030	-0.440
9	-12.56	0.65	-2.456	-0.118	-0.074	0.127	2.23	0.081	-0.395
10	-8.87	1.33	-1.648	-0.072	-0.072	0.119	2.08	0.201	-0.333
11	-5.80	2.56	-1.154	-0.037	-0.064	0.109	1.91	0.327	-0.206
12	-1.94	9.65	-0.382	-0.006	-0.023	0.100	1.75	0.352	-0.066
13	1.88	13.51	0.367	0.0	0.023	0.091	1.60	0.326	-0.001
14	5.65	3.83	1.112	-0.018	0.068	0.084	1.47	0.295	0.052
15	9.22	1.97	1.834	-0.059	0.102	0.078	1.36	0.234	0.141
16	11.57	1.36	2.151	-0.094	0.094	0.074	1.30	0.128	0.205
17	14.87	0.84	2.906	-0.140	0.087	0.072	1.03	0.046	0.220
18	17.51	1.26	3.868	-0.192	0.059	0.073	1.04	0.016	0.229
19	16.98	1.33	3.683	-0.185	0.0	0.077	1.10	0.002	0.233
20	16.31	1.42	3.475	-0.174	-0.050	0.084	1.20	-0.018	0.245
21	15.05	1.63	3.213	-0.155	-0.093	0.094	1.35	-0.053	0.267
22	11.17	1.55	2.468	-0.110	-0.106	0.105	1.85	-0.175	0.300
23	5.77	3.74	1.325	-0.042	-0.076	0.116	2.04	-0.367	0.212
24	1.27	20.56	0.245	-0.003	-0.015	0.125	2.19	-0.401	0.050

X-TWIST = 0.000091433 RAD./IN.   CHECKS, MXX = 81.596   FXX = -0.070   IYZ = -0.0073   AREA = 36.525
Y-CURV. = -0.00022920 RAD./IN.   MXY = -61.516   FXY = -2.957   IYY = 2714.4353   YCENT = -0.000
Z-CURV. = -0.000179301 RAD./IN.   MXZ = -492.728   FXZ = -1.134   IZZ = 2754.1482   ZCENT = 0.404

TABLE XII. TYPICAL STRESSES FOR BOOM CONCEPT 2

AH-1G BOOM SHELL, CONTOUR 2 A 1-19-73 SHELL-D USES
COND V8-1, YAW +15, LIMIT INCH-KIP SYSTEM

CASE 5.12
INPUT DATA

BASIC MODULI
STRINGER E = 4693.
SKIN G = 1263.

	STATION 122.33 COORDINATES		STATION 41.00 COORDINATES		COMP.	TENS.	CRITICAL STRESS		REL.	SKIN	SKIN			
ELEM.	Y	Z	Y	Z	AREA	AREA	COMP.	TENS.	MOD.	THICK.	MOD.	AST	CF	TF
1	0.0	12.931	0.0	17.950	0.1920	0.2199	-14.40	32.45	1.00	0.0800	1263.	0.0000	15.0	0.500
2	-2.75	12.931	-3.82	17.950	0.1920	0.2741	-14.40	32.45	1.00	0.0800	1263.	0.0000	15.0	0.500
3	-6.80	12.267	-9.28	16.750	0.1920	0.3296	-14.40	32.45	1.00	0.0800	1263.	0.0000	15.0	0.500
4	-10.02	9.679	-12.93	12.480	0.1920	0.2920	-14.40	32.45	1.00	0.0800	1263.	0.0000	15.0	0.500
5	-11.43	6.844	-14.01	8.420	0.1920	0.2696	-14.40	32.45	1.00	0.0800	1263.	0.0000	15.0	0.500
6	-12.14	3.342	-14.56	4.180	0.1920	0.2766	-14.40	32.45	1.00	0.0800	1263.	0.0000	15.0	0.500
7	-12.10	0.0	-14.60	0.0	0.1920	0.2785	-14.40	32.45	1.00	0.0800	1263.	0.0000	15.0	0.500
8	-11.65	-3.592	-14.49	-4.430	0.1920	0.2763	-14.40	32.45	1.00	0.0800	1263.	0.0000	15.0	0.500
9	-10.81	-6.772	-13.99	-8.740	0.1920	0.2527	-14.40	32.45	1.00	0.0800	1263.	0.0000	15.0	0.500
10	-9.43	-9.465	-12.76	-12.760	0.1920	0.2611	-14.40	32.45	1.00	0.0800	1263.	0.0000	15.0	0.500
11	-6.74	-11.709	-9.37	-16.240	0.1920	0.2800	-14.40	32.45	1.00	0.0800	1263.	0.0000	15.0	0.500
12	-3.38	-12.682	-4.74	-17.680	0.1920	0.2757	-14.40	32.45	1.00	0.0800	1263.	0.0000	15.0	0.500
13	0.0	-12.931	0.0	-17.950	0.1920	0.2713	-14.40	32.45	1.00	0.0800	1263.	0.0000	15.0	0.500
14	3.38	-12.682	4.74	-17.680	0.1920	0.2757	-14.40	32.45	1.00	0.0800	1263.	0.0000	15.0	0.500
15	6.74	-11.709	9.37	-16.240	0.1920	0.2800	-14.40	32.45	1.00	0.0800	1263.	0.0000	15.0	0.500
16	9.43	-9.465	12.76	-12.760	0.1920	0.2611	-14.40	32.45	1.00	0.0800	1263.	0.0000	15.0	0.500
17	10.81	-6.772	13.99	-8.740	0.1920	0.2527	-14.40	32.45	1.00	0.0800	1263.	0.0000	15.0	0.500
18	11.65	-3.592	14.49	-4.430	0.1920	0.2763	-14.40	32.45	1.00	0.0800	1263.	0.0000	15.0	0.500
19	12.10	0.0	14.60	0.0	0.1920	0.2785	-14.40	32.45	1.00	0.0800	1263.	0.0000	15.0	0.500
20	12.14	3.342	14.56	4.180	0.1920	0.2766	-14.40	32.45	1.00	0.0800	1263.	0.0000	15.0	0.500
21	11.43	6.844	14.01	8.420	0.1920	0.2696	-14.40	32.45	1.00	0.0800	1263.	0.0000	15.0	0.500
22	10.02	9.679	12.93	12.480	0.1920	0.2920	-14.40	32.45	1.00	0.0800	1263.	0.0000	15.0	0.500
23	6.80	12.267	9.28	16.750	0.1920	0.3296	-14.40	32.45	1.00	0.0800	1263.	0.0000	15.0	0.500
24	2.75	12.931	3.82	17.950	0.1920	0.2741	-14.40	32.45	1.00	0.0800	1263.	0.0000	15.0	0.500

TABLE XII - Continued

AH-1G BOOM SHELL, CONTOUR 2 A — 1-19-73 — SHELL-D USES INCH-KIP SYSTEM

COND VB-1, YAW +15, LIMIT

CASE 5.12 — LOAD Y = 0.0 — MXX = 81.596 — FXX = -0.070

STA. 122.33 — POINT Z = 8.48 — MXY = -61.516 — FXY = -2.957

MXZ = -492.730 — FXZ = -1.134

NO.	AXIAL STRESS	M.S.	COMPONENTS OF FORCE X	Y	Z	SHEAR FLOW	SHEAR STRESS	SKIN FORCE COMP. Y	Z
1	-1.32	9.90	-0.290	[illegible] 0	0.018	0.137	1.71	-0.368	0.0
2	-3.84	2.75	-1.050	-0.[illegible]14	0.065	0.143	1.79	-0.479	-0.048
3	-7.48	0.93	-2.459	-0.07[illegible]	0.136	0.147	1.84	-0.528	-0.238
4	-10.16	0.42	-2.962	-0.106	[illegible].102	0.146	1.83	-0.340	-0.398
5	-11.15	0.29	-3.003	-0.095	0.0[illegible]9	0.143	1.78	-0.154	-0.457
6	-11.43	0.26	-3.161	-0.094	0.033	0.136	1.70	-0.048	-0.478
7	-11.04	0.30	-3.074	-0.095	0.0	0.128	1.60	0.031	-0.457
8	-10.27	0.40	-2.836	-0.099	-0.029	0.117	1.46	0.078	-0.416
9	-9.18	0.57	-2.316	-0.091	-0.056	0.106	1.33	0.123	-0.329
10	-7.64	0.89	-1.990	-0.082	-0.081	0.094	1.18	0.200	-0.248
11	-4.95	1.91	-1.382	-0.045	-0.077	0.081	1.02	0.263	-0.145
12	-1.77	7.15	-0.486	-0.008	-0.030	0.071	0.88	0.257	-0.048
13	1.36	22.94	0.367	0.0	0.023	0.062	0.78	0.225	-0.001
14	4.43	6.33	1.218	-0.020	0.075	0.056	0.70	0.200	0.035
15	7.41	3.38	2.069	-0.067	0.115	0.053	0.66	0.166	0.087
16	9.63	2.37	2.510	-0.103	0.102	0.053	0.67	0.108	0.132
17	10.61	2.06	2.679	-0.105	0.065	0.056	0.70	0.06[illegible]	0.161
18	11.05	1.94	3.050	-0.106	0.031	0.062	0.77	0.037	0.200
19	11.08	1.93	3.084	-0.095	0.0	0.070	0.87	0.011	0.227
20	10.78	2.01	2.979	-0.089	-0.031	0.080	1.00	-0.027	0.257
21	9.77	2.32	2.631	-0.083	-0.051	0.092	1.15	-0.093	0.271
22	8.19	2.96	2.389	-0.0[illegible]5	-0.082	0.106	1.32	-0.235	0.267
23	4.97	5.52	1.636	-0.050	-0.090	0.121	1.51	-0.415	0.177
24	1.20	26.12	0.327	-0.004	-0.020	0.131	1.63	-0.424	0.040

X-TWIST = 0.000077049 RAD./IN. — CHECKS, MXX = 81.596 — FXX = -0.070 — IYZ = 0.0000 — AREA = 6.623

Y-CURV. = -0.000022051 RAD./IN. — MXY = -61.516 — FXY = -2.957 — IYY = 601.1584 — YCENT = 0.000

Z-CURV. = -0.000195160 RAD./IN. — MXZ = -492.733 — FXZ = -1.134 — IZZ = 539.0564 — ZCENT = 0.272

TABLE XIII. TYPICAL STRESSES FOR BOOM CONCEPT 3

AH-1G BOOM SHELL, CONTOUR 3 E   12-19-72   SHELL-D USES
COND VB-1, YAW +15, LIMIT   INCH-KI[illegible] [illegible]YSTEM

CASE 5.12
INPUT DATA

BASIC MODULI
STRINGER E = 1000.
SKIN G = 1000.

	STATION 122.33 COORDINATES		STATION 41.00 COORDINATES		COMP.	TENS.	CRITICAL STRESS		REL.	SKIN	SKIN			
ELEM.	Y	Z	Y	Z	AREA	AREA	COMP.	TENS.	MOD.	THICK.	MOD.	AST	CF	TF
1	-6.50	15.383	-6.50	20.450	0.1440	0.1440	-38.00	46.00	10.50	C.0320	4C00.	0.1440	0.0	0.0
2	-6.85	15.157	-6.85	20.250	0.1162	0.1121	-22.23	42.49	5.75	0.0820	848.	0.0000	15.0	0.500
3	-8.57	13.249	-9.65	17.350	0.2017	0.2404	-22.23	42.49	5.75	0.0820	848.	0.0000	15.0	0.500
4	-10.45	10.548	-13.00	12.500	0.2017	0.2738	-22.23	42.49	5.75	0.0820	848.	0.0000	15.0	0.500
5	-11.43	7.306	-14.01	8.420	0.2017	0.2860	-22.23	42.49	5.75	C.C820	848.	0.0000	15.0	0.500
6	-11.92	3.750	-14.56	4.180	0.2017	0.2820	-22.23	42.49	5.75	0.0820	848.	0.0000	15.0	0.500
7	-11.90	0.462	-14.60	0.0	0.2017	0.2799	-22.23	42.49	3.75	0.0820	848.	0.0000	15.0	0.500
8	-11.57	-3.061	-14.49	-4.430	0.1585	0.2459	-19.02	38.42	5.53	0.0620	955.	0.0C00	15.0	0.500
9	-10.82	-6.225	-13.99	-8.740	C.0841	0.1646	-14.12	31.02	4.87	0.0420	1164.	0.C000	15.0	0.500
10	-9.56	-8.988	-12.76	-12.760	0.0529	0.1383	-14.12	31.02	4.44	0.0420	1164.	0.0000	15.0	0.500
11	-6.97	-11.417	-9.37	-16.240	0.0529	0.1510	-14.12	31.02	4.44	0.0420	1164.	0.0000	15.0	0.500
12	-3.53	-12.598	-4.74	-17.680	0.0529	0.1508	-14.12	31.02	4.44	0.C420	1164.	0.0C00	15.0	0.5C0
13	0.0	-12.883	0.0	-17.950	C.0529	0.1485	-14.12	31.02	4.44	0.0420	1164.	0.0000	15.0	0.500
14	3.53	-12.598	4.74	-17.680	0.0529	0.1508	-14.12	31.02	4.44	0.0420	1164.	0.0000	15.0	0.500
15	6.97	-11.417	9.37	-16.240	0.0529	0.1510	-14.12	31.02	4.44	0.0420	11[illegible]	[illegible].0000	15.0	0.500
16	9.56	-8.988	12.76	-12.760	0.0529	0.1383	-14.12	31.02	4.44	0.C420	11[illegible]	[illegible].0C00	15.0	0.500
17	10.82	-6.225	13.99	-8.740	0.0841	0.1646	-14.12	31.02	4.87	0.0320	9[illegible]	[illegible].0000	15.0	0.500
18	11.57	-3.061	14.49	-4.430	0.1585	0.2459	-19.02	38.42	5.53	0.0820	84[illegible]	[illegible].0000	15.0	0.500
19	11.90	0.462	14.60	0.0	C.2017	0.2799	-22.23	42.49	5.75	C.C820	84[illegible]	[illegible].0000	15.0	0.500
20	11.92	3.750	14.56	4.180	0.2017	0.2820	-22.23	42.49	5.75	0.0820	84[illegible]	[illegible].0000	15.0	0.500
21	11.43	7.306	14.01	8.420	0.2017	0.2860	-22.23	42.49	5.75	0.0820	84[illegible]	[illegible].0000	15.0	0.500
22	10.45	10.548	13.00	12.500	0.2017	0.2738	-22.23	42.49	5.75	0.0820	848.	[illegible].0000	15.0	0.500
23	8.57	13.249	9.65	17.350	C.2017	0.2404	-22.23	42.49	5.75	0.0820	848.	0.0000	15.0	0.500
24	6.85	15.157	6.85	20.250	0.1162	0.1121	-22.23	42.49	5.75	0.0320	4000.	0.0000	15.0	0.500
25	6.50	15.383	6.50	20.450	0.1440	0.1440	-38.00	46.00	10.50	0.0320	4000.	0.1440	0.0	0.0
26	6.15	15.733	6.15	20.800	0.0418	0.1451	-14.12	31.02	4.44	0.0420	1164.	0.CCCC	15.0	0.500
27	0.0	17.933	0.0	23.0C0	0.0529	0.2743	-14.12	31.02	4.44	0.0420	1164.	0.0000	15.0	0.500
28	-6.15	15.733	-6.15	20.800	0.0418	0.1451	-14.12	31.02	4.44	0.0320	4000.	0.0000	15.0	0.500

TABLE XIII - Continued

AH-1G BOOM SHELL, CONTOUR 3 E　　12-19-72　　SHELL-D USES
COND VB-1, YAW +15, LIMIT　　INCH-KIP SYSTEM
CASE 5.12　LOAD Y = 0.0　MXX = 81.596　FXX = -0.070
STA. 122.33　POINT Z = 8.48　MXY = -61.516　FXY = -2.957
MXZ = -492.730　FXZ = -1.134

NO.	AXIAL STRESS	M.S.	COMPONENTS OF FORCE X	Y	Z	SHEAR FLOW	SHEAR STRESS	SKIN FORCE COMP. Y	Z
1	-14.24	1.67	-2.047	0.0	0.128	0.139	4.35	-0.048	-0.040
2	-8.12	1.74	-0.908	0.0	0.057	0.140	1.71	-0.145	-0.150
3	-9.57	1.32	-2.296	-0.030	0.116	0.139	1.70	-0.252	-0.322
4	-11.07	1.01	-3.029	-0.095	0.073	0.135	1.64	-0.197	-0.407
5	-11.62	0.91	-3.321	-0.105	0.045	0.126	1.54	-0.097	-0.442
6	-11.64	0.91	-3.282	-0.107	0.017	0.114	1.39	-0.030	-0.412
7	-11.21	0.98	-3.137	-0.104	-0.018	0.100	1.22	0.018	-0.364
8	-10.03	0.90	-2.465	-0.089	-0.041	0.086	1.38	0.049	-0.312
9	-7.88	0.79	-1.295	-0.050	-0.040	0.077	1.82	0.080	-0.242
10	-5.95	1.37	-0.821	-0.032	-0.038	0.069	1.64	0.139	-0.190
11	-3.74	2.78	-0.563	-0.017	-0.033	0.061	1.45	0.194	-0.120
12	-1.00	13.18	-0.150	-0.002	-0.009	0.054	1.28	0.200	-0.044
13	1.72	17.05	0.255	0.0	0.016	0.048	1.14	0.180	-0.001
14	4.38	6.09	0.659	-0.010	0.041	0.044	1.04	0.160	0.033
15	6.89	3.50	1.038	-0.031	0.062	0.041	0.97	0.128	0.075
16	8.62	2.60	1.189	-0.047	0.055	0.040	0.95	0.078	0.105
17	10.20	2.04	1.677	-0.065	0.052	0.041	0.46	0.040	0.120
18	11.90	2.23	2.923	-0.105	0.049	0.044	0.54	0.023	0.142
19	12.25	2.47	3.428	-0.114	0.019	0.052	0.63	0.008	0.164
20	11.85	2.59	3.339	-0.108	-0.018	0.062	0.76	-0.015	0.196
21	10.91	2.89	3.119	-0.099	-0.043	0.075	0.92	-0.052	0.233
22	9.54	3.45	2.609	-0.082	-0.063	0.089	1.09	-0.121	0.242
23	7.34	4.79	1.763	-0.023	-0.089	0.102	1.24	-0.172	0.218
24	5.40	6.86	0.605	0.0	-0.038	0.108	3.37	-0.107	0.109
25	9.19	4.01	1.320	0.0	-0.082	0.122	3.80	-0.040	0.033
26	3.58	7.66	0.519	0.0	-0.032	0.127	3.03	-0.413	0.161
27	-1.32	9.69	-0.362	0.0	0.023	0.136	3.23	-0.809	-0.009
28	-5.79	1.44	-0.839	0.0	0.052	0.137	4.28	-0.441	-0.173

X-TWIST = 0.000108105 RAD./IN.　CHECKS, MXX = 81.596　FXX = -0.070　IYZ = 0.0018　AREA 31.373
Y-CURV. = -0.000022336 RAD./IN.　MXY = -61.516　FXY = -2.957　IYY = 2787.0801　YCENT = 0.000
Z-CURV. = -0.000171295 RAD./IN.　MXZ = -492.728　FXZ = -1.134　IZZ = 2876.4150　ZCENT = 4.643

TABLE XIV. TYPICAL STRESSES FOR BOOM CONCEPT 4

AH-1G BOOM SHELL, CONTOUR 4 B   1-23-73   SHELL-D USES
COND VB-1, YAW +15, LIMIT   INCH-KIP SYSTEM

CASE 5.12
INPUT DATA

BASIC MODULI
STRINGER E = 1000.
SKIN G = 1000.

	STATION 122.33 COORDINATES		STATION 41.00 COORDINATES		COMP.	TENS.	CRITICAL STRESS		REL.	SKIN	SKIN			
ELEM.	Y	Z	Y	Z	AREA	AREA	COMP.	TENS.	MOD.	THICK.	MOD.	AST	CF	TF
1	-6.50	15.383	-6.50	20.450	0.1440	0.1440	-38.00	46.00	10.50	0.0320	4000.	0.1440	0.0	0.0
2	-6.85	15.157	-6.85	20.250	0.1263	0.1172	-20.80	41.69	5.74	0.0860	943.	0.0000	15.0	0.500
3	-8.57	13.249	-9.65	17.350	0.2219	0.2523	-20.80	41.69	5.74	0.0860	943.	0.0000	15.0	0.500
4	-9.87	10.220	-12.30	12.050	0.2219	0.2819	-20.80	41.69	5.74	0.0860	943.	0.0000	15.0	0.500
5	-10.84	7.105	-13.25	8.150	0.2219	0.2941	-20.80	41.69	5.74	0.0860	943.	0.0000	15.0	0.500
6	-11.31	3.557	-13.80	3.780	0.2219	0.2819	-20.80	41.69	5.74	0.0860	943.	0.0000	15.0	0.500
7	-11.26	0.582	-13.80	0.120	0.2219	0.2744	-20.80	41.69	5.74	0.0860	943.	0.0000	15.0	0.500
8	-10.99	-2.813	-13.75	-4.150	0.2219	0.2821	-20.80	41.69	5.74	0.0860	943.	0.0000	15.0	0.500
9	-10.28	-5.886	-13.30	-8.300	0.1668	0.2248	-20.24	32.80	4.96	0.0610	1187.	0.0000	15.0	0.500
10	-9.05	-8.539	-12.05	-12.200	0.1116	0.1901	-20.24	32.80	4.21	0.0610	1187.	0.0000	15.0	0.500
11	-6.67	-10.831	-9.00	-15.500	0.1116	0.2086	-20.24	32.80	4.21	0.0610	1187.	0.0000	15.0	0.500
12	-3.34	-11.999	-4.45	-16.880	0.1116	0.2098	-20.24	32.80	4.21	0.0610	1187.	0.0000	15.0	0.500
13	0.0	-12.316	0.0	-17.250	0.1116	0.2044	-20.24	32.80	4.21	0.0610	1187.	0.0000	15.0	0.500
14	3.34	-11.999	4.45	-16.880	0.1116	0.2098	-20.24	32.80	4.21	0.0610	1187.	0.0000	15.0	0.500
15	6.67	-10.831	9.00	-15.500	0.1116	0.2086	-20.24	32.80	4.21	0.0610	1187.	0.0000	15.0	0.500
16	9.05	-8.539	12.05	-12.200	0.1116	0.1901	-20.24	32.80	4.21	0.0610	1187.	0.0000	15.0	0.500
17	10.28	-5.886	13.30	-8.300	0.1668	0.2248	-20.24	32.80	4.21	0.0860	943.	0.0000	15.0	0.500
18	10.99	-2.813	13.75	-4.150	0.2219	0.2821	-20.80	41.69	4.96	0.0860	943.	0.0000	15.0	0.500
19	11.26	0.582	13.80	0.120	0.2219	0.2744	-20.80	41.69	5.74	0.0860	943.	0.0000	15.0	0.500
20	11.31	3.557	13.80	3.780	0.2219	0.2819	-20.80	41.69	5.74	0.0860	943.	0.0000	15.0	0.500
21	10.84	7.105	13.25	8.150	0.2219	0.2941	-20.80	41.69	5.74	0.0860	943.	0.0000	15.0	0.500
22	9.87	10.220	12.30	12.050	0.2219	0.2819	-20.80	41.69	5.74	0.0860	943.	0.0000	15.0	0.500
23	8.57	13.249	9.65	17.350	0.2219	0.2523	-20.80	41.69	5.74	0.0860	943.	0.0000	15.0	0.500
24	6.85	15.157	6.85	20.250	0.1263	0.1172	-20.80	41.69	5.74	0.0320	4000.	0.0000	15.0	0.500
25	6.50	15.383	6.50	20.450	0.1440	0.1440	-38.00	46.00	10.50	0.0320	4000.	0.1440	0.0	0.0
26	6.15	15.733	6.15	20.800	0.0418	0.1451	-14.12	31.02	4.44	0.0420	1164.	0.0000	15.0	0.500
27	0.0	17.933	0.0	23.000	0.0529	0.2743	-14.12	31.02	4.44	0.0420	1164.	0.0000	15.0	0.500
28	-6.15	15.733	-6.15	20.800	0.0418	0.1451	-14.12	31.02	4.44	0.0320	4000.	0.0000	15.0	0.500

TABLE XIV - Continued

AH-1G BOOM SHELL, CONTOUR 4 B 1-23-73 SHELL-D USES

COND VB-1, YAW +15, LIMIT INCH-KIP SYSTEM

CASE 5.12	LOAD Y = 0.0	MXX =	81.596	FXX =	-0.070
STA. 122.33	POINT Z = 8.48	MXY =	-61.516	FXY =	-2.957
		MXZ =	-492.730	FXZ =	-1.134

NO.	AXIAL STRESS	M.S.	COMPONENTS OF FORCE X	Y	Z	SHEAR FLOW	SHEAR STRESS	SKIN FORCE COMP. Y	Z
1	-14.55	1.61	-2.091	0.0	C.130	0.145	4.54	-0.050	-0.04[illegible]
2	-8.28	1.51	-0.969	0.0	0.061	0.146	1.70	-0.151	-0.154
3	-9.79	1.13	-2.466	-0.033	0.124	0.145	1.68	-0.220	-0.359
4	-10.72	0.94	-3.019	-0.090	0.068	0.140	1.63	-0.162	-0.438
5	-11.30	0.84	-3.323	-0.059	C.043	0.132	1.54	-0.099	-0.453
6	-11.33	0.84	-3.193	-0.098	0.009	0.121	1.41	-0.028	-0.415
7	-10.91	0.91	-2.993	-0.093	-0.017	0.109	1.26	0.017	-0.365
8	-10.21	1.04	-2.878	-0.098	-0.047	0.094	1.09	0.048	-0.328
9	-7.86	1.57	-1.765	-C.C66	-C.052	0.082	1.35	0.084	-0.253
10	-5.52	2.67	-1.047	-0.039	-0.047	0.073	1.20	0.138	-0.193
11	-3.52	4.74	-0.733	-0.021	-0.042	0.064	1.05	0.195	-0.122
12	-0.93	20.78	-0.195	-0.CC3	-0.012	0.056	0.92	0.201	-0.046
13	1.59	19.62	0.325	0.0	0.020	0.050	0.82	0.178	-0.001
14	4.05	7.10	0.848	-0.012	0.051	0.046	0.75	0.159	0.035
15	6.43	4.10	1.338	-0.038	0.077	0.043	0.71	0.127	0.076
16	8.00	3.10	1.517	-C.C56	C.068	0.043	0.71	0.078	0.107
17	8.66	2.79	1.944	-0.072	0.058	0.045	0.52	0.042	0.126
18	10.49	2.97	2.957	-0.100	0.049	0.049	0.58	0.023	0.153
19	11.98	2.48	3.287	-0.102	C.019	0.058	0.67	0.008	0.170
20	11.65	2.58	3.282	-0.1C1	-C.009	C.068	0.79	-0.015	0.206
21	10.72	2.89	3.152	-0.094	-0.041	0.081	0.94	-0.055	0.247
22	9.35	3.46	2.634	-0.079	-0.059	G.095	1.11	-0.131	0.271
23	7.65	4.45	1.928	-0.026	-0.097	0.109	1.26	-0.155	0.248
24	5.66	6.36	0.663	0.0	-0.041	0.115	3.59	-0.114	0.117
25	9.65	3.76	1.388	0.0	-0.086	0.128	4.01	-0.043	0.035
26	3.77	7.22	0.546	0.0	-0.034	0.134	3.19	-0.435	0.170
27	-1.28	9.99	-0.352	0.C	C.022	0.142	3.38	-0.849	-0.009
28	-5.91	1.39	-0.856	0.0	0.053	0.143	4.47	-0.461	-0.181

X-TWIST = 0.000101867 RAD./IN.	CHECKS, MXX =	81.596	FXX =	-0.070	IYZ =	33.2839	AREA =	33.835
Y-CURV. = -0.000C22178 RAD./IN.	MXY =	-61.516	FXY =	-2.957	IYY =	3076.7991	YCENT =	-0.123
Z-CURV. = -0.000176967 RAD./IN.	MXZ =	-492.728	FXZ =	-1.134	IZZ =	2788.2927	ZCENT =	3.922

STIFFNESS

The three boom contours differ appreciably in their efficiency for stiffness. Table XV summarizes the results of a preliminary study to assess the relative efficiencies, wherein section properties were determined for a shell of uniform moduli and uniform thickness of .01 inch. The columns of relative properties for equal areas in Table XV may be interpreted as factors for an increase in effective modulus due to geometry. The improvements are significant, particularly in torsion and lateral bending.

TABLE XV. SECTION PROPERTIES FOR UNIFORM SHELLS

Boom Sta.	Contour	Area ($in.^2$)	Area Properties ($in.^4$) J	I_y	I_z	Relative Properties for Equal Areas J	I_y	I_z
80.4	1	.953	198.8	123.9	90.9	1.0	1.0	1.0
	2	.968	213.6	126.0	100.2	1.06	1.0	1.08
	3	1.023	245.5	161.3	104.9	1.15	1.21	1.07
122.4	1	.795	115.2	71.8	52.7	1.0	1.0	1.0
	2	.828	137.0	72.4	67.3	1.14	.97	1.23
	3	.885	163.2	102.4	71.1	1.27	1.31	1.21
164.2	1	.635	59.1	36.8	27.0	1.0	1.0	1.0
	2	.694	81.2	41.1	43.1	1.26	1.02	1.46
	3	.749	101.7	60.1	45.8	1.46	1.39	1.44
194.3	1	.522	32.7	20.4	15.0	1.0	1.0	1.0
	2	.602	52.1	24.6	30.4	1.38	1.04	1.76
	3	.653	68.7	38.4	32.1	1.68	1.50	1.71

Detailed analyses using the appropriate materials for each concept were also made. The results are shown and compared to the unbuckled section properties for the existing structure in Figures 35 through 40. The unbuckled properties were calculated from data presented in reference 3. Calculations are required because the section properties presented in reference 3 are the buckled properties corresponding to limit load conditions. To obtain the unbuckled properties, new calculations were made using the tension areas for each element as reported in reference 3.

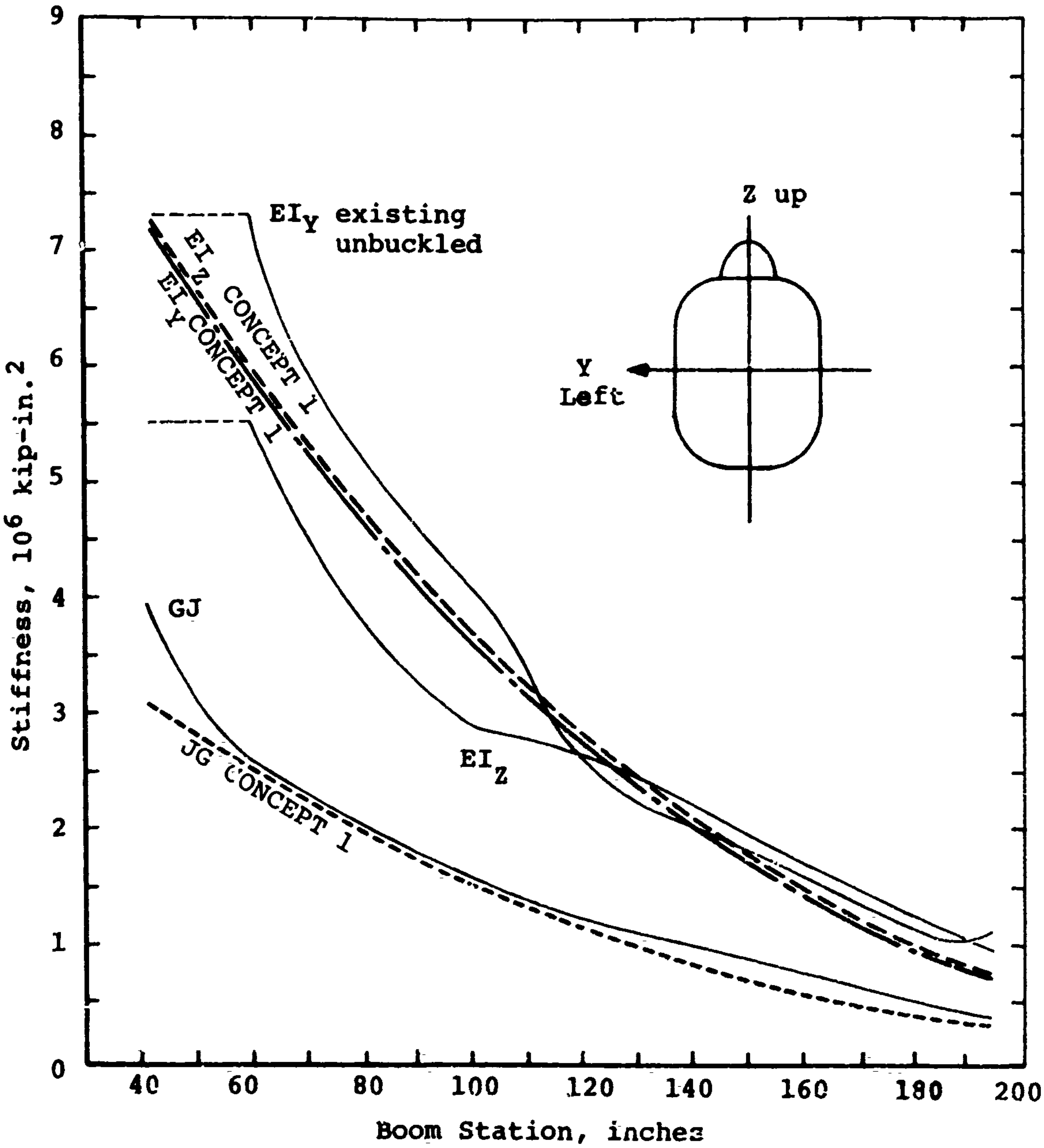

Figure 35. Section Properties for Existing Boom and Boom Concept 1.

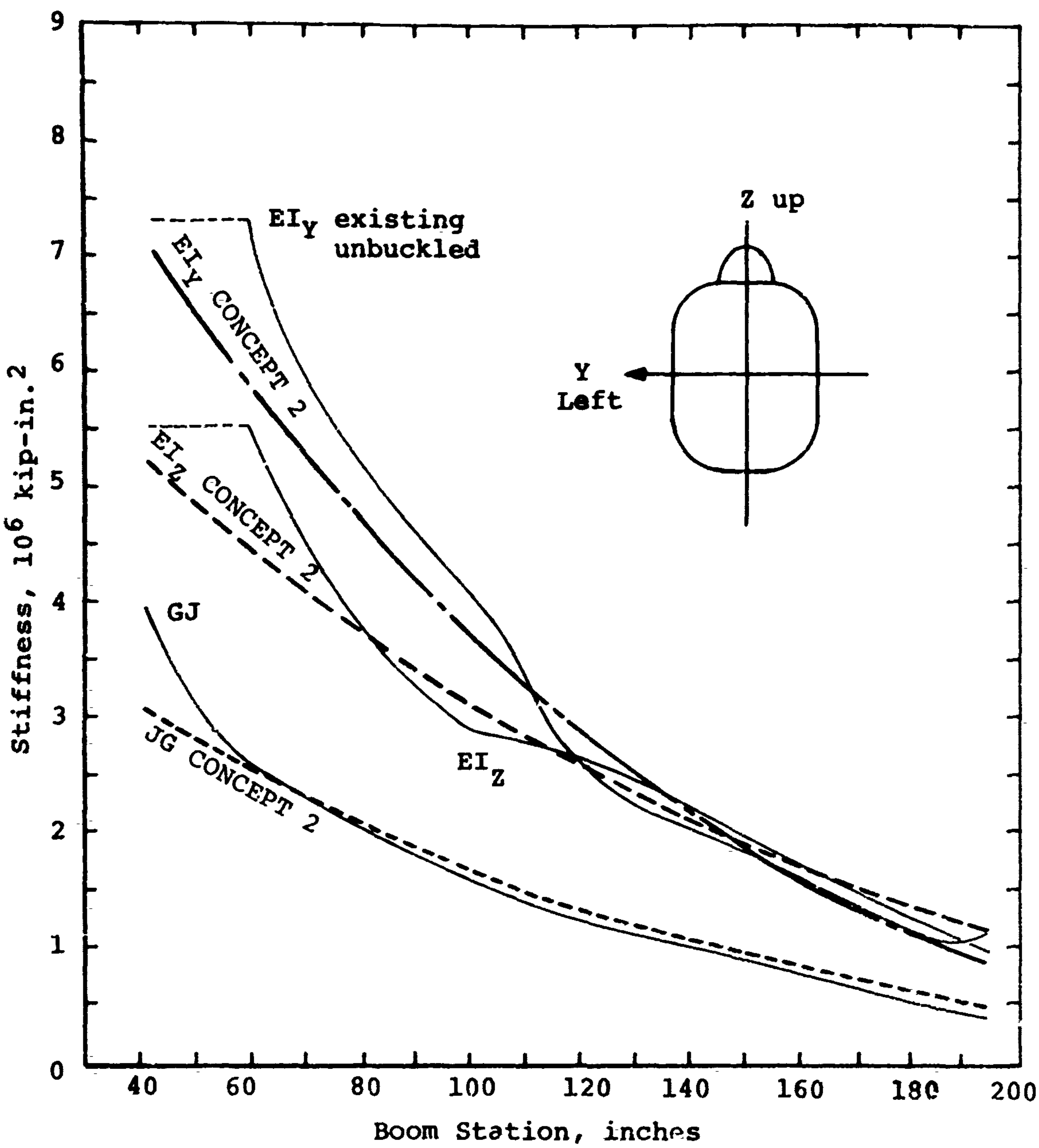

Figure 36. Section Properties for Existing Boom and Boom Concept 2.

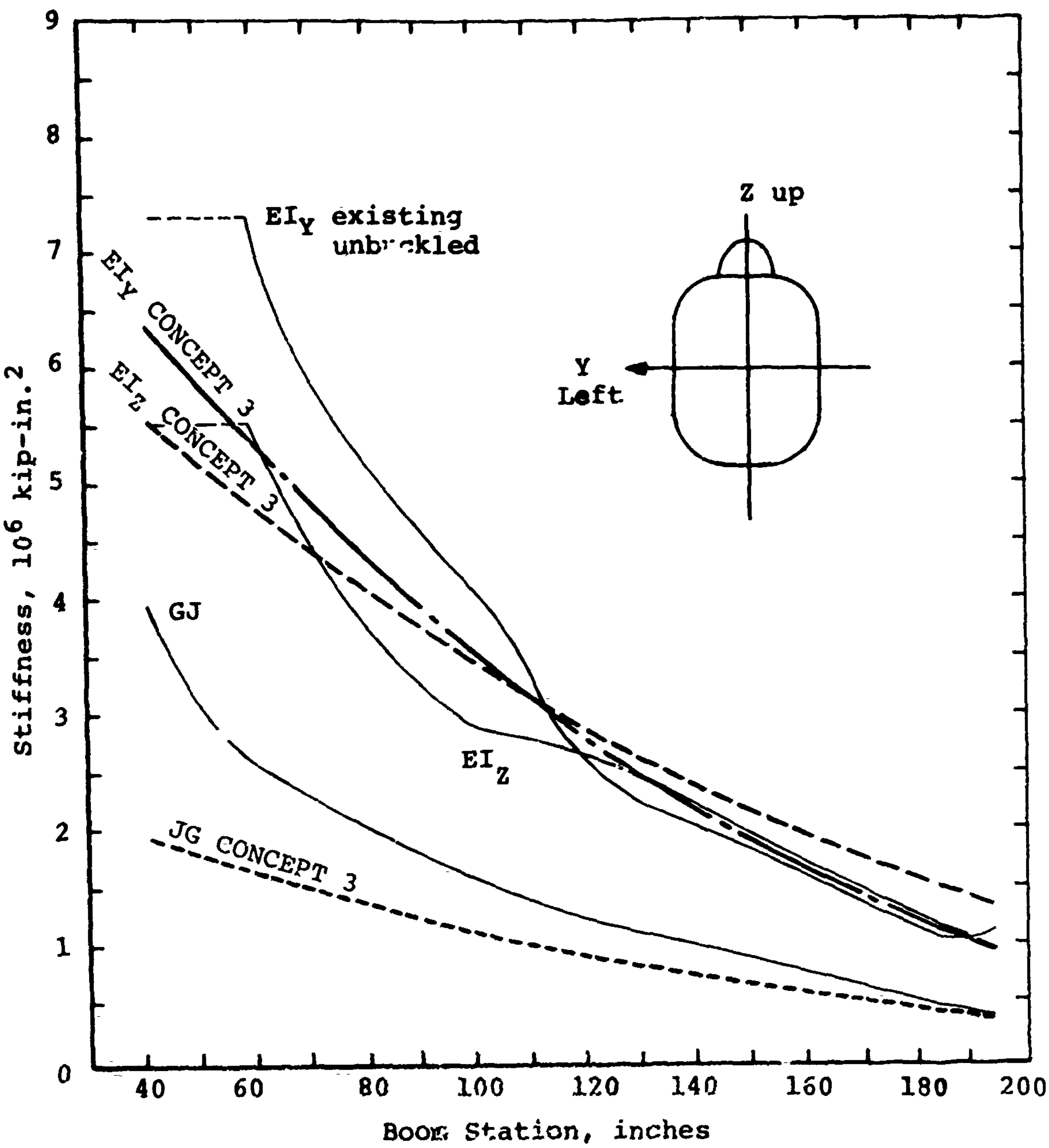

Figure 37. Section Properties for Existing Boom and Boom Concept 3.

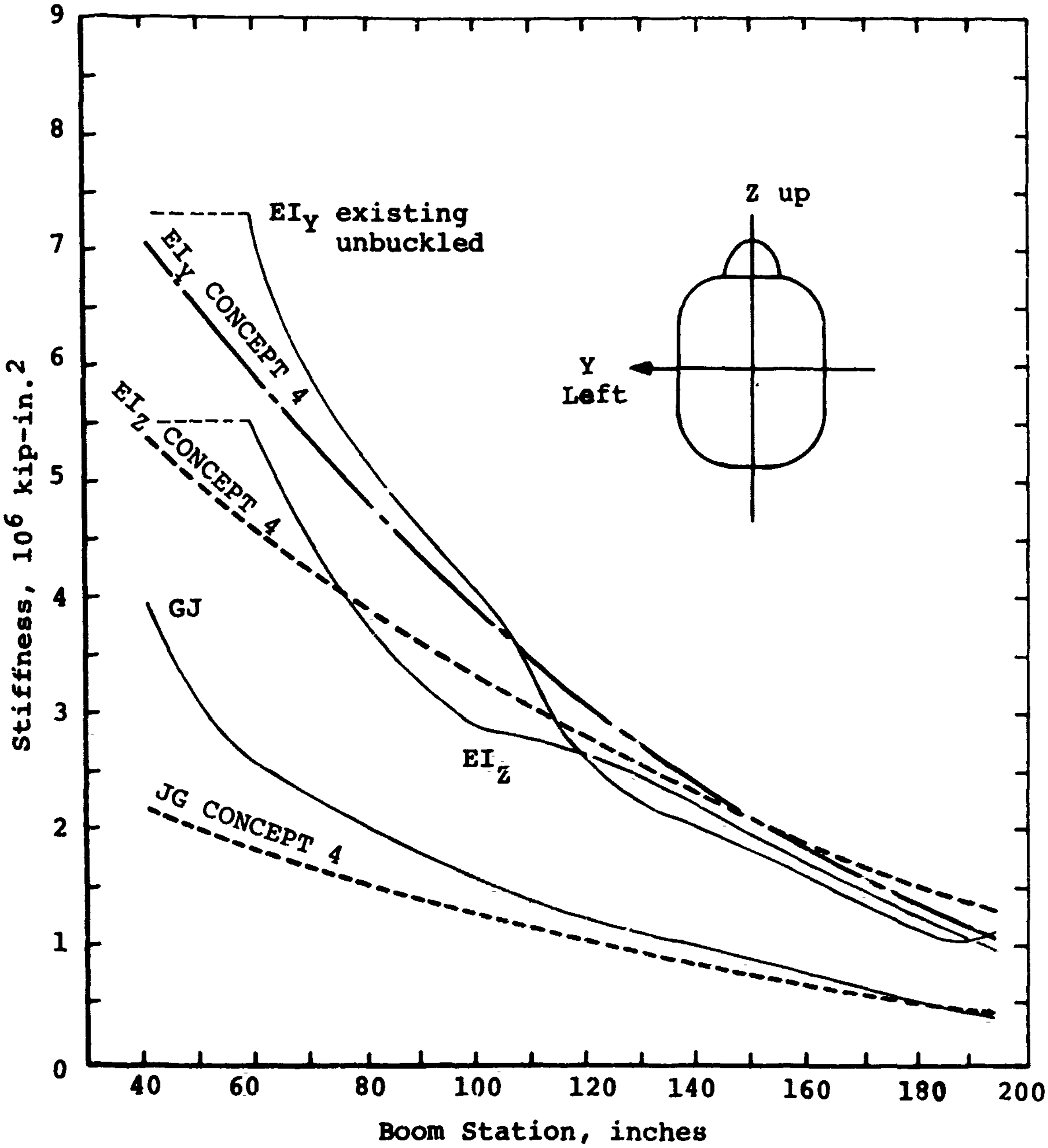

Figure 38 . Section Properties for Existing Boom and Boom Concept 4.

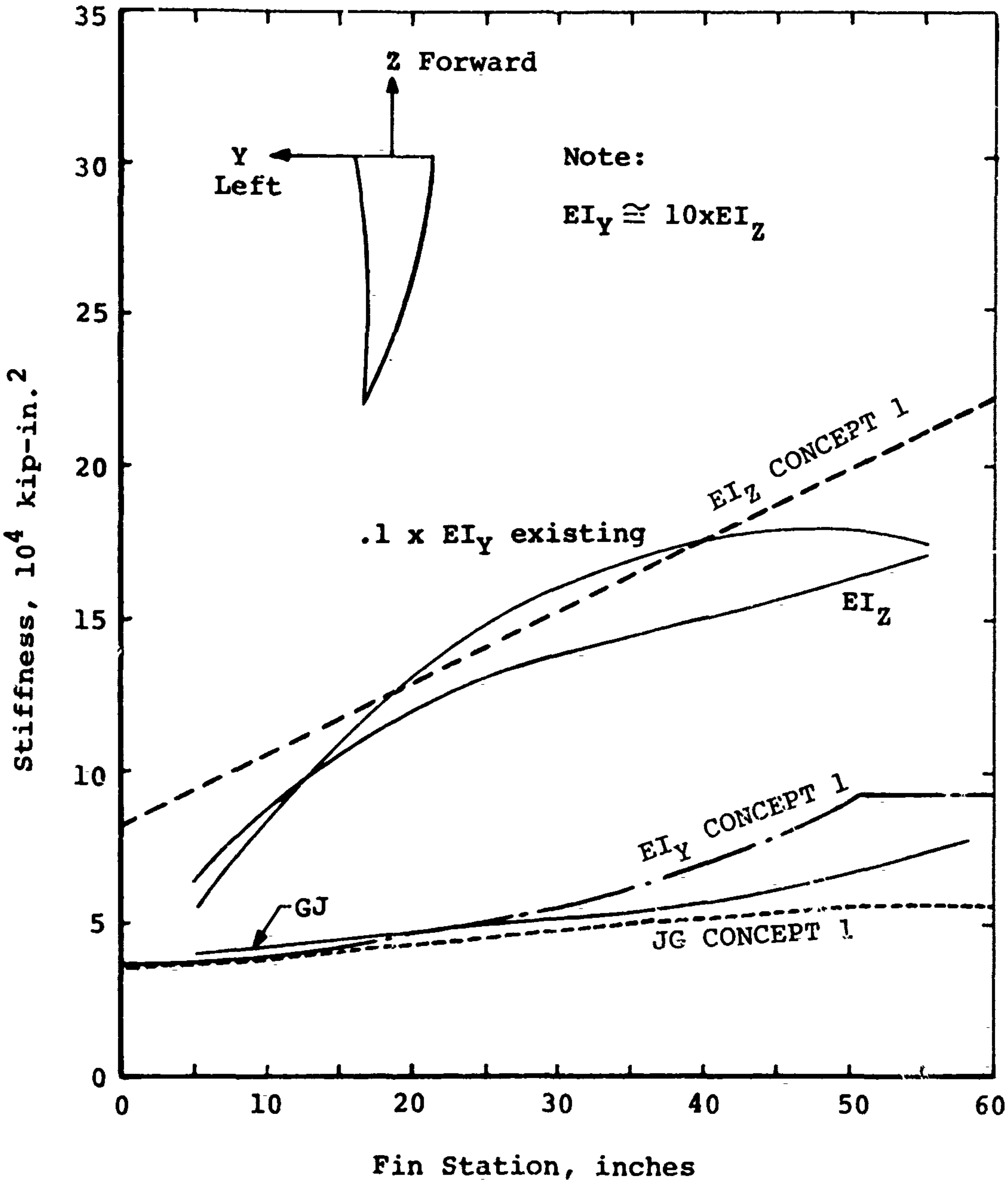

Figure 39. Section Properties for Existing Fin and Fin Used in Boom-Fin Concept 1.

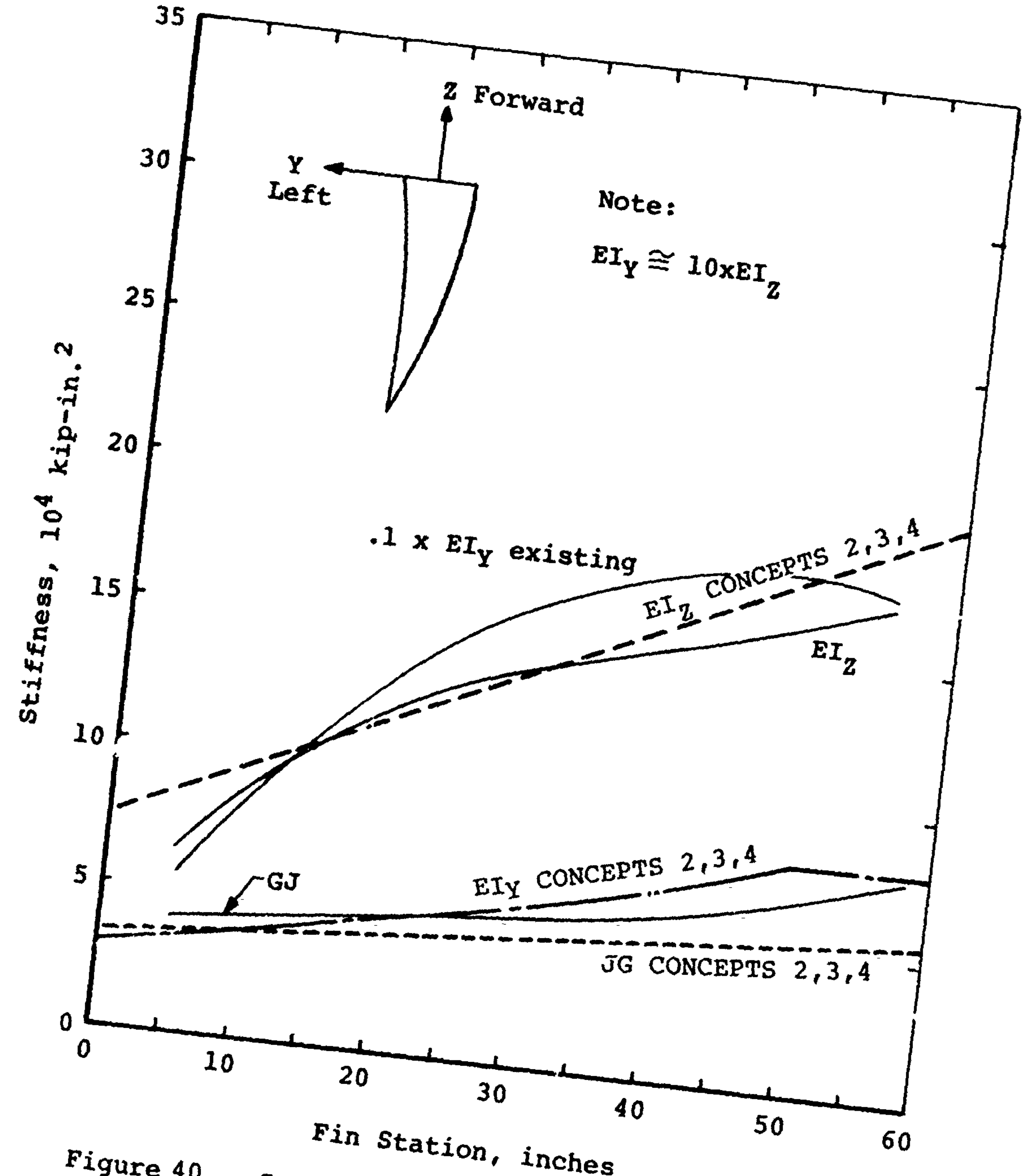

Figure 40 . Section Properties for Existing Fin and Fin Used in Boom-Fin Concepts 2, 3, and 4.

It is apparent from Figures 35, 36, and 39 that concepts 1 and 2 approximately match the stiffness of the existing unbuckled structure at every station. Concepts 3 and 4, however, deviate significantly from the existing structure. In general, the torsional stiffness is less than that of the existing boom and the lateral stiffness is slightly higher than that of the existing boom. Additional analysis shows that these deviations are self compensating, and that the entire boom-fin assembly has essentially the same stiffness as the existing structure. For example, if boom-fin concept 3 and the existing assembly were each cantilevered from a rigid wall and loaded with a 1-kip load at the 90° gearbox, the following deflections and rotations at the 90° gearbox would occur:

1. vertical deflection from a vertical load
   1.136 inches for the existing design
   1.262 inches for concept 3

2. lateral deflection from a lateral load
   2.81 inches for the existing design
   2.65 inches for concept 3

3. angular rotation (change in angle of attack) of the fin from a lateral load
   1.062 degrees for the existing design
   1.064 degrees for concept 3

Additional calculations were made to provide some insight into the relative importance of the stiffnesses of the boom and the fin. Of particular interest is the question: what are the origins of lateral deflection at the 90° gearbox in response to lateral load at the 90° gearbox? In the existing structure the following are the origins:

44.3% from lateral bending of the boom
19.6% from torsional twisting of the boom
33.7% from lateral bending of the fin
2.4% from torsional twisting of the fin

These percentages help in visualizing the consequences of changes in a particular component of stiffness. In one respect, however, the percentages do not reflect the full significance of the lateral stiffness of the fin itself. Lateral stiffness of the fin is strongly coupled to changes in angle of attack because of the sweepback of the fin. Lateral bending of the fin in response to a control input produces a change in angle of attack of the fin that would in forward flight produce air loads that reduce the effectiveness of the control input. The significant fact is that the control "feel" of the aircraft can be affected by the lateral bending

stiffness of the fin.

One additional feature of the new design is noteworthy. In the new fin concepts described herein, the elastic axis of the fin moves forward to approximately the location of the forward spar. This is advantageous because it is more nearly in line with the line of action of the lateral loads on the fin, resulting in less torsional deflection.

WEIGHT

Table XVI lists the calculated weights for each of the new design concepts. It can be seen that the designs include a significant allowance of 15 pounds in concepts 1, 2, and 3, and 21 pounds in concept 4 under the category of "Other" to account for miscellaneous reinforcement, fasteners, brackets, etc. The allowance for concept 4 is larger to account for sandwich reinforcement around the top opening.

TABLE XVI. WEIGHTS FOR NEW CONCEPT ASSEMBLIES (LB)				
	Concept			
Item	1	2	3	4
Shell, BS 41 to BS 194	51.15	80.43	72.04	71.62
BS 194 to FS 50	14.12	20.51	17.96	17.84
FS 50 to FS -22.5	17.36	19.98	19.80	19.78
Covers, fin and 42^{O} gearbox	5.15	5.15	5.15	5.15
Electronics shelf	3.66	3.66	3.66	3.66
Elevators, concept 4	23.00	23.00	23.00	23.00
Bulkheads and frames	8.90	8.90	9.50	9.50
Bumper, aux. tail gear	4.50	4.50	4.50	4.50
Fittings, BS 41	4.40	4.40	4.40	4.40
Exterior finish	3.20	3.20	3.20	3.20
Penalties	3.75	3.75	2.50	2.50
Covers, boom, concept 3	8.20	8.20	0.00	0.00
Fasteners, boom opening	.00	.00	2.41	2.41
Other	15.00	15.00	15.00	21.00
Lightning protection	10.00	.00	.00	.00
Total Weight	1[illegible].39	200.68	183.12	188.56

RELIABILITY ANALYSIS

The reliability analysis consists primarily of performing failure mode and effects analyses of those boom-fin, elevator and secondary structure design concepts selected for detailed evaluation in order to estimate qualitatively the reliability of advanced aft-fuselage designs compared to the existing AH-1G structure. The results are then applied to available historical failure data, and quantitative reliability estimates are generated for input to the life-cycle cost evaluation model.

Detailed tabulations of the results of the failure mode and effects analyses are presented in Tables XXV through XXVII of Appendix II. A discussion of these results for the boom-fin, elevator and secondary structure design concepts considered is presented in the following paragraphs.

BOOM-FIN FAILURE MODE AND EFFECTS ANALYSIS

Failure mode and effects analyses (FMEA) have been performed for each of the four boom-fin concepts selected for detailed evaluation. In performing these analyses, it was evident that the structural design features which significantly affect reliability are quite similar for the four concepts. The conceptual design level FMEA applied during this program does not involve sufficient quantitative analysis to permit easy recognition of slight differences in failure modes and effects among the competing design concepts. For this reason, and to avoid repetitive listing of identical failure modes, a single boom-fin FMEA is presented in Table XXV. This FMEA is applicable to the four design concepts under evaluation and makes liberal use of notes throughout the failure mode tabulation to indicate those differences among the concepts which should be highlighted.

Table XXV shows that the failure probability codes assigned to the assumed failure modes are all quite low, either class C or class D. This is so primarily because the possibility of these failures occurring was considered during the design process, and specific design features were incorporated in the boom-fin concepts to eliminate, or at least to minimize, the probability of such failures. For example, metal-to-metal contacts are used at all attachment and fastening points, wherever possible, to minimize the probability of loosening and wear at these locations, even when this requires the insertion of the metal into the outer skin during the bonding process. Similarly, the outer skins of the advanced concepts have been designed with sufficient strength to tolerate delamination, bond separation, punctures and tears over small areas with no significant effect on the load-carrying capability of the skin.

The large majority of assumed failures listed in Table XXV have little effect on safety of flight and have been assigned criticality codes in the negligible and/or marginal categories. The only failures which might be serious enough to be categorized as critical or catastrophic involve fracture and/or buckling of the outer skin or internal frames/bulkheads, or the loss of frame to skin attachments; however, these failures are all assigned to class D, indicating that they are not expected to occur during the service life of the aircraft. The design strength of the advanced boom-fin concepts makes failures of this type extremely unlikely.

As mentioned previously, there appear to be only slight differences in the predicted reliability of the advanced boom-fin concepts evaluated. The thickness of the fiberglass sandwich outer skin of concepts 2 and 3 is dictated by stiffness requirements, and as a result, this skin is actually stronger than the advanced composite sandwich skin of concept 1. Thus concepts 2 and 3 exhibit greater resistance to cracks, fractures, buckling, dents and punctures. The corrugated fiberglass laminated skin of concept 4 is judged to be superior in resistance to delamination and is also highly dent resistant. On the other hand, concepts 3 and 4 have a larger envelope because of the location of the drive train within the shell. These concepts also require an increased number of mechanical fasteners to secure the panels. Concepts 1 and 2, however, mount the drive train on top of this primary structure shell and require secondary structure covers to enclose it. In general, it is felt that the concepts utilizing fiberglass skin construction are more desirable from a reliability standpoint than concept 1, which uses an advanced composite sandwich skin. However, at this stage of the design process there is little basis for establishing differences in the reliability of the three boom-fin concepts that utilize fiberglass skins.

Any one of the four advanced boom-fin concepts should produce a structure with reliability characteristics significantly superior to the existing AH-1G metal boom-fin. This increased reliability results primarily from a reduction in the total number of parts, a reduction in the number of mechanical fasteners used, the elimination of production operations, and simplification of assembly. Each of the advanced concepts yields a clean structure with high fatigue strength and excellent resistance to impact damage. Structural efficiency and long fatigue life are enhanced by the absence of a mechanical joint between the boom and the fin and by the improved design of removable panels and covers.

ELEVATOR FAILURE MODE AND EFFECTS ANALYSIS

The FMEA for the four elevator advanced design concepts selected for detailed evaluation is presented in Table XXVI. For the same reasons cited in discussing boom-fin failure modes and effects, a single FMEA applicable to all four elevator concepts has been tabulated.

As a result of design efforts to maximize the resistance of elevator concepts to both inherent and external failure causes, all assumed failures listed in Table XXVI have been categorized as either class C or class D failures. This indicates that their probabilities of occurrence are relatively low. In addition, it is noted that almost all of the assumed failures have been assigned to either the negligible or the marginal criticality categories, the one exception being inherent crack or fracture failures of the elevator spar resulting from overload or fatigue. Since this type of failure is difficult to detect in its early stages, it is conceivable that a serious fracture failure might eventually occur sequentially from an initial minor crack. In the most extreme case imaginable, separation of the elevator from the aircraft could result, which warrants categorization of spar fractures as possible critical failures. All elevator design concepts, including the existing AH-1G elevator design, are susceptible to this failure mode. Again, it is pointed out here that spar crack/fracture failures have been recognized as a potentially critical failure mode, and every effort has been made to preclude the occurrence of such failures in evolving the elevator design concepts. Thus, it is unlikely that serious spar fracture failures will be experienced during the service life of the aircraft.

Improved reliability has been a factor of prime concern in developing each of the elevator advanced design concepts; because of this, the differences in predicted reliability among the four concepts evaluated are expected to be small. An aluminum tube and two ribs are the main load-bearing members in concept 1. The leading- and trailing-edge outer skin of this design is well supported and lightly loaded. As a result, concept 1 is not likely to experience cracks, fractures or buckling of the outer skin from inherent causes. Furthermore, the increased thickness of the leading edge increases its resistance to damage from foreign object impacts. Concept 2 is similar to concept 1; however, the one-piece, D-shaped spar eliminates the leading edge to spar bond found in concept 1. Concept 3 utilizes a fiberglass spar bonded to a one-piece, load-carrying skin. This design eliminates the buried outer rib and is more resistant to impact damage because of the increased strength of the outer skin. Concept 4 is unique in

that it uses only two pieces: the elevator itself and the end fitting. This is a highly reliable design since it is completely integral and involves only primary bonds. A redundant feature is provided by the two spars of the box beam. Stainless steel bearing plates, interleaved in the caps of the box beam, aid in the transfer of load to the fitting at the root. The end fitting is a forging with integral lugs and attachment fittings, thus eliminating metal-to-metal bonding operations found in the other elevator concepts.

Although these advanced elevator design concepts exhibit wear, fretting and corrosion failures similar to those experienced by the existing elevator and will utilize essentially the same one-bolt attachment to the control shaft, it is evident from the preceding discussion that each of the advanced concepts incorporates features which result in an improvement in reliability compared to the existing AH-1G elevator design, through the principles of parts reduction, elimination of fabrication operations, and simplified assembly.

COVER FAILURE MODE AND EFFECTS ANALYSIS

Table XXVII presents the FMEA for four secondary structure drive-shaft cover design concepts that have been selected for evaluation. As was done previously for the boom-fin and elevator, a single FMEA is applied to the four drive-shaft cover concepts, with appropriate notes being used to highlight differences among the concepts. The data of Table XXVII show that none of the failure modes assumed for the drive-shaft covers will seriously affect aircraft performance; therefore, all have been assigned to the negligible criticality category. The success of attempts made during the design effort to minimize failure occurrences is evidenced by the fact that most of the drive-shaft cover failures listed in the FMEA are not expected to occur in service and have been assigned to probability class D. The remainder of the failures are considered to be random occurrences, and thus they are ranked in probability class C. These include fastener wear and fretting and battle damage for all four concepts evaluated, torn hinges for those concepts using polypropylene hinges, and foreign object damage for the two fiberglass design concepts.

There is considerable similarity in the reliability aspects of the four drive-shaft cover design concepts, but there are also differences which uniquely affect reliability. All use the same type quick-release fasteners and overlap adjacent covers, so each is mechanically entrapped in the event of a fastener failure. Overlapping the covers also precludes foreign matter being carried by the airstream from blowing in under the covers.

Concept 1 is a fiberglass sandwich composite structure bolted at the corners on one side to a short-length aluminum hinge which in turn is bolted to the fuselage at two points. Adjacent covers are attached to the same hinge. Since the covers can be removed without extracting the hinge pin, the pin can be locked in place. Although this hinge is of heavy gauge aluminum and uses a cadmium-plated steel hinge pin, it might still experience wear, fretting and corrosion failures to some degree.

Concepts 2, 3 and 4 all use a full-length one-piece polypropylene molded hinge. This type of hinge is not susceptible to wear, fret and corrosion failures; however, possible tearing of the hinge is of some concern, particularly at very low temperatures. As a precautionary measure, a thin-gauge stainless steel rip-stopper is used at the leading fastener hole of each polypropylene hinge to limit any tearing that might occur. In concept 2 the hinge is riveted to the laminated fiberglass cover. Concepts 3 and 4 are molded in one piece so that the hinge is an integral part of the cover, along one edge in concept 3 and along both edges in concept 4. This design eliminates hinge-to-cover attachment problems.

Concept 1 is susceptible to bond separation failures, while both concepts 1 and 2 might experience delamination failures at the edges of the cover. Because concepts 3 and 4 are molded polypropylene, neither is susceptible to either of these failure modes. In addition, the resiliency of polypropylene makes both concepts 3 and 4 relatively immune to puncture/tear and foreign object damage. Since concept 4 does not have a stiff lateral load path, as provided in concept 3 by the molded-in arch-shaped stiffeners extending all the way to the fastener holes at the free edge, it will be subject to more hinge flexing and will probably be fabricated in a heavier gauge. This will further enhance the resistance of concept 4 to external damage events.

Based on these considerations, it seems possible that concepts 3 and 4 might prove to be somewhat more desirable from a reliability standpoint than either concept 1 or 2. However, all four of the advanced concepts evaluated show promise of increased reliability compared to the existing AH-1G drive-shaft cover designs, due primarily to reduction in the number of parts and fasteners, choice of material, and simplified assembly.

These advanced design concepts are also under consideration for secondary structure fairing and access door applications. Thus, fairings and access doors are expected to exhibit essentially the same failure modes and effects as the drive-shaft covers. No separate FMEA is presented here for the fairings

and access doors, since the FMEA for the drive-shaft covers shown in Table XXVII is also applicable to other secondary structure components using the same design concepts.

The FMEA for the tail skid secondary structure is summarized in Table XXVII. The simple steel tube structure of the tail skid is susceptible to very few failure modes, none of which is considered serious enough to warrant a criticality code classification beyond marginal. Of the three assumed failure modes tabulated, corrosion and battle damage are expected to be highly unlikely occurrences for the tail skid and have been grouped in probability class L. Should a projectile hit result in a hole in the tail skid tube, the tube should be replaced; thus, battle damage is assigned a possible marginal criticality code as indicated in Table XXVII. A bent tail skid tube caused by a hard landing is considered to be a random occurrence and is assigned to probability class C. If the tube is bent severely, it should be replaced; therefore, a marginal criticality code is appropriate for this failure mode.

The proposed tail skid design concept does not differ radically from the existing AH-1G tail skid; however, a bending failure of the new design is less likely to result in the fuselage structure's contacting the ground. This in itself is a noteworthy reliability improvement.

RELIABILITY ESTIMATES FOR ADVANCED DESIGN CONCEPTS

In discussing the failure mode and effects analyses for the boom-fin, elevator and secondary structure advanced design concepts, it was noted that all the concepts under consideration are expected to result in a significant reliability improvement compared to the existing AH-1G aft-fuselage structure. Possible areas of improved reliability have been mentioned based on a qualitative assessment of the proposed design concepts. However, in order to evaluate the reduction in program costs that can be achieved by using an advanced aft-fuselage design for the AH-1G, it is necessary to derive a quantitative reliability comparison. Reliability estimates for the existing AH-1G aft fuselage and for the promising advanced design concepts can be made based on available 3M data for the AH-1G/J helicopter.

The most recent available 3M data summary of the detailed maintenance actions list for Marine Corps AH-1G/J aircraft tabulates all recorded malfunctions/failures for the two-year period from June 1969 through July 1971. Since the aft-fuselage section is listed as a segregated work unit code in this summary, all the failure modes of interest are conveniently grouped together. Under the aft-fuselage work unit code, the recorded malfunction/failure events are classified among approximately

twenty-five malfunction codes. For the purpose of this analysis, these events have been reapportioned among nine general categories which correspond more closely to the assumed failure modes of the boom-fin, elevator and secondary structure FMEA's discussed previously. Table XVII shows the 3M failure/damage data grouped under these nine categories, as well as the percentage of total events falling within each category. The two-year period covered by the 3M data involved a total of 23,948 flight hours. Thus, the 225 failures recorded during this period yield a mean time between failures of 106.4 hours. The data given in Table XVII provide a basis for estimating the number of malfunctions/failures and the coincident MTBF that might be expected for the advanced aft-fuselage design concepts, operating under the same conditions, through the application of engineering judgment and a detailed knowledge of the promising concepts.

As noted previously, the advanced aft-fuselage design concepts selected for evaluation are all expected to exhibit improved reliability characteristics compared to the existing AH-1G aft fuselage, resulting primarily from their common advantageous features of a reduction in total number of parts and total number of mechanical fasteners used, elimination of production operations, and simplification of assembly. In general, differences expected in reliability among the various aft-fuselage design concepts themselves are difficult to evaluate at the conceptual design level of analysis. One significant difference is noted, however, in that the outer skin of the fiberglass boom-fin concepts is stronger than the outer skin of the advanced composite boom-fin concept. Because of this, the fiberglass designs of boom-fin concepts 2, 3 and 4 offer greater resistance to cracks, fractures, buckling, dents and punctures than the advanced composite design of boom-fin concept 1. In addition, the technology involved in fabrication and production of fiberglass structures is further developed than the corresponding technology for advanced composite materials. For these reasons it is possible to distinguish between the fiberglass and advanced composite skin structures in estimating the expected number of malfunction/failure events from the 3M data of Table XVII.

Table XVIII presents the predicted number of malfunction/failure events for advanced aft-fuselage designs using the fiberglass outer skin of boom-fin concepts 2, 3 or 4, based on estimated percentage reductions in the number of events recorded in the 3M data as indicated for each of the nine failure event categories. A reduction of 70 percent is estimated for broken/loose/missing hardware failures because of the reduction in total number of parts and particularly in the number of mechanical fasteners used in the advanced design concepts. In the

crack/fracture/buckling category, the estimated reduction is 60 percent, due primarily to the increased skin strength of the fiberglass designs. Note that these two categories, where the largest percentage reductions in the number of malfunction/failure events are expected, account for more than half the total events recorded. Reductions are estimated to be 50 percent in the wear category due to design features for minimizing wear, and 50 percent in the foreign object damage and puncture/tear categories due to inherent skin strength; while 30 percent reductions are estimated for the corrosion and improper adjustment/alignment categories. The noncorrosive properties of fiberglass are responsible for the estimated reduction in corrosion failures, and fewer number of mechanical fasteners and simplified assembly account for the estimated reduction in improper adjustment/alignment failures. All predicted reductions in the number of malfunction/failure events are considered to be conservative, but reasonable. No reductions are estimated for the number of events in the battle damage and no defect categories in the interest of maintaining this conservative approach. The resulting number of predicted malfunction/failure events for the fiberglass skin aft-fuselage designs is 116.9, which yields a mean time between failures of 204.9 hours.

The aft-fuselage design using the advanced composite skin of boom-fin concept 1 is considered in Table XIV. Here it is noted that the estimated reduction in the number of malfunction/failure events for the advanced composite skin design is the same as that for the fiberglass skin designs for all failure categories except those where failure occurrences depend on the strength of the fuselage outer skin; namely, crack/fracture/buckling, foreign object damage, and puncture/tear. Because the advanced composite outer skin of boom-fin concept 1 is not as strong as the fiberglass skin of boom-fin concepts 2, 3 and 4, a reduction of only 30 percent is estimated in the number of crack/fracture/buckling failures. For similar reasons, and in keeping with the conservative approach of the analysis, reductions of only 25 percent are assumed in the number of failures occurring in the foreign object damage and puncture/tear categories. With these differences accounted for, the number of malfunction/failure events predicted for the advanced composite aft-fuselage design is 138.2, yielding a mean time between failures of 173.3 hours.

In summary, available 3M data records for the AH-1G/J aircraft have been used to predict the expected mean time between failures for promising aft-fuselage design concepts. The analysis indicates that design concepts using fiberglass fuselage skins are expected to show an increase in MTBF of approximately 93 percent. For the aft-fuselage concept using advanced composite

skin, the expected increase in MTBF is about 63 percent. Because the analysis has been performed at the conceptual design level, no attempt has been made to evaluate slight differences in the overall reliability of the promising aft fuselage designs that might result from possible differences in the reliability of the elevator and secondary structure design concepts described previously.

The expected reliability of advanced aft-fuselage design concepts has been compared to the reliability of the existing AH-1G aft fuselage in terms of the mean time between failures. This particular reliability parameter has been chosen because it is a primary input to the cost model, which is the principal tool of the methodology for evaluating the cost effectiveness of promising design concepts.

TABLE XVII. REAPPORTIONED 3M FAILURE DATA FOR AH-1G/H AIRCRAFT

Failure Event Category	Number of Recorded Events	Percentage of Total Events
Wear/Fretting	17	7.6
Corrosion	5	2.2
Broken/Loose/Missing Hardware	67	29.8
Crack/Fracture/Buckle/ Bond Failure	50	22.2
Foreign Object Damage	7	3.1
Puncture/Tear	18	8.0
Battle Damage	12	5.3
Improper Adjustment/ Alignment	29	12.9
No Defect	20	8.9
Totals	225	100.0

Total Flight Hours = 23,948
MTBF = 106.4 Hours

TABLE XVIII. PREDICTED FAILURE EVENTS FOR FIBERGLASS SKIN AFT-FUSELAGE DESIGN CONCEPTS

Failure Event Category	Expected % Reduction in No. of Events	Estimated No. of Events	% of Total Events
Wear/Fretting	50	8.5	7.3
Corrosion	30	3.5	3.0
Broken/Loose/Missing Hardware	70	20.1	17.2
Crack/Fracture/Buckle/ Bond Failure	60	20.0	17.1
Foreign Object Damage	50	3.5	3.0
Puncture/Tear	50	9.0	7.7
Battle Damage	-0-	12.0	10.2
Improper Adjustment/ Alignment	30	20.3	17.4
No Defect	-0-	20.0	17.1
Totals		116.9	100.0

Total Flight Hours = 23,943
MTBF = 204.9 Hours

TABLE XIX. PREDICTED FAILURE EVENTS FOR ADVANCED COMPOSITE SKIN AFT-FUSELAGE DESIGN CONCEPTS

Failure Event Category	Expected % Reduction in No. of Events	Estimated No. of Events	% of Total Events
Wear/Fretting	50	8.5	6.2
Corrosion	30	3.5	2.5
Broken/Loose/Missing Hardware	70	20.1	14.5
Crack/Fracture/Buckle/ Bond Failure	30	35.0	25.3
Foreign Object Damage	25	5.3	3.8
Puncture/Tear	25	13.5	9.8
Battle Damage	-0-	12.0	8.7
Improper Adjustment/ Alignment	30	20.3	14.7
No Defect	-0-	20.0	14.5
Totals		138.2	100.0

Total Flight Hours = 23,948
MTBF = 173.3 Hours

COST

METHODOLOGY

The objective of the cost analysis is to determine and compare the total cost per aircraft life cycle for the existing structure and four new concepts for the aft fuselage. The life-cycle cost per aircraft is defined herein as the total cost for each aircraft in a fleet maintained at a constant size for a specified time. For this study, a fleet size of 1000 and a life time of 10 years are used.

The principal tool for cost analysis is the cost model shown schematically in Figure 41. Input data for the model considers the structural design concept itself and a scenario of life-cycle events which is applied to each design concept. The scenario has been developed by Kaman from past field experience of the AH-1G/J helicoper as reported in Marine Corps 3M data covering the two-year period from June 1969 through July 1971 involving a total of 23,948 flight hours. This baseline data defining structure damage causes, types and distribution is further developed and refined by reliability and maintainability analysis and then applied to each design concept. Both external damage causes, such as normal incidents, hangar rash and ballistic impacts, and inherent damage events, such as fatigue, bond failures and loose/broken fittings, are considered. With the composite tail assembly repair/scrap criteria established, cost elements either supplied by the Government or determined by Kaman are applied to compute the total cost per aircraft for the tail assembly during the life cycle of the AH-1G helicopter.

Tail assembly life-cycle costs are generated in the following basic categories:

1. Acquisition
2. Operation
3. Attrition

Acquisition costs are incurred in producing the particular tail assembly design and providing pipeline spares and materials. They include, but are not limited to, the following elements:

1. Engineering design, research, development, test, and evaluation costs
2. Unit cost of producing the tail assembly as a function of quantity
3. Nonrecurring and rate tooling costs
4. Profit

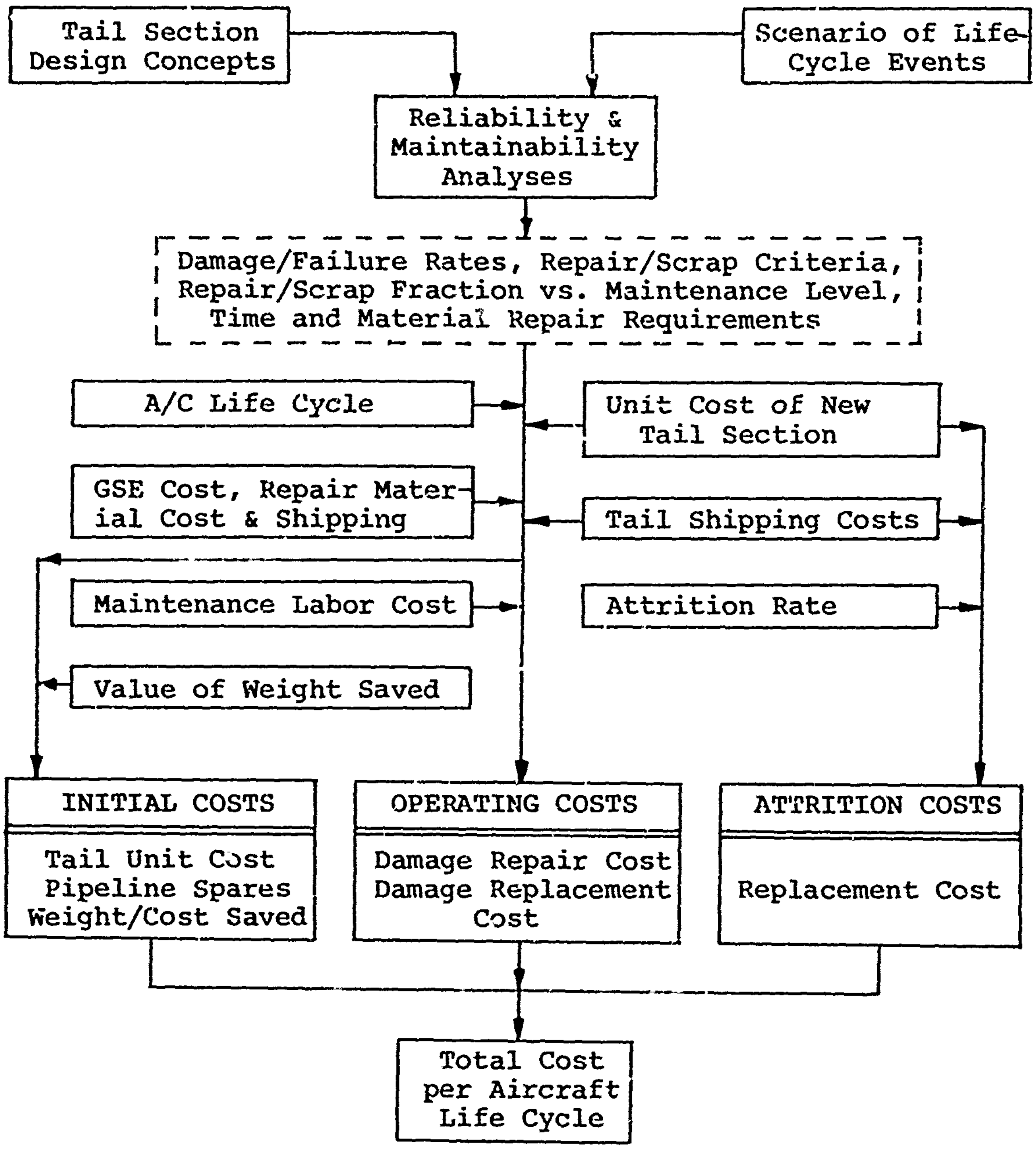

Figure 41. Cost Model.

Operating costs are determined from the results of the reliability and maintainability analysis for the scenario of life-cycle events applied to the tail assembly design concept. The following cost elements and maintenance parameters are considered in this category:

1. Mean time between damage (MTBD) and mean time to repair (MTTR) criteria
2. Military and civilian labor including inspection, disposition, requisition and repair requirements
3. Packaging and shipping costs
4. Repair or replacement material costs, other GSE and support equipment costs
5. Repair level of maintenance (organizational, intermediate, depot)

Attrition costs consist of replacement costs for damage due to other than tail assembly damage-related causes and are included in the model to provide a realistic appraisal of total unit quantities required during the aircraft life cycle.

The cost model generates a summation of the tail assembly cost per aircraft life cycle in the three basic categories discussed above. This cost per aircraft multiplied by the desired fleet size yields the total program tail assembly life-cycle cost.

COST MODEL EQUATIONS

Number of Damaged Tail Sections per Aircraft Life Cycle

$$N_D = \frac{L}{MTBD}$$

where N_D = number of damaged tail sections per aircraft life cycle

L = aircraft life cycle, flight hours

$MTBD$ = tail section mean time between damage

Initial Costs

The initial costs consist of tail section unit cost, pipeline spares costs, and weight cost.

a. Unit Cost

C_O = acquisition cost for one tail section

b. Weight Cost

Cost comparisons of different designs should be based upon equal effectiveness in terms of mission performance. The tail sections in this study have essentially equal mission performance with only one significant exception: weight. In order to account for this difference, a dollar value is determined for the weight difference and is applied to each design as an adjustment in the initial cost. The existing metal tail section is the baseline; its weight cost is zero. Typically the new concepts are lighter than the existing structure, and thus the weight cost adjustment is a lowering of the cost.

$$C_W = D_W W_S$$

where C_W = cost adjustment for weight

D_W = dollar value per pound of structural weight

W_S = weight of existing tail section minus weight of new concept

c. Pipeline Spares

The initial spares requirement assumes that all tail sections scrapped and all tail sections repaired at the depot level, as well as all repair meterials, over a 6-month period must be procured to establish the pipeline.

$$C_S = N_D(0.5/Y)((K_{TS}+K_{RD})(C_O+C_C+C_{AS})+(K_{RO}+K_{RI})$$
$$(C_M+C_M C_{MS}))+C_{ER}(0.5/Y)$$

where C_S = initial spares cost per aircraft life cycle

K_{TS} = total fraction of damaged sections scrapped

K_{RD} = fraction of damaged sections repaired at depot

K_{RO} = fraction of damaged sections repaired at organizational level

K_{RI} = fraction of damaged sections repaired at intermediate level

C_M = average cost of meterial per repair

C_{MS}= shipping cost of material per repair as a fraction of material cost

C_{ER}= cost of special ground support equipment required

C_C= cost of shipping container

C_{AS}= cost of air shipping tail section from CONUS

Y= aircraft life cycle, years

d. Total Initial Cost

$$C_{TO} = C_O + C_S + C_W$$

where C_{TO}= total initial costs per aircraft life cycle

Operating Costs

The operating costs consist of tail section repair and scrap costs summed for organizational/intermediate and depot level maintenance.

a. Organizational/Intermediate Level Repair Costs

$$C_{RO} = N_D (C_{MH} (M_1 + T_{RO}) K_{RI} + C_{MH} (M_1 + T_{RO}) K_{RO} + (K_{RO} + K_{RI}) (C_M + C_M C_{MS})) + C_{ER}$$

where C_{RO}= organizational/intermediate level repair costs

C_{MH}= organizational/intermediate level labor rate

M_1= MMH to inspect and determine damage

T_{RO}= mean field repair time, including time to remove and replace 1.3% of damaged tail sections

b. Organizational/Intermediate Level Scrap Costs

$$C_{SO} = N_D K_{SO} (C_{MH} M_3 + C_O + C_{AS} + C_{SC})$$

where C_{SO}= organizational/intermediate level scrap costs

K_{SO}= fraction of damaged sections scrapped at organizational/intermediate level

M_3= MMH to inspect and determine damage, remove and replace tail section, requisition and obtain replacement

C_{SC}= container surface shipping cost

c. Depot Level Repair Costs

$$C_{RD}= N_D K_{RD}(C_{MH}M_3+C_{SS}+2C_{PS}+C_{AS}+C_{MD}M_4+D_{RD})$$

where C_{RD}= depot level repair costs

D_{RD}= average depot repair cost per tail section

C_{SS}= tail section surface shipping cost to CONUS

C_{PS}= shipping preparation cost

C_{MD}= depot level labor rate

M_4= MMH to receive and inspect at depot

d. Depot Level Scrap Costs

$$C_{SD}= N_D K_{SD}(C_{MH}M_3+C_{PS}+C_{SS}+C_{MD}M_5+C_O+C_{AS})$$

where C_{SD}= depot level scrap costs

M_5= MMH at depot level to receive, inspect, and dispose of scrap

K_{SD}= fraction of damaged tail sections scrapped at depot level

e. Total Operating Costs

$$C_{TM}= C_{RO}+C_{SO}+C_{RD}+C_{SD}$$

where C_{TM}= total operating costs per aircraft life cycle

Attrition Costs

The attrition costs consist of the cost of new tail sections and the associated transportation charges to replace tail

sections lost to causes other than damage to the tail section.

$$C_A = N_A(C_O + C_{AS})$$

where C_A = attrition costs per aircraft life cycle

N_A = number of tail sections lost to attrition

Total Tail Section Costs

The total tail section costs are the sum of the initial, operating and attrition costs.

$$C_{LC} = C_{TO} + C_{TM} + C_A$$

where C_{LC} = total tail section costs per aircraft life cycle

Lists and Diagrams

Figures 42 and 43 list and diagram the cost elements.

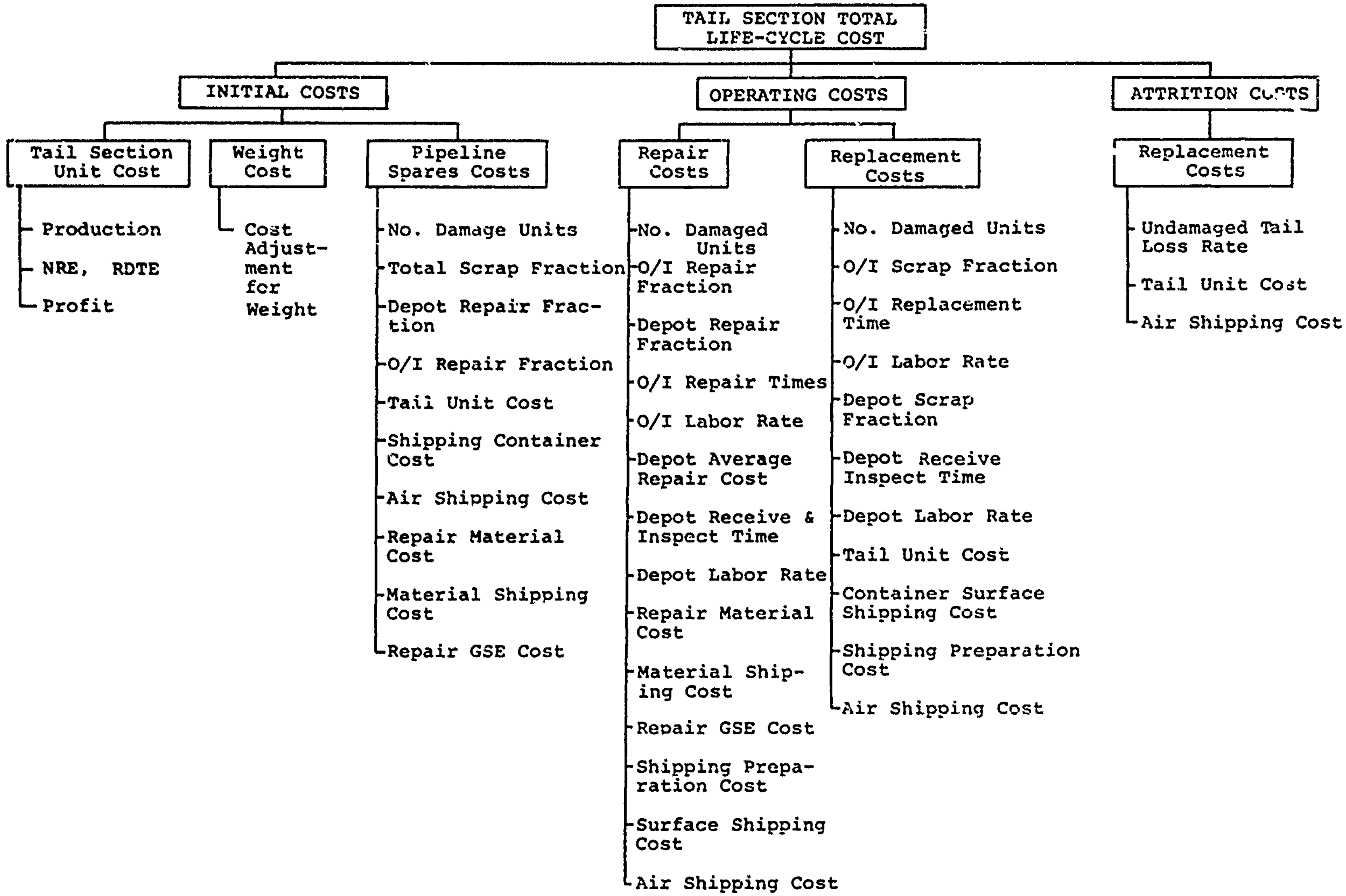

Figure 42. Individual Cost Element Breakdown.

A

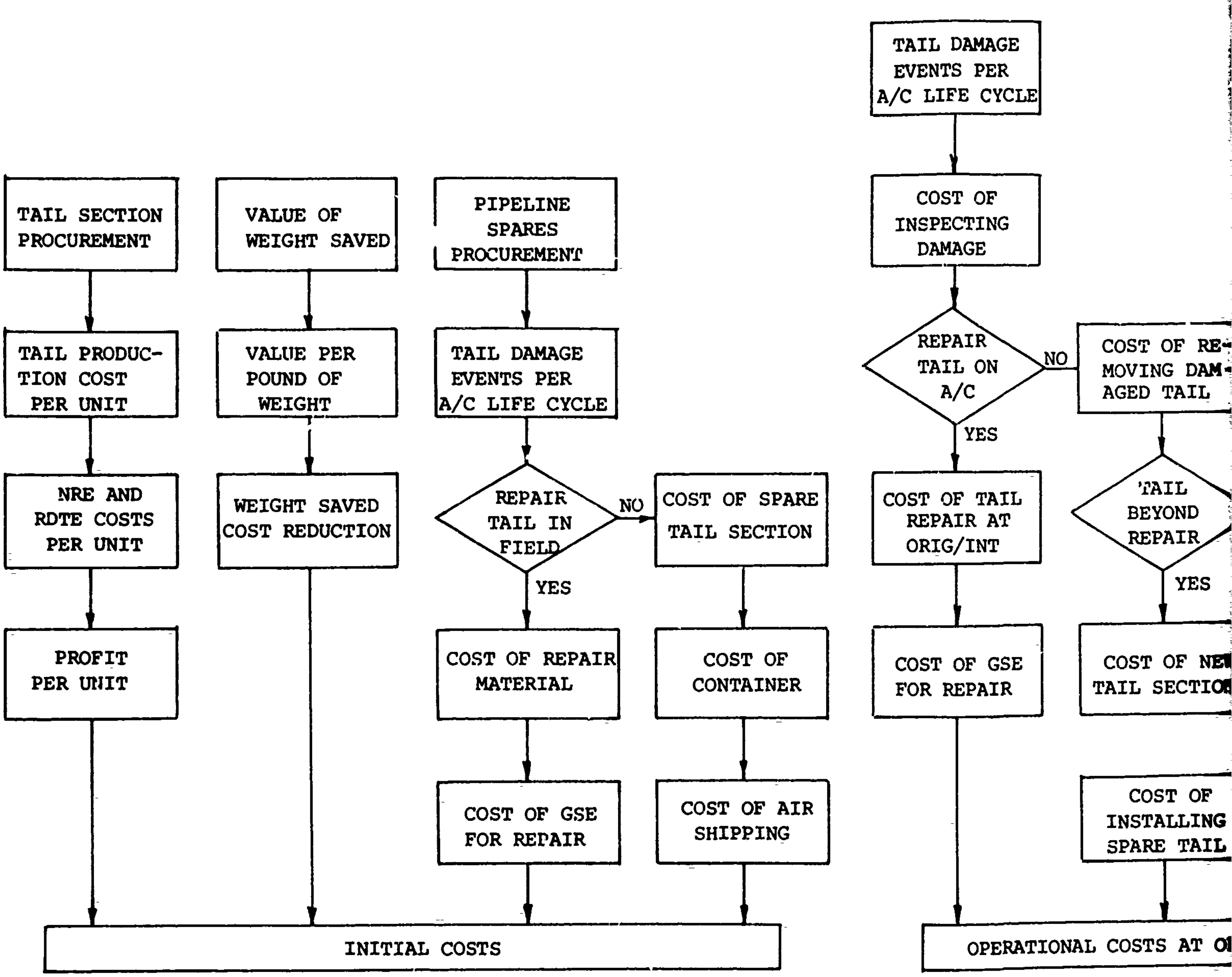

Figure 43. Cost Diagnosis.

B

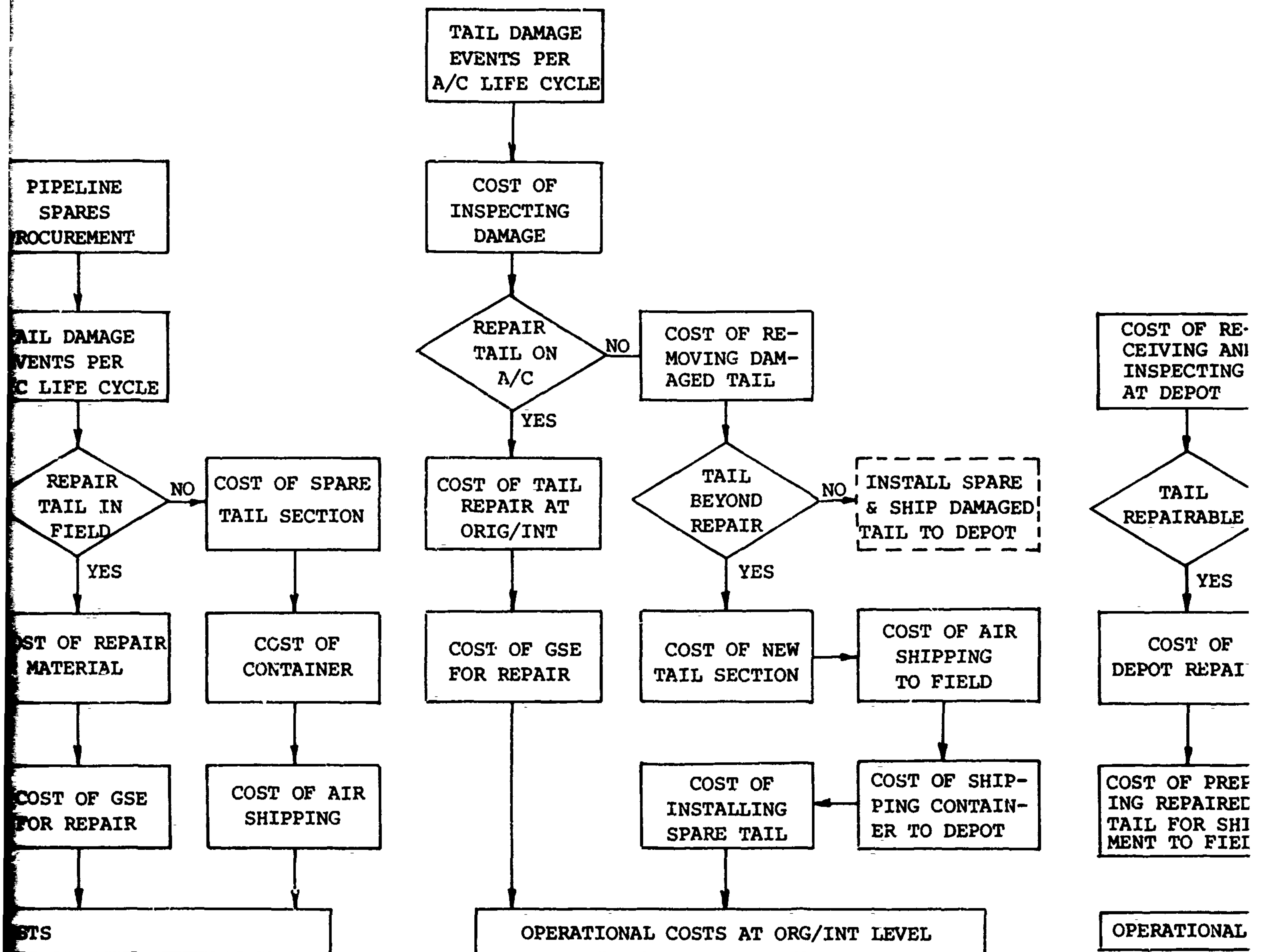

Cost Diagnosis.

C

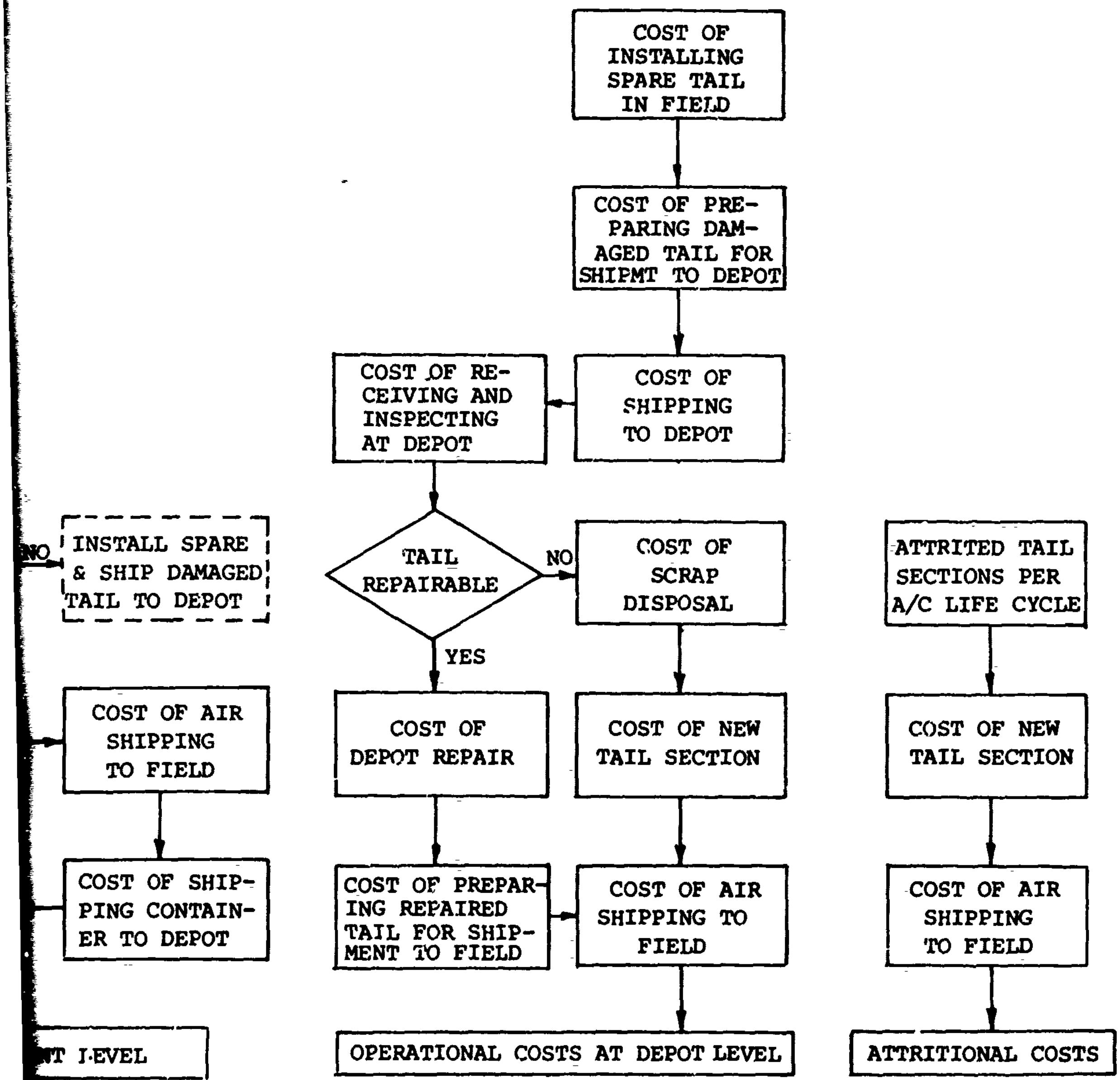

COST OF INSTALLING SPARE TAIL IN FIELD
COST OF PRE-PARING DAM-AGED TAIL FOR SHIPMT TO DEPOT
COST OF SHIPPING TO DEPOT
COST OF RE-CEIVING AND INSPECTING AT DEPOT
NO
INSTALL SPARE & SHIP DAMAGED TAIL TO DEPOT
TAIL REPAIRABLE
NO
YES
COST OF SCRAP DISPOSAL
ATTRITED TAIL SECTIONS PER A/C LIFE CYCLE
COST OF AIR SHIPPING TO FIELD
COST OF DEPOT REPAIR
COST OF NEW TAIL SECTION
COST OF NEW TAIL SECTION
COST OF SHIP-PING CONTAIN-ER TO DEPOT
COST OF PREPAR-ING REPAIRED TAIL FOR SHIP-MENT TO FIELD
COST OF AIR SHIPPING TO FIELD
COST OF AIR SHIPPING TO FIELD
T LEVEL
OPERATIONAL COSTS AT DEPOT LEVEL
ATTRITIONAL COSTS

PRODUCTION COSTS

The cost estimating department at Kaman Aerospace Corporation prepared estimates for the production costs for each of the new design concepts. Table XX summarizes these estimates and also lists the weight for each concept. The following notes describe the basis for the estimate.

1. All costs are the fully burdened cost to the customer. The costs include all overheads and a 12% profit.

2. The total production run is 2000 aft-fuselage assemblies. This quantity is the approximate number required to maintain a constant fleet size of 1000 for a 10-year period using the historical attrition rate of 10% per year.

3. Constant 1974 dollars are used.

4. Tooling costs include both materials and labor. Tooling costs are distributed equally to each unit.

5. Material costs for composite materials and core materials include a 15% allowance for losses from cutting & trimming.

6. Material costs for other materials include a 1.9% allowance for losses.

7. Production labor costs are computed using $17/hour. Average hours for the total production run were used with an 87% learning curve.

8. Prices used for the most significant raw materials are listed below. All composite materials listed are pre-impregnated with a low-temperature epoxy resin.

Material	Price, dollars/sq yd
Fabric 913 Style, S-Glass	7.25
Fabric 120 Style, E-Glass	3.75
Fabric 181 Style, E-Glass	5.50
Fabric 181 Style, PRD 49	21.00
Unidirectional E Glass, T=.009 in.	2.40
Unidirectional S-1014 Glass, T=.010 in.	8.10
Unidirectional Graphite SP-288-T2	37.00
PVC core R-400, T=.25 in.	4.95

These prices were received from the following suppliers:

B. F. Goodrich Corporation
Minnesota Mining and Manufacturing Corporation
United States Polymeric Corporation

TABLE XX. SUMMARY OF PRODUCTION COSTS AND WEIGHT						
		Average Cost (dollars)				Weight
Concept		Tooling	Material	Labor	Total	(lb)
Elevators (set of 2)	1	38	186	368	592	26.4
	2	57	198	351	606	26.0
	3	76	187	302	565	25.2
	4	76	179	266	521	23.0
Covers (set of 4 over boom)	1	24	83	281	388	5.7
	2	32	65	387	484	6.4
	3	10	23	28	61	8.2
	4	10	23	28	61	8.2
Boom-Fin	1	122	5200	3230	8552	141.1
	2	122	1939	3335	5396	169.3
	3	153	1843	3296	5292	160.0
	4	169	1899	3173	5241	165.6
Aft Fuselage Assembly	1	208	5402	3524	9134	172.3
	2	208	2141	3626	5975	200.5
	3	229	2022	3562	5813	183.0
	4	245	2078	3439	5762	188.6

Notes:

1. Average costs per unit are calculated assuming an 87% learning curve and a total purchase of 2000 aft fuselage assemblies.

2. The boom-fin includes the primary structure for each concept and the leading edge cover on the fin. For concepts 1 and 2, it does not include secondary covers for the drive shaft over the boom. For concepts 3 and 4, no such covers are required.

3. Concept 1 requires an unknown additional cost for lightning protection The weight for concept 1 includes a 10-lb allowance for lightning protection.

4. The aft fuselage assembly includes:

   numbered boom-fin
   + elevator concept 4
   + covers concept 3, for boom-fin concepts 1 and 2

LIFE-CYCLE COSTS

Tables XXI and XXII present the final results from the analysis of life-cycle costs using the cost model. Table XXI shows the cost in dollars for each unit of the fleet, and Table XXII shows the cost relative to the cost of the existing aft fuselage, concept 0, taken as 100. In order to assess the sensitivity of the costs to changes in value of input parameters, several variations are shown. These include:

- best estimate
- ±15% changes in purchase price
- ±50% changes in mean time between damage
- ±50% changes in cost of a typical repair
- ±50% changes in the scrap rate
- ±100% change in the value of a pound saved

In all cases, these changes were found to have a relatively minor effect upon the costs and the relative rankings of the concepts. The most significant savings (30 to 40%) are found in concepts 2, 3, and 4, which use glass reinforcement.

Table XXIII summarizes the input data used for the best-estimate cost analysis. The origins of these data have already been presented in the sections describing the cost model and the reliability analysis. Table XIV shows in more detail the distribution of costs corresponding to the best estimate of cost for each concept.

TABLE XXI. TOTAL COST (DOLLARS) FOR EACH UNIT OF THE FLEET					
	Concept				
Circumstances	0	1*	2	3	4
Best Estimate	21251	20922	14644	13684	13768
.85 x Unit purchase price	18517	17933	12714	11804	11907
1.15 x Unit purchase price	23986	23911	16674	15558	15629
.5 x MTBD	25775	23913	16689	15703	15780
1.5 x MTBD	19744	19928	13961	13008	13097
.5 x Cost of typ. repair	20390	20394	14197	13235	13321
1.5 x Cost of typ. repair	22112	21451	15091	14130	14215
.5 x Scrap rate	19903	19986	14095	13146	13235
1.5 x Scrap rate	22599	21859	15193	14219	14301
0 x Value of lb saved	21251	22217	14952	14603	14493
2 x Value of lb saved	21251	19627	14336	12763	13043

* Concept 1 requires an unknown additional cost for lightning protection.

TABLE XXII. RELATIVE TOTAL COST (SEE NOTE 1)					
	Concept				
Circumstances	0	1	2	3	4
Best Estimate	100	98	69	64	65
.85 x Unit purchase price	87	84	60	56	56
1.15 x Unit purchase price	113	113	78	73	74
.5 x MTBD	121	113	79	74	74
1.5 x MTBD	93	94	66	61	62
.5 x Cost of typ. repair	96	96	67	62	63
1.5 x Cost of typ. repair	104	101	71	66	67
5. x Scrap rate	94	94	66	62	62
1.5 x Scrap rate	106	103	71	67	67
0 x Value of lb saved	100	105	70	69	68
2 x Value of lb saved	100	92	67	60	62

Note:

1. Best estimate for concept 0 taken as 100.
2. Concept 1 requires an unknown additional cost for lightning protection.

TABLE XVIII. SUMMARY OF COST MODEL INPUT PARAMETERS FOR BEST ESTIMATES

Symbol	Units	Concept 0	1	2	3	4
C_{AS}	dollars	850.0	same, unless noted			
C_C	dollars	200.0				
C_{ER}	dollars	0.0	100.0	100.0	100.0	100.0
C_M	dollars	25.0				
C_{MH}	dollars/hour	4.0				
C_{MS}	fraction	0.10				
C_O	dollars	7939.0	9134.0	5975.0	5813.0	5762.0
C_{SC}	dollars	125.0				
C_W	dollars	0.0	-1295.0	-308.0	-920.5	-725.0
K_{RI}	fraction	0.994				
K_{RO}	fraction	0.0				
K_{SO}	fraction	0.007				
K_{TS}	fraction	0.006				
L	flight hours	5000.0				
M_1	hours	0.5				
M_3	hours	59.7				
MTBD	flight hours	106.4	173.3	204.9	204.9	204.9
N_A	fraction	1.0				
T_{RO}	hours	2.0				
Y	years	10.0				

TABLE XXIV. DETAILED COSTS IN BEST ESTIMATE FOR EXISTING STRUCTURE AND NEW CONCEPTS*

		Concept				
Symbol	Definition	0	1	2	3	4
N_D	number of damaged tail sections	47.0	28.9	24.4	24.4	24.4
C_S	initial spares cost	191	133	90	89	88
C_{TO}	total initial cost	8130	7972	5757	4981	5125
C_{RO}	repair cost, org/int level	1752	1175	1010	1010	1010
C_{SO}	scrap cost, org/int level	2581	1791	1053	1029	1021
C_{RD}	repair cost, depot level	0	0	0	0	0
C_{SD}	scrap cost, depot level	0	0	0	0	0
C_{TM}	total operating cost	4332	2967	2062	2038	2031
C_A	attritional cost	8789	9984	6825	6663	6612
C_{LC}	total life-cycle cost	21251	20922	14644	13682	13768

* All costs in dollars per aircraft life cycle

DOLLAR VALUE FOR A POUND SAVED

One parameter, C_W, the adjustment for weight, deserves additional discussion. C_W is the product of a difference in weight and the dollar value per pound of structural weight. The latter is potentially controversial because in engineering practice it can take on several different values during the design cycle. First, there is a true economic value which is believed to be \$35 per pound. Rationale for this number is presented in this section. Second, there is a legal or contractual value which can vary from near nil to several hundred dollars, depending on the penalty terms of a contract and the relationship of the aircraft to the contractual specifications.

The economic value can be derived by considering the aircraft to consist of a transporter and a load to be transported. The transporter supports the load and must grow in weight in response to an increase in the load if performance (speed and maneuverability) is kept constant. For the AH-1G helicopter, the transporter consists of the following groups:

Group	Weight, lb (Ref. 5)
Rotor	929.1
Tail	59.2
Total Basic Structure	801.3
Landing	108.3
Flight Control	382.2
Propulsion	1404.4
Hydraulic/Pneumatic	91.0
	3775.5

The load consists of all other items, such as crew, instruments, armament, fuel, etc. For its basic mission, the gross weight of the AH-1G is 8621.0 lb (Ref. 5). Thus

$$\text{load} = \text{gross} - \text{transporter}$$
$$\text{load} = 8621.0 - 3775.5 = 4845.5 \text{ lb}$$

On the average, 3775.5/4845.5 = .779 lb of transporter is required to support each pound of load.

Now, consider that two hypothetical tail sections exist that are functionally identical but differ in weight by 1 pound. If the lighter tail section were used, one could reason that the transporter could be designed .779 lb lighter. At current prices for the AH-1G, the transporter costs \$60 per

pound. The value of a pound of weight saved in this case is then .779 x 60.00 = $46.70 in initial cost. Fuel costs over the lifetime of the aircraft would add another $1.40, bringing the total to $48.10. This estimate, however, is too high for two reasons:

1. The slope of the tangent to the curve of transporter weight versus load is less than that of the secant, as shown in Figure 44.

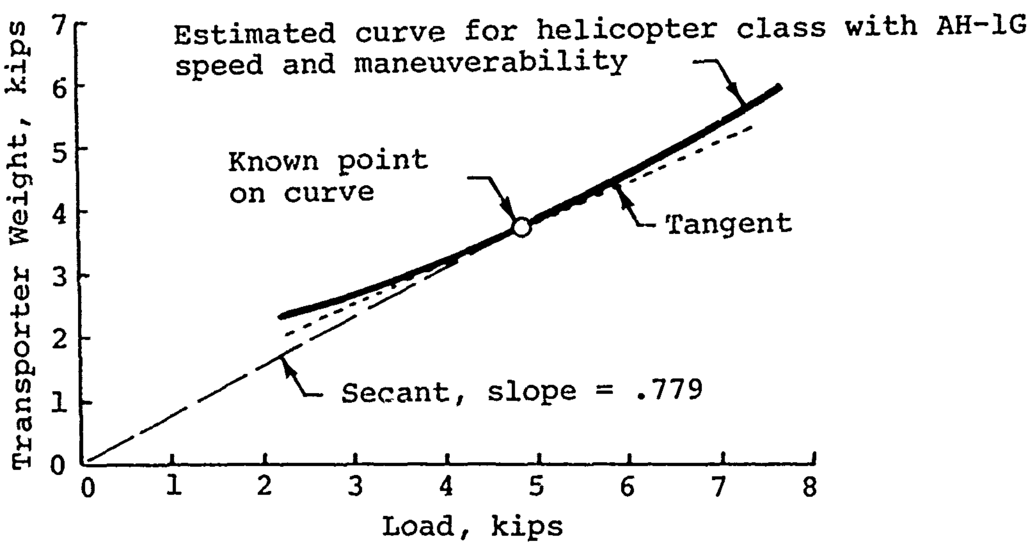

Figure 44. Transporter Weight Versus Load.

2. The law of marginal utility. The last increment of load is less useful than the first.

For these reasons, the true economic value of a pound saved is estimated to be only $35 in the design stage. This value was used in the calculation of the best estimates of life-cycle cost. Life-cycle costs with the value of a pound saved at $0 and $70 are also shown in the sensitivity analysis, Tables XXI and XXII.

CONCLUSIONS

1. The new concepts for the aft fuselage provide significant savings in life-cycle costs over the existing metal aft fuselage. The preferred concepts save 36% in life-cycle cost.

2. The new concepts have a lower unit purchase price. The unit purchase price of the preferred concepts is 26% less. The new one-phase fabrication methods for the boom, elevators, and covers are very significant factors in achieving the low unit purchase prices.

3. The new concepts provide increased safety, reliability, and maintainability.

4. The new concepts save weight. The preferred concept (No. 3) is 12% lighter.

5. Fuselage concepts 2, 3, and 4 (the glass composite concepts) are significantly more cost effective than concept 1. The principal reason for their advantage is the lower cost of the material.

6. The differences in cost between fuselage concepts 2, 3, and 4 are not great. The respective life-cycle cost savings for fuselage concepts 1, 2, 3, and 4 are 1%, 31%, 36%, and 35%.

7. Fuselage concept 3 is selected as the best concept because it offers the greatest cost saving and significant weight savings. It also provides excellent access to the interior of the boom via removable panels over its entire length.

8. Fuselage concept 2 is a very close second to concept 3. Concept 2 provides less, but still good, cost savings; less weight savings; and less access to the interior. However, concept 2 has some compensating virtues. These include: (1) increased structural integrity that accrues from a completely monolithic boom without joints and an increase in thickness for the outer facings, and (2) easier access to the drive shaft over the boom.

9. Elevator concept 4 is an easy winner. It enjoys the lowest cost, lightest weight, greatest reliability, and best salvageability.

10. Cover concept 3 is also an easy winner. It has very low cost and is the most rugged.

11. In general, the low life-cycle costs reported herein are attributed to the fact that the design concepts:

   a. Reduce the number of parts.

   b. Eliminate production operations.

   c. Simplify assembly.

   d. Improve field maintainability.

LITERATURE CITED

1. Arvin, G. H., et al, STRUCTURAL DESIGN GUIDE FOR ADVANCED COMPOSITE APPLICATIONS, North American Rockwell Corporation; Advanced Composite Division, Air Force Materials Laboratory, Air Force Systems Command, Wright-Patterson Air Force Base, Ohio, January 1971.

2. Anon, DS, GS, AND DEPOT MAINTENANCE MANUAL ARMY MODEL AH-1G HELICOPTER, TM55-1520-221-35, Headquarters, Department of the Army, April 1969.

3. Ambrose, E., and Clarke, D., TAILBOOM, VERTICAL FIN AND HORIZONTAL STABILIZER STRUCTURAL ANALYSIS, Bell Helicopter Company Report 209-099-056, Fort Worth, Texas, January 1967.

4. Montgomery, B. L., and Balke, R. W., RESULTS OF GROUND VIBRATION SURVEY, VOLUME I OF II, Bell Helicopter Company Report 209-099-017, Fort Worth, Texas, February 1969.

5. Noyes, J. K., ACTUAL WEIGHTS AND BALANCE AH-1G, Bell Helicopter Company Report 209-099-264, Fort Worth, Texas, June 1971.

6. Ashton, J. E., Halpin, J. C., and Petit, P. H., PRIMER ON COMPOSITE MATERIALS: ANALYSIS, Technomic Publishing Company, Stamford, Connecticut, 1969.

7. Anon, PLASTICS FOR AEROSPACE VEHICLES, PART I. REINFORCED PLASTICS, MIL-HDBK-17A, Department of Defense, Washington, D. C., January 1971.

8. Anon, PRD-49, DU PONT'S NEW HIGH MODULUS ORGANIC FIBER FOR PLASTICS REINFORCEMENT, BALLISTIC ARMOR, AND TENSION CABLE APPLICATIONS, PRELIMINARY DATA, E. I. DuPont de Nemours and Company, Wilmington, Delaware, September 1971.

9. Anon, "SCOTCHPLY" SP-286 PREPREG GRAPHITE TAPE, Minnesota Mining and Manufacturing Company, Saint Paul, Minnesota, January 1972.

10. Durchlaub, E., Sacco, P., FRACTURE MECHANICS AND DAMAGE TOLERANCE OF S GLASS COMPOSITES, AFFDL-TR-72-82, The Boeing Company, Vertol Division; Air Force Flight Dynamics Laboratory, Air Force Systems Command, Wright-Patterson Air Force Base, Ohio, August 1972.

11. Anon, FERRO ZERO TWIST FABRICS, S GLASS, Ferro Corporation, Nashville, Tennessee, undated.

12. Anon, RIGICELL, RIGID VINYL FOAM DATA SHEET, B. F. Goodrich Industrial Products Company, Akron, Ohio, undated.

APPENDIX

FAILURE MODE AND EFFECTS ANALYSES

The failure mode and effects analysis (FMEA) is a basic analytical tool for design evaluation and reliability improvement. This technique involves a systematic assessment of every possible potential failure mode within a hardware design based on an empirical knowledge of the design and historical statistical data when available. By following this approach, the weakness or limitations of a design can be pinpointed and appropriate engineering attention directed toward improving critical reliability areas of the design.

The simplified functional flow block diagram of Figure 45 shows the basic functions which the aft fuselage must perform as an assembly of the helicopter system. For the purposes of the FMEA's, it is sufficient to summarize the functional requirements as follows:

> Transfer Loads - The aft-fuselage structure must have sufficient strength to receive input loads from the tail rotor, elevator, and tail skid, and to transfer these to the main fuselage.
>
> Meet Stiffness Requirements - The advance design concepts must provide adequate stiffness to assure that natural frequencies are not adversely affected.
>
> Provide Access - The advanced concepts must have enough access panels, covers and/or doors to permit drive train maintenance, flight control maintenance, structural repair and inspection.
>
> Provide Environmental Durability - The advanced concepts must be at least comparable to the existing aft fuselage in resistance to erosion, corrosion, foreign object and ballistic damage, and hangar rash incidents.

The functional flow block diagram of Figure 46 and preliminary design drawings of the boom-fin, elevator and secondary structure advanced design concepts serve as a basis for preparing the simplified aft-fuselage reliability block diagram and the aft-fuselage component level reliability block diagram presented in Figures 46 and 47 respectively. The latter diagram isolates and itemizes those components whose successful performance is essential to proper performance of the overall aft fuselage structure. The FMEA methodically evaluates each of these essential components in turn to establish possible failure

modes, causes of failure, effects of failure on aft fuselage structural performance, methods of detection, qualitative estimates of failure criticality to safety and mission success, and subjective classifications of expected failure probabilities of occurrence. To facilitate the analysis procedure, all potential inherent and external modes of failure are sorted into the following basic failure groups:

Inherent - Wear/Fretting
Corrosion
Loose/Broken Hardware
Delamination
Bond Separation
Crack/Fracture/Buckling

External - Dent
Puncture/Tear
Battle Damage

Failure criticality codes are defined as follows in accordance with MIL-STD-882:

Category I - Negligible - Any nuisance failure not serious enough to be classified in a higher category, but requiring corrective action during routine preventive maintenance.

Category II - Marginal - Any failure which is expected to degrade performance, which can be tolerated throughout a mission, but which should be corrected immediately upon completion of the mission.

Category III - Critical - Mandatory Abort - Any failure expected to cause personnel injury/hazard or major aircraft system damage, or requiring immediate corrective action for survival. A time-dependent repair action which can cause a catastrophic failure if uncompensated.

Category IV - Catastrophic - Any failure expected to cause death/serious injury, or loss of the aircraft.

To provide a qualitative estimate of the probability of failure occurrence, the following subjective classifications are used:

Class A - Probability of failure is not remote.
Class B - Probability of failure is remote.
Class C - Subject to rare, random failures.
Class D - Not expected to fail in service.

Tables XXV through XXVII present the detailed results of the failure mode and effects analyses.

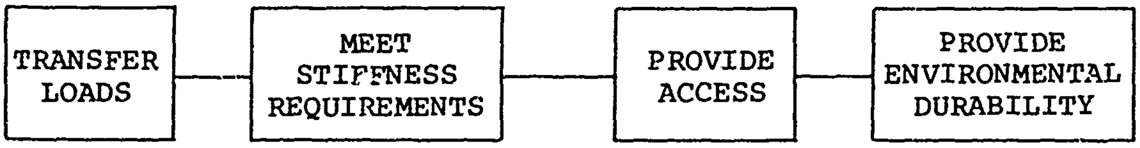

Figure 45. Simplified Functional Block Diagram.

Figure 46. Simplified Reliability Block Diagram.

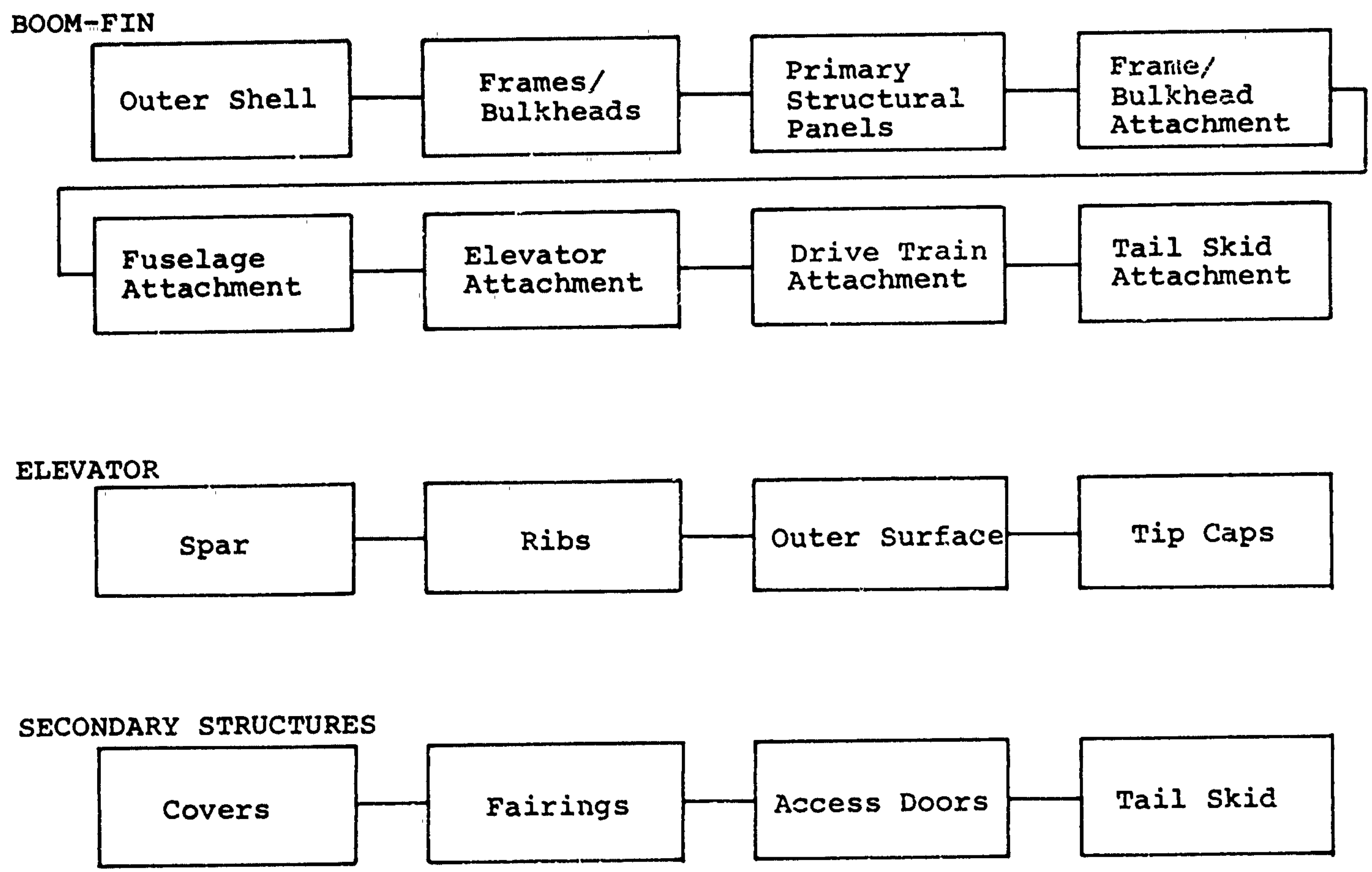

Figure 47. Aft-Fuselage Component Level Reliability Block Diagram.

TABLE XXV. FAILURE MODE AND EFFECTS ANALYSIS FOR BOOM-FIN CONCEPTS

Item Name	Assumed Failure	Possible Cause	Effect	Detection Method	Criticality Code	Probability Class
Outer Shell	Fretting of fin spar	Vibration, loose bolts	Could lead to fatigue cracks at bolt holes	Visual with fin cover open: loose parts and metal powder	Negligible to marginal	D
	Corrosion of aluminum edge members	Exposure to weather, corrosive agents	Could lead to fatigue cracks	Visual with covers open or internal inspection	Negligible to marginal	D
	Delamination of skin (See Note 1)	Vibration, defect in manufacture	Possible loss of structural integrity if area is large (See Note 2)	Visual, coin topping, spongy feel	Negligible to marginal	C small D large
	Crack, fracture or buckling of skin (See Note 3)	Overload, fatigue	Fracture could lead to structural failure	Visual, increased vibration	Negligible to catastrophic depending on severity	D
	Dent (See Note 4)	Foreign object, tool impacts, mishandling	Generally, small dents will not affect performance; large dents could result in local loss of structural integrity	Visual	Negligible to marginal	C
	Puncture/tear (See Note 5)	Foreign object, tool impacts, mishandling	Small punctures or tears will not affect performance; large ones could result in local loss of structural integrity	Visual	Negligible to marginal	D
	Battle damage	Projectile hit	Individually minor effect: produces localized hole	Visual	Negligible to marginal	C

TABLE XXV - Continued

Item Name	Assumed Failure	Possible Cause	Effect	Detection Method	Criticality Code	Probability Class
Frames/Bulkheads	Wear/fretting	Vibration, loose bolts	Could lead to fatigue cracks	Visual during internal inspection; feel of bolts	Negligible	D
	Corrosion of aluminum	Exposure to weather, corrosive agents	Could lead to fatigue cracks	Visual during internal inspection	Negligible to marginal	D
	Crack, fracture or buckling	Overload, vibration	Some loss of load transfer capability and shell stability	Visual	Negligible to critical depending on severity	D
	Dent	Tool impacts, projectile hits	No effect on performance	Visual during internal inspection	Negligible	D
	Battle damage	Projectile hit	Individual bullet holes have little immediate effect; repair should be made to prevent cracks and restore integrity	Visual during internal inspection	Negligible	C or D
Primary Structure Panels (Avionics door, access doors, drive train covers) (See Note 6)	Wear/fretting at edges	Vibration	Loosening of door or cover; could lead to fatigue cracks	Visual; feel of fasteners	Negligible to marginal	D
	Dent (See Note 4)	Foreign object, tool impact, mishandling	Small dents will not affect performance; large dents could cause local loss of integrity	Visual	Negligible to marginal	C

TABLE XXV - Continued

Item Name	Assumed Failure	Possible Cause	Effect	Detection Method	Criticality Code	Probability Class
Primary Structure Panels (continued)	Puncture/tear (See Note 5)	Foreign object, tool impact, mishandling	Small punctures/tears have little effect; large punctures/tears could result in local loss of structural integrity	Visual	Negligible to marginal	D
	Battle damage	Projectile hit	Individually minor effect: produces localized hole	Visual	Negligible to marginal	C
Frame/Bulkhead Attachment	Fastener pulled through skin	Overload	Loss of support and stability of skin; reduction of skin load-carrying capability	Visual	Marginal to critical	D
	Bond separation from shell	Fatigue, vibration	Reduction of skin load-carrying capability	Visual	Negligible to marginal	C
	Battle damage	Projectile hit	Local reduction of skin load-carrying capability	Visual	Negligible	D
Fuselage Attachment	Corrosion of fittings	Exposure to weather, corrosive agents	Could lead to fatigue cracks	Visual	Negligible to marginal	D
	Crack, fracture, bond failure	Overload, loose bolt, fatigue	Fracture could lead to structural failure	Visual, increased vibration	Marginal to catastrophic depending on severity	D

TABLE XXV - Continued

Item Name	Assumed Failure	Possible Cause	Effect	Detection Method	Criticality Code	Probability Class
Fuselage Attachment (continued)	Battle damage	Projectile hit	Mission can probably be completed without serious failure if maneuvers and speed are restricted; replace fitting before next flight	Visual, increased vibration	Marginal to catastrophic depending on severity	D
	Loose bolt	Overload, defective nut, improper installation	Could lead to fatigue cracks	Visual via torque stripe, feel, increased vibration	Negligible to marginal	C
Elevator Attachment	Delamination	Overload, vibration.	Crazing, cracking, or buckling of outer skin; increased vibration	Visual	Marginal	D
Drivetrain Attachment (See Note 7)	Loose bolt	Vibration	Could lead to fatigue cracks at attachment points	Visual with covers open	Negligible to marginal	C
Tail Skid Attachment	Missing bolt	Vibration; improper installation/maintenance	Tail skid would rotate on ground contact and be ineffective; side load could cause skid to separate from fuselage	Visual	Marginal	C

TABLE XXV - Continued

NOTES:

1. In Concept 4 this failure is applicable to the fin only, since the corrugated fiberglass skin of the boom is much less likely to delaminate compared to the sandwich skin of the fin and the other boom-fin design concepts.

2. The probability of skin delamination in the fiberglass sandwich construction is considered to be somewhat less than in the advanced fiber composite sandwich construction because of the more advanced state of the art of fiberglass technology.

3. The probability of cracks, fractures or buckling is considered to be less for the fiberglass sandwich skin than for the advanced fiber sandwich skin since the fiberglass sandwich used in concepts 2 and 3 possesses better strength properties.

4. Because of its greater strength, the fiberglass sandwich construction of concepts 2 and 3 is less susceptible to dent and puncture/tear types of damage than the advanced fiber sandwich skin of concept 1.

5. Puncture/tear damage is applied only to the composite sandwich construction of concepts 1, 2 and 3.

6. Drive train covers are primary structure on concepts 3 and 4 only. These covers are secondary structure on concepts 1 and 2.

7. Drive train includes drive shaft, 42° gearbox, 90° gearbox, and tail rotor.

TABLE XXVI. FAILURE MODE AND EFFECTS ANALYSIS FOR ELEVATOR CONCEPTS

Item Name	Assumed Failure	Possible Cause	Effect	Detection Method	Criticality Code	Probability Class
Spar	Crack/fracture	Overload, fatigue	Increased vibration; adverse effect on handling qualities of the aircraft; loss of elevator control; possible separation of elevator from aircraft	Difficult to detect prior to serious failure; possibly visual if bent or misaligned	Marginal to critical	D
	Battle damage	Projectile hit	Mission can probably be completed without serious failure, but elevator should be replaced/repaired before next flight (See Note 1)	Possibly visual through bullet hole or probing through the hole	Marginal	D
Ribs	Bond separation (See Note 2)	Vibration, defect in manufacture	Nuisance failure with no effect on performance when area affected is small, but could progress to a critical failure if not repaired	Visual, tapping, feel	Negligible to marginal	C small D large
	Foreign object damage	Impact with foreign object	Could cause bond separation at rib/skin interface, but would be limited by rivets (See Note 2)	Difficult to detect	Negligible	C

TABLE XXVI - Continued

Item Name	Assumed Failure	Possible Cause	Effect	Detection Method	Criticality Code	Probability Class
Ribs (Continued)	Battle damage	Projectile hit	Mission can probably be completed without serious failure: Repair if inboard rib is damaged; replace elevator if outboard rib is damaged (See Note 3)	Visual	Marginal	D
Outer Surface & Tip Caps	Delamination	Poor sealing at edges allowing moisture to enter	Nuisance failure with no effect on performance, but could progress to more serious failure if not repaired	Visual, feel	Negligible	C
	Bond separation	Vibration; defect in manufacture	Nuisance failure when affected area is small, but could progress to more serious failure if not repaired	Visual, tapping, feel	Negligible to marginal	C small D large
	Foreign object damage	Impact with foreign object or tools	Could cause dent, puncture or tear with no major effect on structural integrity	Visual	Marginal	C
	Crack in aft skin (See Note 4)	Fatigue, pulsating air loads	Nuisance failure, but should be repaired to prevent crack from progressing	Visual	Negligible	C
	Crack/fracture at rivets (See Note 5)	Vibration	Primarily a nuisance failure	Visual	Negligible	D
	Battle damage	Projectile hit	No major effect on structural integrity of skin	Visual	Marginal	C

TABLE XXVI -Continued

NOTES:

1. In concepts 1 and 2 the elevator must be replaced. In concept 4, the spar can be replaced if damaged. In concept 4, the end fitting can be removed and salvaged. In addition, the spar in concept 4 is accessible for repair after the removal of the end fitting.

2. The outboard rib of concepts 1 and 2 is also riveted to the outer skin to limit the extent of any skin/rib bond separation that might occur. Concepts 3 and 4 do not have an outboard rib.

3. Concepts 3 and 4 do not have an outboard rib.

4. The trailing-edge skin of concept 1 is well supported by a honeycomb core. For this reason, concept 1 is not expected to be susceptible to this type of failure.

5. This type of failure is applicable only to concept 4, which incorporates a riveted skin-to-spar attachment.

TABLE XXVII. FAILURE MODE AND EFFECTS ANALYSIS FOR SECONDARY STRUCTURES

Item Name	Assumed Failure	Possible Cause	Effect	Detection Method	C[illegible]ality [illegible]e	Probability Class
Covers	Wear/fretting at hinge (See Note 1)	Vibration	Hinge becomes loose due to pin wear; could lead to broken hinge pin	Visual, sloppy feel	Negligible	D
	Wear/fretting at fasteners	Vibration	Fasteners become loose; could lead to broken fasteners	Visual, sloppy feel	Negligible	C
	Corrosion of hinges (See Note 1)	Exposure to elements, corrosive agents	Could lead to broken hinge	Visual	Negligible	D
	Loose/broken hinge (See Note 1)	Excessive wear; corrosion	Cover becomes loose	Visual	Negligible	D
	Loose/broken fasteners	Excessive wear	Cover becomes loose	Visual	Negligible	D
	Torn hinge (See Note 2)	Vibration, flexing	Nuisance failure, rip-stopper will limit extent	Visual, feel	Negligible	C
	Delamination (See Note 3)	Poor sealing at edges allowing moisture to enter	Nuisance failure without serious consequences	Visual, feel	Negligible	D
	Bond separation (See Note 4)	Vibration, defect in manufacture	Nuisance failure without serious consequences	Visual, feel, tapping	Negligible	D
	Foreign object damage (See Note 5)	Foreign object impact; tools	Could cause dent, puncture or tear. Large dent might interfere with drive shaft.	Visual	Negligible	C
	Battle damage	Projectile hit	No significant effect	Visual	Negligible	C

TABLE XXVII - Continued

Item Name	Assumed Failure	Possible Cause	Effect	Detection Method	Criticality Code	Probability Class
Tail Skid	Corrosion	Exposure to elements, corrosive agents	Nuisance failure, not likely unless protective paint is worn off	Visual	Negligible	D
	Bent tube	Overload caused by hard landing	Tube should be replaced or possibly repaired	Visual	Negligible to Marginal	C
	Battle damage	Projectile hit	Hole in tube or tube dented	Visual	Negligible to Marginal	D

NOTES:

1. This failure mode is applicable only to the aluminum hinges of concept 1. The polypropylene hinges of concepts 2, 3 and 4 are not susceptible to this failure.
2. This failure mode is applicable only to the polypropylene hinges of concepts 2, 3 and 4.
3. This failure mode is applicable only to concepts 1 and 2. The polypropylene covers of concepts 3 and 4 are not laminated.
4. This failure mode is applicable only to concept 1. None of the other secondary structure concepts involve bonded construction.
5. This failure mode is applicable only to concepts 1 and 2. Because of their resiliency, the polypropylene covers of concepts 3 and 4 are not susceptible to this failure.